

**Calculation of stress tensor
within the *ab-initio* full-potential
linearized augmented plane wave method**

Diplomarbeit in Physik
zur Erlangung des Grades eines Diplom-Physikers

vorgelegt am
01. Februar 2012

der
**Fakultät für Mathematik, Informatik und
Naturwissenschaften**
der Rheinisch-Westfälischen Technischen Hochschule Aachen

von
Dipl.-Math. Daniel Aaron Klüppelberg
geboren am 11.08.1983 in Dormagen

angefertigt am
Peter Grünberg Institut (PGI)
Forschungszentrum Jülich

Betreuer: Prof. Dr. Stefan Blügel
Zweitgutachter: Prof. Dr. Marjana Ležaić

Contents

1. Introduction	1
2. Theoretical background	7
2.1. Stress and strain in solids	7
2.2. The many-body Hamiltonian	8
2.3. Density functional theory	9
2.3.1. The Kohn-Sham System	10
2.3.2. The exchange-correlation functional	13
3. Electronic structure methods	15
3.1. The APW method	17
3.2. The LAPW method	19
3.3. The FLAPW method	21
3.3.1. Stars as symmetrized plane waves	22
3.3.2. Lattice harmonics	24
3.3.3. The Weinert method	25
3.3.4. Construction of the exchange-correlation energy density and potential	30
3.3.5. Construction of the Hamilton and overlap matrices	32
3.4. Local orbitals	35
3.5. Variational total energy for metals	37
4. Forces from total energy calculations	39
4.1. The Hellman-Feynman force	40
4.2. The Pulay correction	41
4.2.1. Core correction	41
4.2.2. Valence correction	42
4.2.3. Discontinuity correction	43
5. Stress from total energy calculations	45
5.1. Recurring relations	46
5.2. Variation of the kinetic energy	48
5.2.1. Contribution of core electrons	49
5.2.2. Contribution of valence electrons	50
5.3. Exchange-correlation contribution	50
5.4. Variation of the electrostatic energy	51
5.4.1. Electrostatic pressure formulas	53

Contents

5.4.2. Variation of the alternative electrostatic potential	54
5.5. The Hellmann-Feynman stress	60
5.6. Computational details	62
5.6.1. Kinetic stress formula	62
5.6.2. Discontinuity correction	63
5.6.3. Valence correction	65
5.6.4. Core correction	68
5.7. Stress from local orbitals	70
5.8. A simple pressure formula	71
6. Discussion	73
7. Application of the stress formalism to aluminum	77
8. Conclusion & Outlook	83
A. Appendix	85
A.1. Proof of (3.27)	85
A.2. Hellmann-Feynman force formula	86
Bibliography	87

1. Introduction

In the first half of the twentieth century, Niels Bohr, Erwin Schrödinger, Werner Heisenberg, Paul Dirac and others laid the foundation of quantum mechanics after it had become apparent that the laws of classical mechanics failed for sub-atomic particles. Quantum mechanics is not just a special theory for microscopic particles but also contains classical mechanics in the limit of macroscopic dimensions and scales. Therefore the description of macroscopic objects from first principles, or *ab-initio*, is possible. With the discovery of quantum mechanics, Dirac pointed out that "the underlying laws necessary for the mathematical theory of a large part of physics and the whole of chemistry are thus completely known" [Dir29], but he also foresaw the main problem, as he continued "the difficulty is only that exact applications of these laws lead to equations which are too complicated to be soluble." Ever since, a large part of condensed-matter theory has been devoted to developing approximate practical methods that are accurate enough to describe the main properties of materials.

The chemical binding of materials is the result of an interplay of the dynamics of electrons and their interactions with the atomic nuclei as well as the interactions among each other. This leads, for example, to the stable periodic arrangement of atomic nuclei in crystals. While the quantum mechanical motion of a single electron, e.g., in a central potential, the hydrogen atom, is a relatively simple problem that can be solved analytically, the equation of motion becomes exponentially more complicated the more electrons are being treated. The main reason for this is that the electrons interact with each other so that their motion is correlated: the motion of any electron depends on the motion of all other electrons. As a consequence, the many-electron wave function becomes so complicated that it is impossible to store it in a computer for systems with more than a few electrons, let alone the billions of billions of electrons in a macroscopic material.

In 1964, Pierre Hohenberg and Walter Kohn revolutionized the calculation of physical properties of atoms, molecules, and solids from first principles by introducing the density-functional theory (DFT). They showed that one does not have to deal with the complex many-electron wave function; already the much simpler electronic density $\rho(\mathbf{r})$, which is just a real-valued scalar function of space, contains all information about the physical system, e.g., the ground-state total energy. Together with a variational principle for the total energy, this allows us, in principle, to determine the ground-state arrangement of the atomic nuclei at zero temperature by minimizing the total energy of the system. While Hohenberg and Kohn proved the theoretical foundation of DFT, Kohn and Sham introduced one year later, in 1965, a mapping of the real interacting

1. Introduction

system to a fictitious non-interacting system of electrons that has made practical calculations possible; the fictitious system of non-interacting electrons is constructed in such a way that its electronic density coincides with that of the real system. Then, the only approximation is the exchange-correlation energy functional, whose exact form is unknown. The success of DFT lies in the observation that rather simple approximations for this quantity are known, e.g., the local-density approximation (LDA) and several generalized gradient approximations (GGAs), yield reliable results for a wide range of materials. The impact of DFT on theoretical chemistry was acknowledged by awarding Walter Kohn and John A. Pople the Nobel prize in chemistry in 1998. Today, DFT is a standard method in theoretical solid-state physics, theoretical chemistry, materials science, mineralogy, bio-physics, etc. It has been used successfully to determine atomic arrangements in molecules and solids, dynamical properties like lattice vibrations, electronic and magnetic properties, etc.

The structure of a binary molecule consisting of two atoms is determined by a simple number, the inter-atomic distance between the nuclei. If the nuclei are displaced relative to each other, forces arise that cause the nuclei to return to their equilibrium distance. Similar restoring forces occur in molecules that contain more than two atoms. Here, the angles between the nuclei are additional parameters that may change during the relaxation. The ground-state geometry of a molecule or cluster, i.e., the agglomerate of several atoms in a stable arrangement, is characterized as the global minimum of the potential energy surface. Any deformation of the structure will give rise to a larger total energy. To find the ground-state geometry within DFT, one could calculate the total energies of several different atomic configurations and then choose the configuration that is lowest in energy. However, since there are infinitely many structures, this is not a viable practical approach. Instead, one uses an iterative optimization procedure that involves the forces acting on the atoms. As long as a stable geometry is not found yet, there are finite restoring forces that drive the atoms toward their equilibrium positions. In each iteration of the geometry optimization one calculates these atomic forces, which are defined as derivatives of the total energy with respect to the atomic positions. Assuming a parabolic shape of the potential energy surface, this information can then be used to extrapolate to a new atomic arrangement, which starts the next iteration. Furthermore, once a stable geometry is found, one can calculate the restoring forces by selectively displacing certain atoms. The restoring forces are directly related to the so-called dynamical matrix, from which the vibrational modes and frequencies of the molecule or cluster can be calculated.

In a solid, atomic forces determine the configuration of the nuclei in the unit cell, too. When using periodic boundary conditions (which is necessary to deal with the infinite number of atoms in a crystal), all copies of an atom in the unit cells move in the same way as the representative atom. Hence, the representative only changes its position relative to the other atoms in the unit cell but not relative to its equivalent atoms. Apparently, a solid possesses additional degrees of freedom, which are related to the arrangement of atoms within the equivalent sets of nuclei. The simultaneous

change of the position of all atoms in a regular but aperiodic manner is called strain. More specifically, strain can be characterized by a three-dimensional tensor $\underline{\underline{\varepsilon}}$; the atomic displacements are given in terms of this tensor by $\mathbf{r} \rightarrow (\underline{\underline{1}} + \underline{\underline{\varepsilon}})\mathbf{r}$. The unit cell of a solid under strain differs in shape or volume from the unit cell of the solid in its equilibrium state. In the strained solid, forces occur that simultaneously drive all atoms back to their equilibrium positions. These forces can be defined to act on the boundary of the unit cell, a special case of which is pressure. In general, they are called stress. Together with the atomic forces, stress can be used to determine the crystal structure of a solid in its ground state, which is defined by the atomic basis and the lattice vectors of the crystal, respectively: Equilibrium is achieved if (i) the total forces vanish on each atom and if (ii) the macroscopic stress equals the externally applied stress. For example, in a liquid the state of the system is fully specified by the volume, pressure and temperature. Note that the elasticity of solids is another property that is directly related to the stress tensor. In this way, we can understand the microscopic origin of elasticity, which is originally a concept used in continuum mechanics.

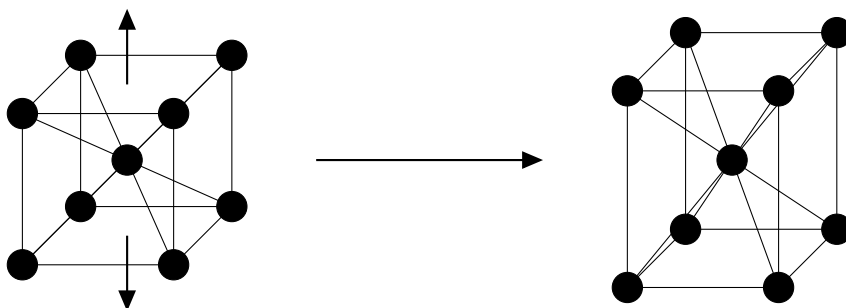


Figure 1.1.: Uniaxial tensile stress transforms a bcc structure into a bct structure.

Stress and strain are interesting not only for finding the ground-state crystal structure of a system. A material can also be forced into a strained geometry. The technique of growing thin films of a certain material onto a substrate material exploits this feature. At the contact zone, interface forces of the substrate exert stress on the film material, and the film adopts the lattice constant of the substrate. Choosing different substrates, one can experimentally tune the lattice constant of the film and in this way study its behavior under different degrees of strain. This enables, for example, the study of the dependence of the easy magnetization axis of iron or nickel films under strain [SK11].

Another example is the study of the deformation of solids induced by a magnetic field. Such a study provides a means to search for new materials to use in transformers, dynamos, and other applications of electric engineering. Severe deformation of the materials embedded in these devices causes them to heat up and to generate a characteristic humming. By knowing how a material changes its shape in a magnetic field, its usability and performance in such devices can be predicted.

1. Introduction

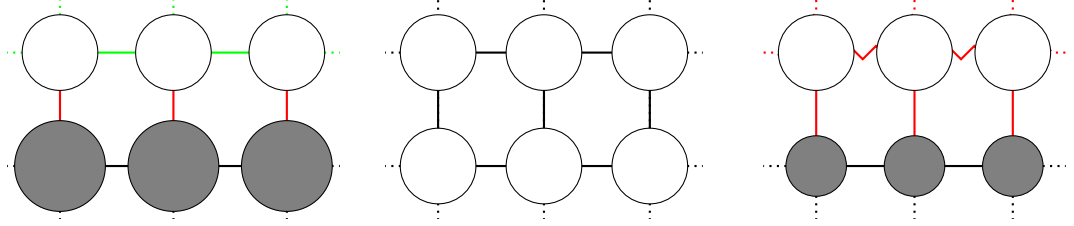


Figure 1.2.: Film (white) on different substrates (gray). In the middle figure, substrate and film are of the same material, the film is under no stress. On the left, the substrate has a greater lattice constant, leading to a tensile stress in the film (thin green lines). On the right, the substrate has a smaller lattice constant. This results in compressive stress in the film (red zigzag lines).

The first derivation of the macroscopic stress tensor from DFT was provided, implemented and tested by Nielsen and Martin [NM85a, NM85b] in the context of the pseudo-potential method, a particular approach to electronic structure methods based on density functional theory, in which plane waves are used as basis sets. An implementation that was later extended to the projector augmented-wave (PAW) method [Blo94, TJB⁺08].

In this thesis, a formalism is presented to obtain the stress tensor of a strained solid from a DFT calculation for an all-electron method, that means an electronic structure method that takes all electrons of an atom into account and can be applied to all atoms of the periodic table and also to magnetic materials with complex magnetic phases. Prerequisite to precise stress tensor calculations is the treatment of the crystal potential and the charge density without approximation of their shapes.

With all these factors in mind, we have chosen the full-potential linearized augmented-plane-wave (FLAPW) method [WKWF81, WWF82, Sin94, BB06, htt12], considered to be the most accurate electronic structure method available with caveat that it is technically and conceptually a rather complex method. The FLAPW method relies on a partitioning of space into non-overlapping atom-centered muffin-tin spheres and the remaining interstitial region. In the latter plane waves are used as basis functions, while in the former one employs superpositions of atomic solutions of the radial Schrödinger equation, as well as the energy derivatives of the atomic solutions. The superpositions are such that they match in value and first radial derivative to the plane waves in the interstitial. A force formalism based on the FLAPW method was derived by Yu *et al.* [YSK91], while a formalism derived by Soler and Williams [SW89] uses a variant of a linearized augmented plane-wave method.

Prior to the results of this thesis, the stress tensor was formulated within the FLAPW method by Thonhauser *et al.* [TADS02], where they give a guideline on how to obtain the stress tensor from total-energy calculations. However, their publication lacks a detailed description of the stress contribution coming from the electrostatic interac-

tion between the particles, which poses a challenge due to the non-local nature of the corresponding energy term. A very rigorous deduction of stress using the basis set of Soler and Williams was done recently by Nagasako and Oguchi [NO11]. Their derivation cannot directly be adopted for the FLAPW method, though.

The formalism presented here will allow to relax the lattice structure of a solid similar to the relaxation of atomic positions within the unit cell. Furthermore, the formalism can be used for studies of the elasticity of materials.

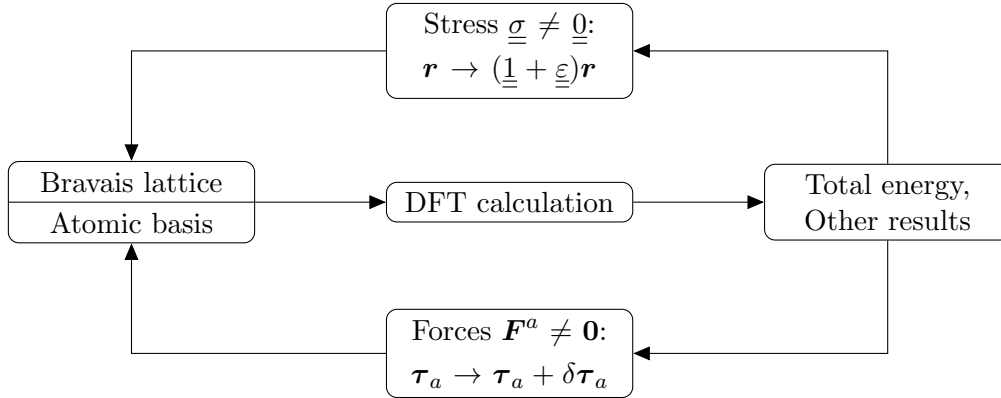


Figure 1.3.: Lattice structure optimization: Start with a guessed lattice geometry. If the resulting atomic forces are non-zero, shift the atoms in the unit cell and continue the optimization until the forces are sufficiently small. If the stress is non-zero, change the Bravais lattice vectors accordingly and continue the optimization until the stress vanishes.

The thesis is divided into seven chapters. Chapter 2 will provide a general theoretical background to stress in solids and an introduction to DFT and the formalism of Kohn and Sham. Chapter 3 explains the FLAPW method starting from the Bloch theorem and gives a detailed overview of the construction of the electrostatic potential. Chapter 4 gives an overview about the force implementation in the FLAPW method following Yu *et al.* Chapter 5 then contains the main part of this thesis, the variation of the total-energy formula by strain. Pressure formulas are provided to compare the stress components to, and the implementation into the FLEUR code is presented. This code is a FLAPW DFT code for energy band calculations, which is developed and maintained in the Peter Grünberg Institut of the Forschungszentrum Jülich. Chapter 6 compares the formulas found in this thesis to the previous works of Nielsen and Martin, Thonhauser *et al.*, and Nagasako and Oguchi. First results for aluminum are presented in chapter 7. In chapter 8, we summarize the thesis and give an outlook. Ways to improve the implementation further are suggested and further problems are discussed to which the formalism can be applied. The appendix provides some important technical details.

2. Theoretical background

2.1. Stress and strain in solids

According to the textbook of Nye [Nye98], a body is said to be in a state of stress if it is acted upon by external forces or if parts of the body exert forces on neighboring parts. In considering a unit cube within a body, stress can be described as force components acting on the surface planes of this cube. We define a second rank stress tensor $\underline{\underline{\sigma}}$. On the center of each surface of the cube, a stress component $\sigma_{\alpha\beta}$ is reserved for each direction given by the area normals of the cube (see fig. 2.1 for clarification).

If a strain $\underline{\underline{\varepsilon}}$ is applied to a solid in its equilibrium state, i.e. if all atoms of the solid are displaced by $(\underline{\underline{1}} + \underline{\underline{\varepsilon}})$, then a state of stress is invoked that forces the solid back into its unstrained shape. Similar to the stress, the strain is a second rank tensor. Its elements $\varepsilon_{\alpha\beta}$ describe the expansion or compression of the body along a certain direction (if $\alpha = \beta$) or a shear of the body perpendicular to the normals of a unit cube inside the solid (if $\alpha \neq \beta$).

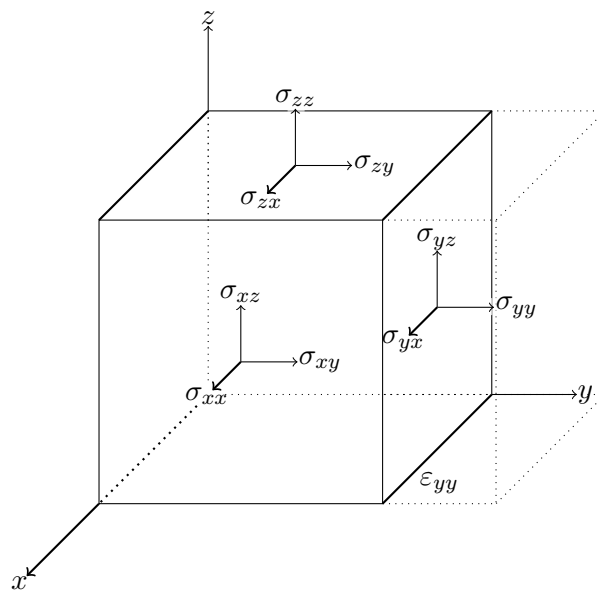


Figure 2.1.: Components of the stress tensor. On each face of the cube, stress can act perpendicular to the surface normal or parallel to it. E.g. the stress component σ_{yy} causes the cube to expand or to shrink by ε_{yy} .

2. Theoretical background

We define both quantities to be symmetric: Antisymmetric strain results in a transformation matrix, which is conceptually of the form

$$\begin{pmatrix} 1 & 0 & \varepsilon_{xz} \\ 0 & 1 & 0 \\ -\varepsilon_{xz} & 0 & 1 \end{pmatrix} \approx \begin{pmatrix} \cos(\varepsilon_{xz}) & 0 & \sin(\varepsilon_{xz}) \\ 0 & 1 & 0 \\ -\sin(\varepsilon_{xz}) & 0 & \cos(\varepsilon_{xz}) \end{pmatrix}.$$

This describes a rotation of the whole body, but no deformation. In turn, antisymmetric stress causes a rotation of the body. Hence, we discard antisymmetric stress and strain.

2.2. The many-body Hamiltonian

The most fundamental and impressive quality of a solid is that it has a variety of characteristics which are not featured by the single atoms the body is composed of. Electric conductivity as well as magnetism arise as collective properties of the particles in the system, while elasticity is a macroscopic property that cannot even be attributed to single atoms. The particles of a solid can be described by the Schrödinger equation

$$\mathcal{H}|\Psi\rangle = i\hbar\frac{\partial}{\partial t}|\Psi\rangle, \quad (2.1)$$

where the Hamiltonian expresses the motion of the particles:

$$\begin{aligned} \mathcal{H} &= -\sum_j \frac{\hbar^2}{2m_e} \nabla_j^2 - \sum_a \frac{\hbar^2}{2M_a} \nabla_a^2 \\ &\quad - \sum_{j,a} \frac{Z_a e^2}{|\mathbf{r}_j - \boldsymbol{\tau}_a|} + \frac{1}{2} \sum_{j,k}^{j \neq k} \frac{e^2}{|\mathbf{r}_j - \mathbf{r}_k|} + \frac{1}{2} \sum_{a,b}^{a \neq b} \frac{Z_a Z_b e^2}{|\boldsymbol{\tau}_a - \boldsymbol{\tau}_b|} \\ \stackrel{\text{Htr. units}}{=} &\quad -\sum_j \frac{1}{2} \nabla_j^2 - \sum_a \frac{1}{2\tilde{M}_a} \nabla_a^2 \\ &\quad - \sum_{j,a} \frac{Z_a}{|\mathbf{r}_j - \boldsymbol{\tau}_a|} + \frac{1}{2} \sum_{j,k}^{j \neq k} \frac{1}{|\mathbf{r}_j - \mathbf{r}_k|} + \frac{1}{2} \sum_{a,b}^{a \neq b} \frac{Z_a Z_b}{|\boldsymbol{\tau}_a - \boldsymbol{\tau}_b|} \end{aligned}$$

The second part of the equation is expressed in Hartree units, which will be used for the remainder of this thesis. In these units, the electron mass m_e as well as the elementary charge e , the reduced Planck's constant \hbar and Coulomb's constant $1/4\pi\epsilon_0$ are set to unity, leaving $\tilde{M}_a = M_a/m_e$ as the relative atomic mass of the nucleus of atom a . \mathbf{r}_j denotes the position of the j -th electron, while $\boldsymbol{\tau}_a$ is the position of the nucleus of atom a . Z_a is that nucleus' charge number. A solution to the Schrödinger equation 2.1 would be a function dependent on the spatial coordinates of all particles in the system and is as such only obtainable for very small systems.

Exploiting the fact that the nuclei are more massive than the electrons by at least three orders of magnitude, both move on different time scales. Due to that it is feasible to fix the atomic positions τ and regard their influence on the system under consideration as an external potential in which the electrons move. This approach is known as the Born-Oppenheimer approximation [BO27]. Still, all solutions of this simplified Schrödinger equation depend on the coordinates of all electrons and are parametrized by the atomic positions.

2.3. Density functional theory

A remedy to deal with the complexity of the aforementioned problem was given in the form of the Hohenberg-Kohn theorem [HK64], for which Kohn was awarded with the Nobel prize in 1998. Hohenberg and Kohn were able to prove that in order to obtain information on the ground state of the system, only the electronic density of the ground state needs to be known. This is a quantity dependent only on one spacial coordinate (i.e. x -, y -, and z -direction) in contrast to the dependencies of the wave functions and as such takes much less effort to be stored and handled. In their publication they recorded that

1. for a given configuration of atomic nuclei, the ground state energy $E[\rho]$ and all other ground state properties of the system are functionals of the electronic density $\rho(\mathbf{r})$ in a unique fashion and that
2. the ground state density $\rho_0(\mathbf{r})$ minimizes the energy functional, if one assumes a fixed number of charges in the system.

$$E[\rho] > E[\rho_0] \text{ for all } \rho(\mathbf{r}) \neq \rho_0(\mathbf{r})$$

Therefore, the theory is called density functional theory (DFT). The second statement allows by means of variational calculus to find the ground state of the system as minimizer to the energy functional, fulfilling

$$\delta E[\rho_0] = 0.$$

It is an integral part of proving the validity of DFT: Assume that ψ and ψ' are different ground states of two different systems with external potentials V_{ext} and V'_{ext} and that they form the same density $\rho = \langle \psi | \sum_i \delta(\mathbf{r} - \mathbf{r}_i) | \psi \rangle$. By the second statement, we see

$$\begin{aligned} E &= \langle \psi | \mathcal{H} | \psi \rangle < \langle \psi' | \mathcal{H} | \psi' \rangle = \langle \psi' | \mathcal{H}' - V'_{\text{ext}} + V_{\text{ext}} | \psi' \rangle \\ &= E' + \int \rho(\mathbf{r}) (V_{\text{ext}}(\mathbf{r}) - V'_{\text{ext}}(\mathbf{r})) d^3r. \end{aligned}$$

Doing the same analysis starting from E' and summing up both inequations, we find the contradiction

$$E + E' < E' + E.$$

2. Theoretical background

So according to their theorem, Hohenberg and Kohn showed that beyond the deduction of ρ by means of the external potential, $V_{\text{ext}} \rightarrow \psi_i \rightarrow \rho$ which is known from textbooks on quantum mechanics, the ground state density also identifies the external potential and in turn the whole Hamiltonian, leading to a direct map between both quantities,

$$V_{\text{ext}} \longleftrightarrow \rho. \quad (2.2)$$

This sketch, which follows closely the original publication of Hohenberg and Kohn, assumes that the ground state is not degenerate and that both external potentials differ by more than just a constant shift so different wave functions are generated.

DFT provides a relevant simplification for obtaining the properties of a solid. While the electronic density still needs to be found, it can now be obtained from a variational ansatz by minimizing the total energy. This avoids the necessity to use many-body wave functions.

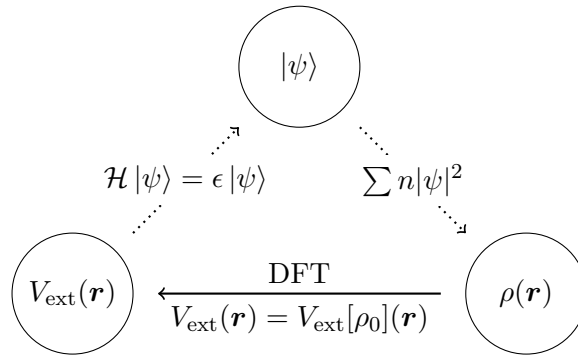


Figure 2.2.: The textbook way of quantum mechanics follows the top, dotted path. Given a potential $V_{\text{ext}}(\mathbf{r})$, one calculates the eigenfunctions of the corresponding Hamiltonian. The electron density $\rho(\mathbf{r})$ is then found as the sum of the eigenfunctions squares. The theorem of Hohenberg and Kohn allows for the lower path from the ground state density $\rho_0(\mathbf{r})$ to the potential, allowing all three quantities to be the starting point of quantum mechanical calculations and introducing the equivalence between ground state density and potential.

2.3.1. The Kohn-Sham System

In order to recast the Hamiltonian into a form that might be easier to use, Kohn and Sham [KS65] formulated the composition of the energy terms as

$$E[\rho] = T_{\text{ni}}[\rho] + U[\rho] + E_{\text{xc}}[\rho],$$

where T_{ni} denotes the kinetic energy of non-interacting electrons and $U[\rho]$ names the Coulomb energy arising from the interaction of the electrons with the nuclei, which pose

an external potential, as well as with all electrons, which is the Hartree expression:

$$\begin{aligned} U[\rho] &= E_{\text{ext}}[\rho] + E_H[\rho] \\ E_{\text{ext}}[\rho] &= \int \rho(\mathbf{r}) V_{\text{ext}}(\mathbf{r}) d^3r \\ E_H[\rho] &= \frac{1}{2} \iint \frac{\rho(\mathbf{r})\rho(\mathbf{s})}{|\mathbf{r} - \mathbf{s}|} d^3s d^3r \end{aligned}$$

Up to this point, the energy functional is rewritten as an expression for electrons that only interact by their Coulomb repulsion and which are exhibited to an external potential. The remaining term, the exchange-correlation functional $E_{\text{xc}}[\rho]$, formally accumulates the finer nuances that have to be considered when using quantum mechanics: In it, the errors made by assuming the electrons as non-interacting in the kinetic energy and the effects of exchange and correlation are subsumed.

The ground state density minimizes this energy functional as we learned in the previous section. Therefore, it fulfills

$$\frac{\delta T_{\text{ni}}}{\delta \rho(\mathbf{r})}[\rho] + \int_{\Omega} \frac{\rho(\mathbf{s})}{|\mathbf{r} - \mathbf{s}|} d^3s + V_{\text{ext}}(\mathbf{r}) + \frac{\delta E_{\text{xc}}}{\delta \rho(\mathbf{r})}[\rho] = 0.$$

This equation has the same form as one obtained for non-interacting particles moving in an effective potential

$$V_{\text{eff}}(\mathbf{r}) = \int_{\Omega} \frac{\rho(\mathbf{s})}{|\mathbf{r} - \mathbf{s}|} d^3s + V_{\text{ext}}(\mathbf{r}) + \mu_{\text{xc}}(\mathbf{r}).$$

Comparing both equations shows that the exchange-correlation potential is given as

$$\mu_{\text{xc}}(\mathbf{r}) = \frac{\delta E_{\text{xc}}}{\delta \rho(\mathbf{r})}[\rho] = \frac{\delta}{\delta \rho(\mathbf{r})} (\rho(\mathbf{r}) \varepsilon_{\text{xc}}[\rho](\mathbf{r})). \quad (2.3)$$

The term $\varepsilon_{\text{xc}}(\mathbf{r})$ represents the exchange-correlation energy density and is such that

$$E_{\text{xc}} = \int \rho(\mathbf{r}) \varepsilon_{\text{xc}}[\rho](\mathbf{r}) d^3r.$$

Using this approach, the density of the original problem can be constructed by solving an auxiliary single particle Schrödinger equation as

$$\left(-\frac{1}{2} \nabla^2 + V_{\text{eff}}(\mathbf{r}) \right) \psi_i(\mathbf{r}) = \epsilon_i \psi_i(\mathbf{r}). \quad (2.4)$$

and then forming the sum of squares of as many Kohn-Sham wave functions as there are electrons in the system, i.e. the sum over all occupied states,

$$\rho(\mathbf{r}) = 2 \sum_i^N n_i |\psi_i(\mathbf{r})|^2, \quad (2.5)$$

2. Theoretical background

where n_i is the occupancy of the state i .

However, as the effective potential in turn depends on the density again, the last two equations have to be solved self-consistently. After application of a convergence scheme from an initial guess for ρ_0 (for example a Broyden mixing [Bro65]), the ground state energy and density meet

$$E_0 = E[\rho_0] = T_{\text{ni}}[\rho_0] + U[\rho_0] + \int \rho_0 V_{\text{ext}}(\mathbf{r}) d^3r + E_{\text{xc}}[\rho_0] \text{ and} \quad (2.6)$$

$$\rho_0(\mathbf{r}) = 2 \sum_i n_i |\psi_i(\mathbf{r})|^2. \quad (2.7)$$

The success of this formalism is based on the observation that the difference between both kinetic energies, the one for the original many body system and the one for the non-interacting particles, is comparably small, as is the contribution from exchange and correlation. By this, the non-interacting system already copes a significant part of the relevant energies, whereas the exchange-correlation functional corrects the energies on a smaller scale.

One should be aware however, that the Kohn-Sham eigenfunctions and their eigenvalues do not actually have a physical meaning. They are merely a means to obtain the density of the system in an easy fashion.

Given the ground state density, we can now formulate the total energy per unit cell Ω of a solid with atoms a placed at $\boldsymbol{\tau}_a$:

$$\begin{aligned} E &= E_{\text{kin}} + E_{\text{xc}} + E_{\text{ee}} + E_{\text{ie}} + E_{\text{ii}} \\ &= \sum_i n_i \epsilon_i - \int_{\Omega} \rho_0(\mathbf{r}) V_{\text{eff}}(\mathbf{r}) d^3r + \int_{\Omega} \rho_0(\mathbf{r}) \varepsilon_{\text{xc}}(\mathbf{r}) d^3r \\ &\quad + \frac{1}{2} \int_{\Omega} \rho_0(\mathbf{r}) \left\{ \int_{\mathbb{R}^3} \frac{\rho_0(\mathbf{s})}{|\mathbf{r} - \mathbf{s}|} d^3s - \sum_b^{\text{atoms}} \frac{Z_b}{|\mathbf{r} - \boldsymbol{\tau}_b|} \right\} d^3r \\ &\quad - \frac{1}{2} \sum_{a \in \Omega}^{\text{atoms}} Z_a \left\{ \int_{\mathbb{R}^3} \frac{\rho_0(\mathbf{s})}{|\boldsymbol{\tau}_a - \mathbf{s}|} d^3s - \sum_{b \neq a}^{\text{atoms}} \frac{Z_b}{|\boldsymbol{\tau}_a - \boldsymbol{\tau}_b|} \right\} \end{aligned} \quad (2.8)$$

The kinetic energy is expressed in this equation as the sum of the Kohn-Sham eigenvalues minus a double counting term. This term is the integral of the electronic density times the effective potential, leaving us with the expression we are looking for. This way to express the kinetic energy is convenient as the Kohn-Sham eigenvalues and the integral containing the electronic density and the effective potential already are quantities easily obtainable from DFT calculations. Furthermore, applying DFT in computational physics, we want to note that a differential operator roughens the function it is applied to, possibly making a numerical description of the functions derivative difficult.

For the remainder of this thesis, we assume that we already have found the ground state density and hence we drop the index 0.

2.3.2. The exchange-correlation functional

The scheme presented so far is exact in principle. However, the actual form of the exchange-correlation energy functional is not known. It is only known that the xc energy density is a functional of the electronic density, making the energy density and potential deviate from each other following (2.3).

In the local density approximation (LDA), ε_{xc} becomes a mere function of the electronic density, making it - as the name suggest - a local approximation. Because it does not vary at all, the density of the homogeneous electron gas (HEG) acts as a model for this approach for systems with a spatially slowly varying density. Even though this approximation is rather crude for computing the properties of a solid, where the density is heavily influenced by the atomic nuclei, it produces surprisingly good results for certain materials. It is believed that the reason for this is the construction of the LDA after an actual physical system. Due to this, the LDA functional automatically respects some conditions that are posed to such a physical system.

The generalized gradient approximation (GGA), another local approximation to the exchange-correlation functional, adds the gradient of the electronic density to the computation of the xc energy density and potential. As the gradient of a function at a certain point contains information on the vicinity of that point, its inclusion should cause an implicit augmentation regarding the non-locality of the real exchange-correlation functional. Therefore, GGA functionals are often called semi-local, even though their exchange-correlation energy density and potential are evaluated only at \mathbf{r} .

A whole zoo of approximations to the xc functional exists, even within the LDA [vBH72, CA80, VWN80, PZ81, CP82, PW92] and GGA [PW86, WP91, PBE96], where the methods to deal with the correlation part or the inclusion of the density gradient are manifold. Yet more sophisticated methods add explicit non-locality as is done with the orbital dependent hybrid functionals [HSE03, BFB10, SBF⁺11], while others deal with exact exchange [Bet11].

We will restrict ourselves to the local density and generalized gradient approximations, though. Both can be described on a similar theoretical footing since their locality allows for certain simplifications. Their explicit expressions will be of no concern to us.

3. Electronic structure methods

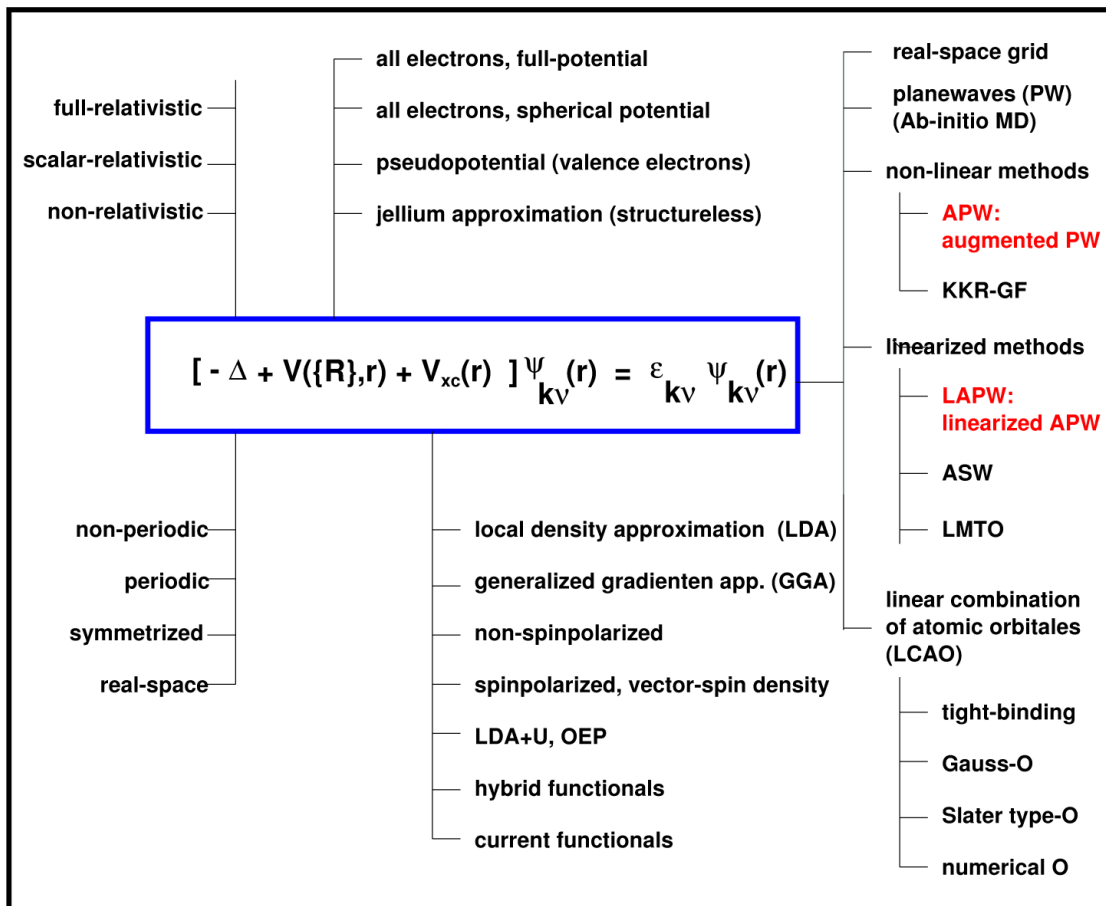


Figure 3.1.: Schematic overview over electronic structure methods. Different parts of the Schrödinger equation can be handled by different techniques. The techniques are chosen with respect to the problem under consideration. [BB06]

As the introductory figure 3.1 indicates, there exists a vast spectrum of methods to perform an electronic structure calculation. Those methods are crafted to fulfill certain needs on the specific topic one wishes to study.

We are interested in solids and the periodicity of a crystalline structure allows the application of Bloch's theorem [Blo28]. Then, the solution of the auxiliary Schrödinger

3. Electronic structure methods

equation are of the form

$$\psi_{i\mathbf{k}}(\mathbf{r}) = e^{i\mathbf{k}\cdot\mathbf{r}} u_{i\mathbf{k}}(\mathbf{r}) \quad (3.1)$$

at each point \mathbf{k} in the first Brillouin zone and we can limit ourselves to the unit-cell volume Ω . The function $u_{i\mathbf{k}}(\mathbf{r})$ has the same periodicity as the crystal potential. Since for each reciprocal lattice vector \mathbf{G} , the plane wave $e^{i\mathbf{G}\cdot\mathbf{r}}$ has the correct periodicity, we can expand $u_{i\mathbf{k}}(\mathbf{r})$ and consequently $\psi_{i\mathbf{k}}(\mathbf{r})$ into plane waves of reciprocal lattice vectors,

$$u_{i\mathbf{k}}(\mathbf{r}) = \sum_{\mathbf{G}} \hat{u}_{i\mathbf{k}}(\mathbf{G}) e^{i\mathbf{G}\cdot\mathbf{r}} \quad \text{and} \quad (3.2)$$

$$\psi_{i\mathbf{k}}(\mathbf{r}) = \sum_{\mathbf{G}} z_{i\mathbf{k}\mathbf{G}} \phi_{\mathbf{k}\mathbf{G}}(\mathbf{r}), \quad \text{with} \quad (3.3)$$

$$\phi_{\mathbf{k}\mathbf{G}}(\mathbf{r}) = \frac{1}{\sqrt{\Omega}} e^{i(\mathbf{k}+\mathbf{G})\cdot\mathbf{r}}. \quad (3.4)$$

Plane waves are a convenient choice because the kinetic energy operator becomes diagonal in reciprocal space, whereas the potential is diagonal in real space. Thus, one can reformulate the Kohn-Sham equation (2.4), which is a differential equation of second order, as an algebraic (generalized) eigenvalue problem:

$$\sum_{\mathbf{G}} H_{\mathbf{G}'\mathbf{G}}(\mathbf{k}) z_{i\mathbf{k}\mathbf{G}} = \epsilon_i(\mathbf{k}) \sum_{\mathbf{G}} S_{\mathbf{G}'\mathbf{G}}(\mathbf{k}) z_{i\mathbf{k}\mathbf{G}} \quad (3.5)$$

The Hamilton and overlap matrices are given as

$$H_{\mathbf{G}'\mathbf{G}}(\mathbf{k}) = \int_{\Omega} \phi_{\mathbf{k}\mathbf{G}'}^*(\mathbf{r}) \left\{ -\frac{1}{2} \nabla^2 + V_{\text{eff}}(\mathbf{r}) \right\} \phi_{\mathbf{k}\mathbf{G}}(\mathbf{r}) d^3r \quad \text{and} \quad (3.6)$$

$$S_{\mathbf{G}'\mathbf{G}}(\mathbf{k}) = \int_{\Omega} \phi_{\mathbf{k}\mathbf{G}'}^*(\mathbf{r}) \phi_{\mathbf{k}\mathbf{G}}(\mathbf{r}) d^3r. \quad (3.7)$$

In the case of plane waves, the overlap matrix is the identity matrix. Thus we see that expanding the solutions of the Kohn-Sham equation into plane waves would in general yield a complete and sufficient representation to find the Kohn-Sham states and their eigenvalues.

However, the number of plane waves one can practically include into electronic structure calculations is limited. That by itself would not pose much of a problem if one could include just as many basis functions as one would need for a decent approximation of the real solution. But in the vicinity of the $1/r$ potential created by the atomic nuclei, the cut-off in the number of basis functions would have to be increased drastically to achieve convergence to the actual solution, up to the point where a computation is not feasible any more. To remedy this behavior, there exist pseudo potential methods, replacing the divergent potential of the atomic nuclei and tightly bound core-electron states by a smooth potential fitted to reproduce good approximations to the chemically important valence states.

We want to include all electrons in the description, though. Therefore, this chapter comprises of an introduction to the all-electron full-potential linearized augmented plane wave method (FLAPW) and we will present the steps taken to obtain this method starting from the simple plane waves we found.

3.1. The APW method

The first augmentation to the use of plane waves distinguishes between the space far away from the atomic nuclei and the space in the vicinity of the atoms. In the former region, the so called interstitial (IS), the potential does not exhibit features that would compromise the use of plane waves for the basis and is approximated as a constant. The near-atom sites are taken as spheres $B_{R_a}(\boldsymbol{\tau}_a)$ around the atomic positions $\boldsymbol{\tau}_a$ of a certain radius R_a . Inside those so called muffin-tins (MT_a), the potential is considered to be spherical and a corresponding solution to the Schrödinger equation are radial functions times spherical harmonics. Both solutions are then matched at the muffin-tin boundary.

This approach was suggested by Slater [Sla37] and is known as the augmented plane wave (APW) method. Beyond the shape approximations to the potential, it is a method distinctively crafted to give a physically appropriate description of the auxiliary basis set. The basis then is

$$\phi_{\mathbf{k}\mathbf{G}}(\mathbf{r}) = \begin{cases} \frac{1}{\sqrt{\Omega}} e^{i(\mathbf{k}+\mathbf{G})\cdot\mathbf{r}} & , \mathbf{r} \in \text{IS} \\ \sum_{lm} a_{lm}^{a\mathbf{k}\mathbf{G}} u_l^a(r_a, E_l^a) Y_{lm}(\hat{\mathbf{r}}_a) & , \mathbf{r} \in \text{MT}_a \end{cases} \quad (3.8)$$

with $\mathbf{r}_a = \mathbf{r} - \boldsymbol{\tau}_a$ being the spatial vector relative to the position of the a -th nucleus. The matching coefficients are found to be

$$a_{lm}^{a\mathbf{k}\mathbf{G}} = \frac{4\pi i^l}{\sqrt{\Omega}} e^{i(\mathbf{k}+\mathbf{G})\cdot\boldsymbol{\tau}_a} Y_{lm}^*(\widehat{\mathbf{k}+\mathbf{G}}) \frac{j_l(|\mathbf{k}+\mathbf{G}|R_a)}{u_l^a(R_a, E_l^a)}$$

and the radial functions u solve

$$\left\{ -\frac{d^2}{dr_a^2} + \frac{l(l+1)}{r_a^2} + V_{\text{eff}00}^a(r_a) - E_l^a \right\} r_a u_l^a(r_a, E_l^a) = 0. \quad (3.9)$$

The E_l are atom specific energy parameters and $Y_{lm}(\hat{\mathbf{r}}_a)$ is a spherical harmonic. $j_l(r)$ are spherical Bessel functions. $V_{\text{eff}00}^a(r_a)$ finally describes the spherical part of the potential around the nucleus at $\boldsymbol{\tau}_a$.

The construction of the radial functions u_l implies that each solution of (3.9) is orthogonal to all other solutions \tilde{u}_l , that are zero at the sphere boundary and beyond. To prove this, multiply the corresponding radial Schrödinger equations by r times the other function and subtract them from each other.

$$\left\{ \tilde{E}_l - \frac{l(l+1)}{r^2} - E_l + \frac{l(l+1)}{r^2} \right\} r^2 u_l \tilde{u}_l = r \tilde{u}_l \frac{d^2}{dr^2} r u_l - r u_l \frac{d^2}{dr^2} r \tilde{u}_l$$

3. Electronic structure methods

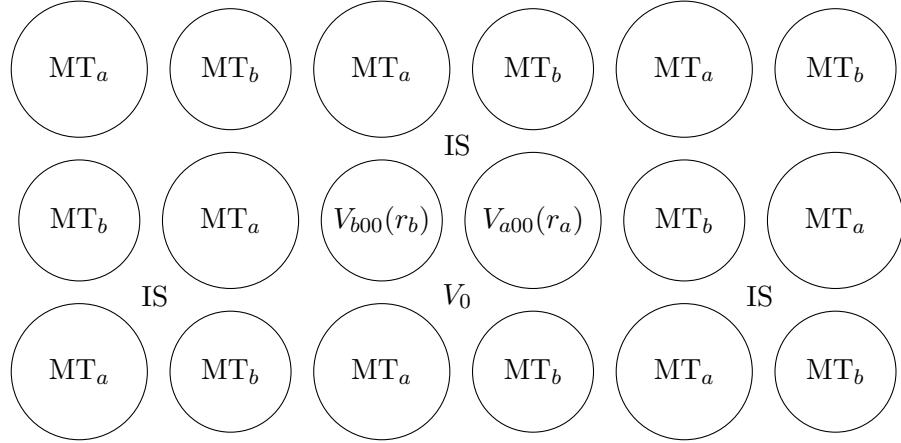


Figure 3.2.: Division of space into an interstitial region between the atomic sites (IS) and spheres centered at the atomic nuclei, the so-called muffin-tin spheres (MT). In the APW method, the interstitial potential is a constant V_0 while the potential in the muffin-tin spheres is spherical with a radial function $V_{00}(r)$.

Integration results in a multiple of the scalar product between u_l and \tilde{u}_l on the left side. The right side becomes after integration by parts

$$\begin{aligned}
 & (\tilde{E}_l - E_l)(u_l, \tilde{u}_l) \\
 & = [r\tilde{u}_l(ru_l)' - ru_l(r\tilde{u}_l)']_0^{R_{\text{MT}}} - \int_0^{R_{\text{MT}}} [(r\tilde{u}_l)'(ru_l)'] - [(ru_l)'(r\tilde{u}_l)'] dr = 0. \quad (3.10)
 \end{aligned}$$

The last equality holds as \tilde{u}_l vanishes at the muffin-tin boundary and beyond, which implies that \tilde{u}_l' , too, vanishes at the muffin-tin boundary. This orthogonality indicates that the space spanned by the APW basis functions does not include states low in energy which are highly localized around the atomic nuclei and which decrease rapidly towards the sphere boundary. Those core states are accounted for separately by solving (3.9). Since the core states are confined within the muffin-tin spheres and don't contribute to chemical bonds, this description already is an adequate representation for them. Hence, the core states do not need to be expanded into a basis.

The energy parameter E_l is a difficulty of the APW method:

First, radial functions that vanish at the muffin-tin boundary will decouple with the plane wave representation of the basis in the interstitial as they appear in the denominator of the matching coefficients a_{lm} evaluated at their zero. This is known as the asymptote problem. Choosing the energies accordingly to prevent zeros of the radial functions at the sphere boundaries circumvents the problem but restricts the choice of energy parameters.

Secondly, fixing the energy parameters at all makes the method impractical: To obtain a good representation of the Kohn-Sham states, the energy parameters would have to be chosen at the band energies of those states. However, those band energies are unknown at this point and in fact they are the quantities that one wants to calculate.

Usually, the E_l are taken as a variational degree of freedom instead. Then their evaluation becomes a non-linear problem and it cannot be found by a simple diagonalization of the Hamiltonian with respect to the basis.

3.2. The LAPW method

In order to obtain a higher variational freedom of the basis functions and to reduce the dependence on the energy parameters E_l , Anderson [And75] proposed to include into the muffin-tin description of the basis the energy derivative of the radial functions, given by differentiating (3.9) with respect to the energy parameter:

$$\left\{ -\frac{d^2}{dr_a^2} + \frac{l(l+1)}{r_a^2} + V_{\text{eff}00}^a(r_a) - E_l^a \right\} r_a \dot{u}_l^a(r_a, E_l^a) = r_a u_l^a(r_a, E_l^a) \quad (3.11)$$

The basis functions then are constructed by matching the muffin-tin representation to the plane waves at the sphere boundaries up to first order in the radial variable.

$$\phi_{\mathbf{k}\mathbf{G}}(\mathbf{r}) = \begin{cases} \frac{1}{\sqrt{\Omega}} e^{i(\mathbf{k}+\mathbf{G})\cdot\mathbf{r}} & , \mathbf{r} \in \text{IS} \\ \sum_{lm} [a_{lm}^{a\mathbf{k}\mathbf{G}} u_l^a(r_a, E_l^a) + b_{lm}^{a\mathbf{k}\mathbf{G}} \dot{u}_l^a(r_a, E_l^a)] Y_{lm}(\hat{\mathbf{r}}_a) & , \mathbf{r} \in \text{MT}_a \end{cases} \quad (3.12)$$

Again, one can show the orthogonality of the radial functions to core states as was done in (3.10), because only properties of the radial function \tilde{u}_l describing a core state were used.

The matching coefficients are given as

$$\begin{pmatrix} a_{lm}^{a\mathbf{k}\mathbf{G}} \\ b_{lm}^{a\mathbf{k}\mathbf{G}} \end{pmatrix} = \frac{4\pi l^l}{\sqrt{\Omega}} e^{i(\mathbf{k}+\mathbf{G})\cdot\boldsymbol{\tau}_a} Y_{lm}^*(\widehat{\mathbf{k}+\mathbf{G}}) \underline{\underline{U}}^{-1} \begin{pmatrix} j_l(|\mathbf{k}+\mathbf{G}|R_a) \\ |\mathbf{k}+\mathbf{G}| j_l'(|\mathbf{k}+\mathbf{G}|R_a) \end{pmatrix}. \quad (3.13)$$

Using the abbreviation $W_l^a(R_a, E_l^a) = u_l^a(R_a, E_l^a) \dot{u}_l^{a'}(R_a, E_l^a) - \dot{u}_l^a(R_a, E_l^a) u_l^{a'}(R_a, E_l^a)$ for the Wronskian determinant, the matrix $\underline{\underline{U}}^{-1}$ is

$$\underline{\underline{U}}^{-1} = \frac{1}{W_l^a(R_a, E_l^a)} \begin{pmatrix} \dot{u}_l^{a'}(R_a, E_l^a) & -\dot{u}_l^a(R_a, E_l^a) \\ -u_l^{a'}(R_a, E_l^a) & u_l^a(R_a, E_l^a) \end{pmatrix}. \quad (3.14)$$

The idea behind taking the energy derivative of the radial function into consideration becomes obvious by Taylor-expanding the radial function around the band energy ϵ :

$$u_l^a(r_a, \epsilon) = u_l^a(r_a, E_l^a) + (\epsilon - E_l^a) \dot{u}_l^a(r_a, E_l^a) + O((\epsilon - E_l^a)^2)$$

Including \dot{u}_l enables valid approximations of $u_l(\epsilon)$ if E_l is chosen to be not too far away from the band energy in contrast to the necessity to hit the band energy on spot. The

3. Electronic structure methods

error made in the wave functions, being of the order of $O((\epsilon - E_l)^2)$, is passed on to the band energies. Choosing those parameters in the middle of an energy window one is interested in should therefore result in decent band structures.

The asymptote problem does not arise in the case of LAPWs as the Wronskian does not vanish at the muffin-tin boundary. This can be proven by multiplying (3.9) and (3.11) of the same l -value with r times the other radial function and subtracting both equations from each other. Integration then gives:

$$\begin{aligned} 1 &= \int_0^{R_a} r^2 u_l^2 dr = \int_0^{R_{\text{MT}}} \left[r \dot{u}_l \frac{d^2}{dr^2} r u_l - r u_l \frac{d^2}{dr^2} r \dot{u}_l \right] dr \\ &= [r \dot{u}_l (r u_l)' - r u_l (r \dot{u}_l)']_0^{R_{\text{MT}}} \\ &= R_{\text{MT}}^2 [\dot{u}_l u_l' - u_l \dot{u}_l'] \end{aligned}$$

The LAPW basis in the muffin-tin spheres depends on \mathbf{G} only through the matching coefficients a and b . Therefore, we can write

$$\begin{aligned} \psi_{i\mathbf{k}}(\mathbf{r})|_{\mathbf{r} \in \text{MT}_a} &= \sum_{\mathbf{G}} z_{i\mathbf{k}\mathbf{G}} \sum_L \left(a_{lm}^{a\mathbf{k}\mathbf{G}} u_l^a(r_a) + b_{lm}^{a\mathbf{k}\mathbf{G}} \dot{u}_l^a(r_a) \right) Y_L(\hat{\mathbf{r}}_a) \\ &= \sum_L \left(A_{lm}^{a\mathbf{k}} u_l^a(r_a) + B_{lm}^{a\mathbf{k}} \dot{u}_l^a(r_a) \right) Y_L(\hat{\mathbf{r}}_a), \end{aligned} \quad (3.15)$$

defining the capital A and B coefficients as

$$A \setminus B_{lm}^{a\mathbf{k}} = \sum_{\mathbf{G}} z_{i\mathbf{k}\mathbf{G}} a \setminus b_{lm}^{a\mathbf{k}\mathbf{G}}. \quad (3.16)$$

Since we will deal with charge densities, the product of two wave functions will have to be calculated. This results in a lengthy formula. For the sake of brevity, we also introduce an index λ which moderates between the quantities belonging to the radial function and its energy derivative for use in the stress chapter:

$$\psi_{i\mathbf{k}}(\mathbf{r})|_{\mathbf{r} \in \text{MT}_a} = \sum_L \sum_{\lambda=0}^1 A_{L\lambda}^{a\mathbf{k}} u_{l\lambda}^a(r_a) Y_L(\hat{\mathbf{r}}_a) \quad (3.17)$$

The assignment of λ is given by

$$A_{L0}^{a\mathbf{k}} u_{l0}^a(r_a) = A_L^{a\mathbf{k}} u_l^a(r_a) \quad (3.18a)$$

$$A_{L1}^{a\mathbf{k}} u_{l1}^a(r_a) = B_L^{a\mathbf{k}} \dot{u}_l^a(r_a). \quad (3.18b)$$

Seeing that the addition of \dot{u} into the calculations increases the flexibility of the basis and thus the efficiency of the method comparing accuracy and complexity, one might be led to conclude that the inclusion of further energy derivatives should bring even more advantages. This is not observed in practice, which is plausible remembering that the inclusion of more energy derivatives makes a matching to higher order necessary

as well. There are two ways to describe an arbitrary smooth function. One way, by the mathematical definition of a function, is to map each of the uncountable many points of the set on which the function is defined onto its image. The other way makes use of the Taylor expansion and identifies the functions by the just countable many expansion coefficients in front of the monomials x^n . As these coefficients are basically the derivatives of the function, this indicates that defining a function by its derivatives is indeed a strong condition.

While adding the first energy derivative into the calculations increases the flexibility in describing the Kohn-Sham states inside the muffin-tin spheres by allowing to deviate from the band energy, adding more derivatives thus fixates the resulting function too firm. The error made around the energy parameter decreases, but in order to retain the variational flexibility to describe the physical system, more basis functions are needed.

3.3. The FLAPW method

In order to drop the shape approximations in the description of the crystal potential and to include its full form into the LAPW method, it seems natural to mimic the twofold description of the wave functions by describing the density and the original potential inside the muffin-tin spheres and the interstitial region on a different footing as well. To that end, the interstitial representation of both quantities is done by an expansion into plane waves, i.e. a Fourier transformation. As the charge density is the square of the wave functions and the reciprocal lattice-vectors form a group, the charge density takes the form

$$\begin{aligned} \rho(\mathbf{r}) &= \sum_{i\mathbf{k}\mathbf{G}\mathbf{G}'} n_{i\mathbf{k}} \frac{z_{i\mathbf{k}\mathbf{G}}^* z_{i\mathbf{k}\mathbf{G}'}}{\Omega} e^{-i(\mathbf{k}+\mathbf{G})\cdot\mathbf{r}} e^{i(\mathbf{k}+\mathbf{G}')\cdot\mathbf{r}} \\ &= \sum_{\mathbf{G}'} \left(\sum_{i\mathbf{k}} \frac{n_{i\mathbf{k}}}{\Omega} \sum_{\mathbf{G}} z_{i\mathbf{k}\mathbf{G}}^* z_{i\mathbf{k}(\mathbf{G}'+\mathbf{G})} \right) e^{i\mathbf{G}'\cdot\mathbf{r}} = \sum_{\mathbf{G}} \hat{\rho}(\mathbf{G}) e^{i\mathbf{G}\cdot\mathbf{r}}. \end{aligned} \quad (3.19)$$

The interstitial description of the potential is more complicated since the Coulomb potential part demands for inclusion of the strongly varying muffin-tin contributions as well. For an accurate description of the interstitial potential, many plane waves would be needed. In section 3.3.3, a detailed formulation of the electrostatic potential will be given that circumvents the need for an excessive amount of plane waves.

3. Electronic structure methods

Inside a muffin-tin, the wave functions are given as an expansion into spherical harmonics. The density around atom a then is expressed by

$$\begin{aligned} \rho^a(\mathbf{r}_a) = & \sum_{st} Y_{st}(\hat{\mathbf{r}}_a) \left[\sum_{i\mathbf{k}} n_{i\mathbf{k}} \sum_{Glm} \sum_{G'l'm'} z_{i\mathbf{k}G}^* z_{i\mathbf{k}G'} \oint Y_{st}^* Y_{lm} Y_{l'm'} dS_2 \right. \\ & \times \left\{ a_{lm}^{a\mathbf{k}G^*} a_{l'm'}^{a\mathbf{k}G'} u_l(r_a) u_{l'}(r_a) + b_{lm}^{a\mathbf{k}G^*} a_{l'm'}^{a\mathbf{k}G'} \dot{u}_l(r_a) u_{l'}(r_a) \right. \\ & \left. \left. + a_{lm}^{a\mathbf{k}G^*} b_{l'm'}^{a\mathbf{k}G'} u_l(r_a) \dot{u}_{l'}(r_a) + b_{lm}^{a\mathbf{k}G^*} b_{l'm'}^{a\mathbf{k}G'} \dot{u}_l(r_a) \dot{u}_{l'}(r_a) \right\} \right] \\ & + \rho_{\text{core}}^a(r_a) Y_{00}(\hat{\mathbf{r}}_a) = \sum_{st} \rho_{st}^a(r_a) Y_{st}(\hat{\mathbf{r}}_a). \end{aligned} \quad (3.20)$$

The muffin-tin potential is similarly given by

$$V^a(\mathbf{r}_a) = \sum_{st} V_{st}^a(r_a) Y_{st}(\hat{\mathbf{r}}_a). \quad (3.21)$$

Its exact form is obtained by solving a Dirichlet boundary value problem. However, knowledge of the interstitial potential is necessary to set up the boundary values. For that reason, we postpone the exact formulas to section 3.3.3, too.

The storage and computational demands to handle the density and potential can be simplified by exploiting lattice symmetries of the solid under consideration. Using these symmetries, several basis functions of the aforementioned expansions can be merged. In case of the plane waves, the symmetrized version is called a star and the spherical harmonics condense to lattice harmonics. We will give an overview over these representations, but we wish to note a critical thing:

Straining the system can explicitly change the symmetry properties of a solid. While stars and lattice harmonics are a good representation to calculate quantities of a system of fixed shape, they are impractical to describe a configuration that is intended to relax according to the stress acting upon it.

Therefore, the next sections mainly will serve as a map between the two forms of representation stars vs. plane waves and lattice harmonics vs. spherical harmonics.

3.3.1. Stars as symmetrized plane waves

A crystal lattice is invariant under its N_{op} space group operations $\{\underline{R}|\underline{\mathbf{t}}\}$. \underline{R} are the rotations of the space group and $\underline{\mathbf{t}}$ are its (non-symmorphic) translations.

$$\{\underline{R}|\underline{\mathbf{t}}\} \mathbf{r} = \underline{R}\mathbf{r} + \underline{\mathbf{t}}$$

This suggests that the description of density and potential of the system along certain directions should stand in some kind of relation.

A star relates plane waves to other plane waves that share a space group equivalent reciprocal lattice vector via

$$\Phi_s(\mathbf{r}) = \frac{1}{N_{op}} \sum_{\underline{R}} e^{i\underline{R}\mathbf{G}_s \cdot (\mathbf{r} - \mathbf{t}_{\underline{R}})}.$$

Onto a representative reciprocal lattice vector \mathbf{G}_s , all space group operations are applied and the results are summed up. Especially those \mathbf{G}_s on high-symmetry directions will reproduce the same reciprocal lattice vector more than once, making this representation more elaborate than necessary for our purposes. Instead, a form can be chosen that sums only once over the m_s distinct plane waves the star is composed of:

$$\Phi_s(\mathbf{r}) = \frac{1}{m_s} \sum_{\mathbf{G}: \mathbf{G} = \underline{R}\mathbf{G}_s \text{ for some } \underline{R}} \phi_{\mathbf{G}} e^{i\mathbf{G} \cdot \mathbf{r}}$$

The occurrence of multiple space group rotations that map the representative vector \mathbf{G}_s onto the same \mathbf{G} is accounted for in the phase factors

$$\phi_{\mathbf{G}} = \frac{m_s}{N_{op}} \sum_{\underline{R}: \underline{R}\mathbf{G}_s = \mathbf{G}} e^{-i\mathbf{G} \cdot \mathbf{t}_{\underline{R}}}.$$

If a plane wave \mathbf{G} is part of a star, it cannot be part of another star due to the group properties of the space group: Assuming \mathbf{G} would be contained in the stars 1 and 2, there exist operations which map the representatives of the stars onto $\mathbf{G} = \underline{R}_1\mathbf{G}_1 = \underline{R}_2\mathbf{G}_2$. Then $\underline{R}_1^{-1}\underline{R}_2$ maps between \mathbf{G}_1 and \mathbf{G}_2 and is an operation of the space group again, making both representatives belong to the same star.

To a star, only plane waves with the same $|\mathbf{G}|$ contribute. The operations \underline{R} preserve the length of a vector when operating on it. This does not imply that all plane waves with the same $|\mathbf{G}|$ are part of the same star.

Thinning out the number of basis functions for the representation of charge and potential by merging them can only decrease the number of effective basis functions, never raise it. In lattices with a high symmetry, the number of stars is much smaller than the number of single plane waves.

Furthermore, each function with the same symmetry as the lattice from which the stars are formed can be expanded in stars, as they are orthogonal:

$$\frac{1}{\Omega} \int_{\Omega} \Phi_s^*(\mathbf{r}) \Phi_{s'}(\mathbf{r}) d^3r = \frac{1}{m_s} \delta_{ss'}$$

The relation between star expansion coefficients and coefficients from a plane wave expansion is in terms of a phase factor.

$$f(\mathbf{r}) = \sum_{\mathbf{G}} \hat{f}(\mathbf{G}) e^{i\mathbf{G} \cdot \mathbf{r}} = \sum_s f_s \frac{1}{m_s} \sum_{\mathbf{G}: \mathbf{G} = \underline{R}\mathbf{G}_s} \phi_{\mathbf{G}} e^{i\mathbf{G} \cdot \mathbf{r}}$$

3. Electronic structure methods

Since the star containing a reciprocal lattice vector is unique, comparison between both representations gives:

$$\hat{f}(\mathbf{G}) = \delta_{s\mathbf{G}} \frac{1}{m_s} \phi_{\mathbf{G}} f_s \text{ or } f_s = m_s \cdot \delta_{s\mathbf{G}} \phi_{\mathbf{G}}^* \hat{f}(\mathbf{G})$$

The Kronecker delta indicates that only \mathbf{G} vectors from the Fourier transformation must be included that belong to the star s . So, if one has given the coefficients of a star expansion, the coefficients of a plane wave expansion can be obtained by looping over all plane waves, finding the star that plane wave is part of, multiplying the phase factor $\phi_{\mathbf{G}}$ to the star coefficient and weighting it by the number of plane waves in that particular star.

3.3.2. Lattice harmonics

The expansion of the density and potential inside the muffin-tin spheres is in terms of spherical harmonics. As with the stars, a high symmetry of the crystal lattice allows for some spherical harmonics to be combined into a symmetrized basis function, the lattice harmonic $K_{\nu}^a(\hat{\mathbf{r}}_a)$. The coordinate origin of each lattice harmonic is at an atom site $\boldsymbol{\tau}_a$ and the coordinates are given relative to this origin. Thus, instead of the full set of space group operations, only those symmetry operations can be taken into account that do not alter the atomic position. The lattice harmonics are constructed to be real and orthonormal and a more detailed overview regarding their synthesis can be found e.g. in the book of Singh [Sin94]. They take the form

$$K_{\nu}^a(\hat{\mathbf{r}}_a) = \sum_m c_{\nu m_{\nu}}^a Y_{l_{\nu} m_{\nu}}(\hat{\mathbf{r}}_a).$$

Only the m and explicitly not the l components of a set of spherical harmonics can be combined as the operations, which allow for the relevant atomic position to be fixed, only consist of rotations. Rotating the argument of a spherical harmonic leaves its l component unchanged, but mixes up several m components. This does not imply that each spherical harmonic with the same l quantum number is contained in the same lattice harmonic.

As they are orthonormal by construction, each function that shares its symmetries with the local symmetry of a lattice site can be expanded into lattice harmonics. Comparing the spherical and lattice harmonic expansions of such a function, we find the map between both representations:

$$f(\mathbf{r}_a) = \sum_{lm} f_{lm}(r_a) Y_{lm}(\hat{\mathbf{r}}_a) = \sum_{\nu} f_{\nu}(r_a) K_{\nu}^a(\hat{\mathbf{r}}_a) = \sum_{\nu m_{\nu}} c_{\nu m_{\nu}}^a f_{\nu}(r_a) Y_{l_{\nu} m_{\nu}}(\hat{\mathbf{r}}_a)$$

This indicates that the radial functions are connected by

$$f_{lm}(r_a) = c_{\nu m_{\nu}}^a f_{\nu}(r_a) \delta_{l_{\nu} l} \delta_{m m_{\nu}}.$$

3.3.3. The Weinert method

To restate the reason for this section, let us briefly repeat the problem posed by the representation of the interstitial potential in terms of plane waves: While the electrostatic potential from the interstitial charge density can be described reasonably well by plane waves, the $1/r$ singularities and the resulting density at the atomic sites inside the muffin-tin spheres demand for an extensive number of plane waves to be included into the basis. This would cause a straight-forward calculation to be computationally expensive.

Weinert [Wei81] solved this problem of constructing the interstitial potential by replacing the muffin-tin density with a more convenient one. In a nutshell, the idea behind this trick is, that in order to calculate the potential of a charge density contained in a volume, only knowledge of the multipole moments of the density is necessary if one is interested in the potential outside of that volume. By this, any density that reproduces the same multipole moments outside this volume will yield the same potential. Thus, exploiting the freedom to choose a convenient charge density in the muffin-tin spheres, the interstitial potential can be obtained with much less computational effort.

The task of finding the muffin-tin potential then becomes rather trivial, as it is given as solution to a Dirichlet boundary value problem with now-known boundary values from the interstitial potential.

During the course of this thesis, we will learn that the electrostatic potential poses an explicit challenge in calculating its stress contribution. The coupling between interstitial and muffin-tin parts in the evaluation of the potential at a certain point is the reason for this challenge. Therefore, we will give a detailed overview over the Weinert method in the following.

Say we have given a total charge-density $n(\mathbf{r})$ from all electrons $\rho(\mathbf{r})$ and the atomic nuclei $Z_a\delta(\mathbf{r}_a)$ in a system dependent on some parameter $\underline{\varepsilon}$. The density is given in terms of interstitial and muffin-tins as

$$n[\underline{\varepsilon}](\mathbf{r}_\varepsilon) = \rho[\underline{\varepsilon}](\mathbf{r}_\varepsilon) = \sum_{\mathbf{G}_\varepsilon} \hat{\rho}[\underline{\varepsilon}](\mathbf{G}_\varepsilon) e^{i\mathbf{G}_\varepsilon \cdot \mathbf{r}_\varepsilon} \quad \text{for } \mathbf{r}_\varepsilon \in \text{IS}_\varepsilon, \quad (3.22a)$$

$$n^a[\underline{\varepsilon}](\mathbf{r}_a) = \sum_{lm} \rho_{lm}^a[\underline{\varepsilon}](r_a) Y_{lm}(\hat{\mathbf{r}}_a) - Z_a \delta(\mathbf{r}_a) \quad \text{for } \mathbf{r}_\varepsilon = \mathbf{r}_a + \boldsymbol{\tau}_a[\underline{\varepsilon}] \in \text{MT}_{a\varepsilon}. \quad (3.22b)$$

While the setup of the system depends on $\underline{\varepsilon}$, it is still set up according to the FLAPW partitioning scheme, meaning that the muffin-tins are spheres. In a local coordinate frame of an atom a that is placed at $\boldsymbol{\tau}_a[\underline{\varepsilon}]$, the relative coordinate \mathbf{r}_a is independent of the parameter.

We now calculate the multipole moments of that density inside the muffin-tin spheres in order to find the condition the smooth replacement density has to fulfill.

$$\begin{aligned} q_{lm}^a[\underline{\varepsilon}] &= \int_{B_{R_a}(\mathbf{0})} Y_{lm}^*(\hat{\mathbf{r}}_a) r_a^l n^a[\underline{\varepsilon}](\mathbf{r}_a) d^3r_a \\ &= \int_0^{R_a} r_a^{l+2} \rho_{lm}^a[\underline{\varepsilon}](r_a) dr_a - \sqrt{4\pi} Z_a \delta_{l0} \end{aligned} \quad (3.23)$$

3. Electronic structure methods

The total charge-density, from which the interstitial electrostatic potential is constructed, then has the form

$$\begin{aligned}
n_{\text{ps}}[\underline{\varepsilon}](\mathbf{r}_\varepsilon) &= \rho[\underline{\varepsilon}](\mathbf{r}_\varepsilon)\Theta(\mathbf{r}_\varepsilon \in \text{IS}_\varepsilon) + \sum_a^{\text{atoms}} \bar{n}^a[\underline{\varepsilon}](\mathbf{r}_a)\Theta(\mathbf{r}_\varepsilon \in \text{MT}_{a\varepsilon}) \\
&= \rho[\underline{\varepsilon}](\mathbf{r}_\varepsilon) + \sum_a^{\text{atoms}} (\bar{n}^a[\underline{\varepsilon}](\mathbf{r}_a) - \rho[\underline{\varepsilon}](\mathbf{r}_a + \boldsymbol{\tau}_a[\underline{\varepsilon}])) \Theta(\mathbf{r}_\varepsilon \in \text{MT}_{a\varepsilon}) \\
&= \rho[\underline{\varepsilon}](\mathbf{r}_\varepsilon) + \sum_a^{\text{atoms}} \tilde{n}_{\text{ps}}^a[\underline{\varepsilon}](\mathbf{r}_\varepsilon - \boldsymbol{\tau}_a[\underline{\varepsilon}]) = \rho[\underline{\varepsilon}](\mathbf{r}_\varepsilon) + \tilde{n}_{\text{ps}}[\underline{\varepsilon}](\mathbf{r}_\varepsilon),
\end{aligned}$$

with $\bar{n}^a[\underline{\varepsilon}]$ providing the same multipoles as the original $n^a[\underline{\varepsilon}]$. In the second line, the plane-wave density from the interstitial is expanded over the whole unit cell and then subtracted from the muffin-tin part, again. Doing this suggests to calculate the multipole moments of the plane-wave charge-density inside the muffin-tin spheres, which leads to a subtraction of

$$\begin{aligned}
q_{lm}^{a,\text{PW}}[\underline{\varepsilon}] &= \frac{\sqrt{4\pi}R_a^3}{3} \hat{\rho}[\underline{\varepsilon}](\mathbf{0})\delta_{l0} \\
&\quad + 4\pi i^l \sum_{\mathbf{G}_\varepsilon \neq \mathbf{0}} \hat{\rho}[\underline{\varepsilon}](\mathbf{G}_\varepsilon) e^{i\mathbf{G}_\varepsilon \cdot \boldsymbol{\tau}_a[\underline{\varepsilon}]} Y_{lm}^*(\mathbf{G}_\varepsilon) \frac{R_a^{l+3} j_{l+1}(G_\varepsilon R_a)}{G_\varepsilon R_a}
\end{aligned} \tag{3.24}$$

from $q_{lm}^a[\underline{\varepsilon}]$. The remaining part of the pseudo charge, $\tilde{\rho}_{\text{ps}}^a[\underline{\varepsilon}]$, then reproduces the multipoles $\tilde{q}_{lm}^a[\underline{\varepsilon}] = q_{lm}^a[\underline{\varepsilon}] - q_{lm}^{a,\text{PW}}[\underline{\varepsilon}]$. We construct this part as a power series in r_a up to a parameter N by defining

$$\tilde{n}_{\text{ps}}^a[\underline{\varepsilon}](\mathbf{r}_a) = \sum_{lm} Q_{lm}^a[\underline{\varepsilon}] Y_{lm}(\hat{\mathbf{r}}_a) \sum_{\eta=0}^N a_\eta[\underline{\varepsilon}] r_a^{l+2\eta}.$$

It then is apparent that the multipoles Q_{lm}^a in the above expansion have to be

$$Q_{lm}^a[\underline{\varepsilon}] = \tilde{q}_{lm}^a[\underline{\varepsilon}] \left[\sum_{\eta=0}^N a_\eta[\underline{\varepsilon}] \frac{R_a^{l+l+2\eta+3}}{l+l+2\eta+3} \right]^{-1}$$

to end up with the correct multipole moments again. Fourier transforming the muffin-tin pseudo charge yields

$$\begin{aligned}
\hat{\tilde{n}}_{\text{ps}}[\underline{\varepsilon}](\mathbf{G}_\varepsilon) &= \frac{1}{\Omega[\underline{\varepsilon}]} \int_{\Omega[\underline{\varepsilon}]} \left[\sum_a \tilde{n}_{\text{ps}}^a[\underline{\varepsilon}](\mathbf{r}_\varepsilon - \boldsymbol{\tau}_a[\underline{\varepsilon}]) \right] e^{-i\mathbf{G}_\varepsilon \cdot \mathbf{r}_\varepsilon} d^3 r_a \\
&= \frac{1}{\Omega[\underline{\varepsilon}]} \sum_{a \in \Omega[\underline{\varepsilon}]} e^{-i\mathbf{G}_\varepsilon \cdot \boldsymbol{\tau}_a[\underline{\varepsilon}]} \int_{B_{R_a}(\mathbf{0})} \tilde{n}_{\text{ps}}^a[\underline{\varepsilon}](\mathbf{r}_a) e^{-i\mathbf{G}_\varepsilon \cdot \mathbf{r}_a} d^3 r_a
\end{aligned}$$

$$\begin{aligned}
 &= \frac{1}{\Omega[\underline{\varepsilon}]} \sum_{lma} Q_{lm}^a[\underline{\varepsilon}] e^{-i\mathbf{G}_\varepsilon \cdot \boldsymbol{\tau}_a[\underline{\varepsilon}]} 4\pi (-i)^l Y_{lm}(\hat{\mathbf{G}}_\varepsilon) \\
 &\quad \times \sum_{\eta=0}^N \frac{a_\eta[\underline{\varepsilon}]}{G_\varepsilon^{l+2\eta+3}} \int_0^{G_\varepsilon R_a} t^{l+2\eta+2} j_l(t) dt
 \end{aligned} \tag{3.25}$$

and

$$\begin{aligned}
 \hat{n}_{\text{ps}}[\underline{\varepsilon}](\mathbf{0}) &= \frac{1}{\Omega[\underline{\varepsilon}]} \sum_{a \in \Omega[\underline{\varepsilon}]} \int_{B_{R_a}(\mathbf{0})} Y_{00}^*(\hat{\mathbf{r}}_a) r_a^0 \tilde{n}_{\text{ps}}^a[\underline{\varepsilon}](r_a) d^3 r_a \sqrt{4\pi} \\
 &= \frac{\sqrt{4\pi}}{\Omega[\underline{\varepsilon}]} \sum_{a \in \Omega[\underline{\varepsilon}]} \tilde{q}_{00}^a[\underline{\varepsilon}].
 \end{aligned} \tag{3.26}$$

By using the equality $\frac{d}{dt}[t^{l+2}j_{l+1}(t)] = t^{l+2}j_l(t)$ of the spherical Bessel functions and integrating η times by parts, the integral in the $\mathbf{G}_\varepsilon \neq \mathbf{0}$ components becomes

$$\begin{aligned}
 \int_0^{G_\varepsilon R_a} t^{l+2\eta+2} j_l(t) dt &= \left[t^{2\eta} t^{l+2} j_{l+1}(t) \right]_0^{G_\varepsilon R_a} - \int_0^{G_\varepsilon R_a} 2\eta t^{2\eta-2} t^{l+3} j_{l+1}(t) dt \\
 &= (G_\varepsilon R_a)^{l+2\eta+2} j_{l+1}(G_\varepsilon R_a) - 2\eta \left[t^{2\eta-2} t^{l+3} j_{l+2}(t) \right]_0^{G_\varepsilon R_a} \\
 &\quad + 2\eta \int_0^{G_\varepsilon R_a} (2\eta - 2) t^{2\eta-4} t^{l+4} j_{l+2}(t) dt = \dots \\
 &= (G_\varepsilon R_a)^{l+2\eta+2} \sum_{\nu=0}^{\eta} \frac{(-1)^\nu 2^\nu \eta!}{(\eta - \nu)!} \frac{j_{l+\nu+1}(G_\varepsilon R_a)}{(G_\varepsilon R_a)^\nu}.
 \end{aligned}$$

Subsequently, the sum over η in the description of $\hat{n}_{\text{ps}}[\underline{\varepsilon}]$ can be rearranged into sums of the same powers of $G_\varepsilon R_a$:

$$\begin{aligned}
 A_l^a[\underline{\varepsilon}] &:= \sum_{\eta=0}^N a_\eta[\underline{\varepsilon}] \frac{R_a^{l+2\eta+3}}{G_\varepsilon R_a} \sum_{\nu=0}^{\eta} \frac{(-1)^\nu 2^\nu \eta!}{(\eta - \nu)!} \frac{j_{l+\nu+1}(G_\varepsilon R_a)}{(G_\varepsilon R_a)^\nu} \\
 &= R_a^{l+3} \sum_{\nu=0}^N (-1)^\nu 2^\nu \frac{j_{l+\nu+1}(G_\varepsilon R_a)}{(G_\varepsilon R_a)^{\nu+1}} \sum_{\eta=\nu}^N \frac{a_\eta[\underline{\varepsilon}] \eta! R_a^{2\eta}}{(\eta - \nu)!}
 \end{aligned}$$

We demand that the last sum be zero for all ν but $\nu = N$. This can be achieved by setting

$$a_\eta[\underline{\varepsilon}] = (-1)^{N-\eta} R_a^{2(N-\eta)} \binom{N}{\eta} a_N[\underline{\varepsilon}]$$

as a simple substitution proves. Consequently, the sum over η becomes

$$A_l^a[\underline{\varepsilon}] = (-1)^N 2^N R_a^{l+3} \frac{j_{l+N+1}(G_\varepsilon R_a)}{(G_\varepsilon R_a)^{N+1}} (a_N[\underline{\varepsilon}] N! R_a^{2N}).$$

3. Electronic structure methods

Coming back to the replacements for the multipole moments, we can insert the $a_\eta[\underline{\varepsilon}]$ there, too:

$$\begin{aligned}
Q_{lm}^a[\underline{\varepsilon}] &= \tilde{q}_{lm}^a[\underline{\varepsilon}] \left[\sum_{\eta=0}^N a_\eta[\underline{\varepsilon}] \frac{R_a^{2l+2\eta+3}}{2l+2\eta+3} \right]^{-1} \\
&= \tilde{q}_{lm}^a[\underline{\varepsilon}] \left[\sum_{\eta=0}^N (-1)^{N-\eta} R_a^{2(N-\eta)} \binom{N}{\eta} a_N[\underline{\varepsilon}] \frac{R_a^{2l+2\eta+3}}{2l+2\eta+3} \right]^{-1} \\
&= \frac{(-1)^N \tilde{q}_{lm}^a[\underline{\varepsilon}]}{a_N[\underline{\varepsilon}] R_a^{2l+2N+3}} \left[\sum_{\eta=0}^N \frac{(-1)^\eta}{2l+2\eta+3} \binom{N}{\eta} \right]^{-1} \tag{3.27a}
\end{aligned}$$

$$\begin{aligned}
&= \frac{(-1)^N \tilde{q}_{lm}^a[\underline{\varepsilon}]}{a_N[\underline{\varepsilon}] R_a^{2l+2N+3}} \left[2^N N! \frac{(2l+1)!!}{(2l+2N+3)!!} \right]^{-1} \tag{3.27b} \\
&= \left((-1)^N 2^N R_a^{l+3} \right)^{-1} \frac{(2l+2N+3)!!}{(2l+1)!! R_a^l} \tilde{q}_{lm}^a[\underline{\varepsilon}] (a_N[\underline{\varepsilon}] N! R_a^{2N})^{-1}
\end{aligned}$$

The transition from the third to the second to last equation will be proven in the appendix A.1 since it demands more analytics than physical understanding. Plugging both $A_l^a[\underline{\varepsilon}]$ and $Q_{lm}^a[\underline{\varepsilon}]$ into the Fourier components of the muffin-tin pseudo charge (3.25), we see that the coefficients $a_N[\underline{\varepsilon}]$ cancel out and we find

$$\begin{aligned}
\hat{n}_{\text{ps}}[\underline{\varepsilon}](\mathbf{G}_\varepsilon) &= \frac{1}{\Omega[\underline{\varepsilon}]} \sum_{lma} Q_{lm}^a[\underline{\varepsilon}] e^{-i\mathbf{G}_\varepsilon \cdot \boldsymbol{\tau}_a[\underline{\varepsilon}]} 4\pi (-i)^l Y_{lm}(\hat{\mathbf{G}}_\varepsilon) A_l^a[\underline{\varepsilon}] \\
&= \frac{4\pi}{\Omega[\underline{\varepsilon}]} \sum_{lma} \frac{(-i)^l (2l+2N+3)!!}{(2l+1)!! R_a^l} \frac{j_{l+N+1}(G_\varepsilon R_a)}{(G_\varepsilon R_a)^{N+1}} \tilde{q}_{lm}^a[\underline{\varepsilon}] e^{-i\mathbf{G}_\varepsilon \cdot \boldsymbol{\tau}_a[\underline{\varepsilon}]} Y_{lm}(\hat{\mathbf{G}}_\varepsilon), \tag{3.28a}
\end{aligned}$$

$$\hat{n}_{\text{ps}}[\underline{\varepsilon}](\mathbf{0}) = \frac{\sqrt{4\pi}}{\Omega[\underline{\varepsilon}]} \sum_{a \in \Omega[\underline{\varepsilon}]}^{\text{atoms}} \tilde{q}_{00}^a[\underline{\varepsilon}]. \tag{3.28b}$$

The total pseudo charge from which the electrostatic potential is constructed then is given by

$$n_{\text{ps}}[\underline{\varepsilon}](\mathbf{r}_\varepsilon) = \sum_{\mathbf{G}_\varepsilon} \left(\hat{\rho}[\underline{\varepsilon}](\mathbf{G}_\varepsilon) + \hat{n}_{\text{ps}}[\underline{\varepsilon}](\mathbf{G}_\varepsilon) \right) e^{i\mathbf{G}_\varepsilon \cdot \mathbf{r}_\varepsilon}.$$

As the electrostatic potential is connected to the (pseudo)charge via the Poisson equation, it can be written as

$$V_C[\underline{\varepsilon}](\mathbf{r}_\varepsilon) = \sum_{\mathbf{G}_\varepsilon} \hat{V}_C[\underline{\varepsilon}](\mathbf{G}_\varepsilon) e^{i\mathbf{G}_\varepsilon \cdot \mathbf{r}_\varepsilon} = \sum_{\mathbf{G}_\varepsilon \neq \mathbf{0}} 4\pi \frac{\hat{n}_{\text{ps}}[\underline{\varepsilon}](\mathbf{G}_\varepsilon)}{G_\varepsilon^2} e^{i\mathbf{G}_\varepsilon \cdot \mathbf{r}_\varepsilon} \tag{3.29}$$

since V_C fulfills

$$\Delta_\varepsilon V_C[\underline{\underline{\varepsilon}}](\mathbf{r}_\varepsilon) = -4\pi \sum_{\mathbf{G}_\varepsilon \neq \mathbf{0}} \hat{n}_{\text{ps}}[\underline{\underline{\varepsilon}}](\mathbf{G}_\varepsilon) e^{i\mathbf{G}_\varepsilon \cdot \mathbf{r}_\varepsilon} = -4\pi n_{\text{ps}}[\underline{\underline{\varepsilon}}](\mathbf{r}_\varepsilon).$$

Note that the $\mathbf{G}_\varepsilon = \mathbf{0}$ component of $\hat{V}_C[\underline{\underline{\varepsilon}}]$ is not explicitly determined by this equation as any shift in the potential would vanish during differentiation, anyway.

Comparing the single expansion coefficients as

$$G_\varepsilon^2 \hat{V}_C[\underline{\underline{\varepsilon}}](\mathbf{G}_\varepsilon) = 4\pi \hat{n}_{\text{ps}}[\underline{\underline{\varepsilon}}](\mathbf{G}_\varepsilon),$$

it becomes prominent that the pseudo density has to fulfill $\hat{n}_{\text{ps}}[\underline{\underline{\varepsilon}}](\mathbf{0}) = 0$. This requirement corresponds to charge neutrality in the whole system since the zero component of the density represents the average density.

A detailed discussion on the choice of the parameter N can be found in the publication by Weinert [Wei81] that introduced this method. Therein he states, that $N - 1$ is the degree to which the pseudo charge is guaranteed to be continuously differentiable on the muffin-tin boundary and that a different N can be chosen for each value of l . To achieve a good convergence of the pseudo charge with respect to the number of \mathbf{G} vectors, the paper presents the criterion to chose $N(l)$ such that the first zero of the spherical function $j_{l+N(l)+1}$ is close to the maximal value of the product $G_\varepsilon R_a$ for each muffin-tin radius and each reciprocal lattice vector included into the computations. According to this criterion, the sum of l and $N(l)$ is independent of l .

We assume that the influence of the parameter $\underline{\underline{\varepsilon}}$ on the maximal value of $G_\varepsilon R_a$ is small, then the choice of N does not depend on $\underline{\underline{\varepsilon}}$.

It should be noted that in his book, Singh [Sin94] argues against the sensitivity of electronic structure calculations to $N(l)$ and suggests a general value of $\max(G_\varepsilon R_a)/2$, independent of l .

Now that the electrostatic potential is known in the interstitial, the potential in the muffin-tin spheres can be constructed by inverting the Poisson equation to a Dirichlet boundary value problem. The Green's function belonging to the homogeneous Laplace equation on a sphere of radius R_a is known to be

$$G(\mathbf{r}_a, \mathbf{s}_a) = 4\pi \sum_{lm} \frac{Y_{lm}^*(\hat{\mathbf{s}}_a) Y_{lm}(\hat{\mathbf{r}}_a)}{2l+1} \frac{r_{<}^l}{r_{>}^{l+1}} \left[1 - \left(\frac{r_{>}}{R_a} \right)^{2l+1} \right] \quad (3.30)$$

with $r_{< \setminus >} = \min \setminus \max(r_a, s_a)$. The Green's function subsequently can be used to construct a function g that solves the inhomogeneous Laplace equation $\Delta g = -f$ with the source term f on the same sphere.

3. Electronic structure methods

Green's identity provides the proof of this statement:

$$\begin{aligned}
& \int_{B_{R_a}(\mathbf{0})} G(\mathbf{r}_a, \mathbf{s}_a) \Delta g(\mathbf{s}_a) - g(\mathbf{s}_a) \Delta G(\mathbf{r}_a, \mathbf{s}_a) d^3 s_a \\
&= \int_{B_{R_a}(\mathbf{0})} \nabla \cdot [G(\mathbf{r}_a, \mathbf{s}_a) \nabla g(\mathbf{s}_a) - g(\mathbf{s}_a) \nabla G(\mathbf{r}_a, \mathbf{s}_a)] d^3 s_a \\
&= \oint_{\partial B_{R_a}(\mathbf{0})} G(\mathbf{r}_a, \mathbf{s}_a) \partial_{s_a} g(\mathbf{s}_a) - g(\mathbf{s}_a) \partial_{s_a} G(\mathbf{r}_a, \mathbf{s}_a) dS_2.
\end{aligned}$$

The Green's function is zero on the sphere boundary and G and g solve their respective Poisson equations. With $g(\mathbf{s}_a) = V_C[\underline{\varepsilon}](\mathbf{s}_a + \boldsymbol{\tau}_a[\underline{\varepsilon}])$ and $f(\mathbf{s}_a) = 4\pi n^a[\underline{\varepsilon}](\mathbf{s}_a)$, the original muffin-tin density, we see:

$$\begin{aligned}
V_C[\underline{\varepsilon}](\mathbf{r}_a + \boldsymbol{\tau}_a[\underline{\varepsilon}]) &= \int_{B_{R_a}(\mathbf{0})} n^a[\underline{\varepsilon}](\mathbf{s}_a) G(\mathbf{r}_a, \mathbf{s}_a) d^3 s_a \\
&\quad - \frac{R_a^2}{4\pi} \oint_{\partial B_1(\mathbf{0})} V_C[\underline{\varepsilon}](R_a \mathbf{s} + \boldsymbol{\tau}_a[\underline{\varepsilon}]) \partial_{R_a s} G(\mathbf{r}_a, R_a \mathbf{s}) dS_2 \quad (3.31)
\end{aligned}$$

The normal derivative of the Green's function evaluated for $s = R_a$ is calculated to be

$$\partial_s G(\mathbf{r}_a, \mathbf{s})|_{s=R_a} = -\frac{4\pi}{R_a^2} \sum_{lm} \left(\frac{r_a}{R_a} \right)^l Y_{lm}^*(\hat{\mathbf{s}}) Y_{lm}(\hat{\mathbf{r}}_a). \quad (3.32)$$

We finally obtain for the electrostatic potential in a muffin-tin sphere the equation

$$\begin{aligned}
& V_C[\underline{\varepsilon}](\mathbf{r}_a + \boldsymbol{\tau}_a[\underline{\varepsilon}]) \\
&= \sum_{lm} Y_{lm}(\hat{\mathbf{r}}_a) \frac{4\pi}{2l+1} \int_0^{R_a} s_a^2 \rho_{lm}^a[\underline{\varepsilon}](s_a) \frac{r_{<}^l}{r_{>}^{l+1}} \left[1 - \left(\frac{r_{>}}{R_a} \right)^{2l+1} \right] ds_a - Z_a \frac{1}{r_a} \left[1 - \frac{r_a}{R_a} \right] \\
&\quad + \sum_{lm} Y_{lm}(\hat{\mathbf{r}}_a) \left(\frac{r_a}{R_a} \right)^l \sum_{\mathbf{G}_\varepsilon \neq \mathbf{0}} e^{i\mathbf{G}_\varepsilon \cdot \boldsymbol{\tau}_a[\underline{\varepsilon}]} \hat{V}_C[\underline{\varepsilon}](\mathbf{G}_\varepsilon) \oint_{B_1(\mathbf{0})} e^{i\mathbf{G}_\varepsilon \cdot R_a \mathbf{s}} Y_{lm}^*(\hat{\mathbf{s}}) dS_2. \quad (3.33)
\end{aligned}$$

With this, we conclude our construction of the parameter dependent electrostatic potential $V_C[\underline{\varepsilon}](\mathbf{r}_\varepsilon)$ using Weinerts construction method. Discarding the parameter gives the general construction scheme used in full-potential codes like FLEUR [htt12].

3.3.4. Construction of the exchange-correlation energy density and potential

In contrast to the electrostatic potential, the quantities corresponding to the exchange-correlation density and potential shift the attention away from a non-local nature of the potential towards the non-linearity of their density-dependence, at least as far as the local density approximation (LDA) and the generalized gradient approximation (GGA)

are concerned. Due to the locality of the energy functional,

$$E_{\text{xc}}[\rho] = \begin{cases} \int_{\Omega} \rho(\mathbf{r}) \varepsilon_{\text{xc}}[\rho](\mathbf{r}) d^3r = \int_{\Omega} \rho(\mathbf{r}) \varepsilon_{\text{xc}}(\mathbf{r}, \rho(\mathbf{r})) d^3r & , \text{LDA} \\ \int_{\Omega} \rho(\mathbf{r}) \varepsilon_{\text{xc}}[\rho, |\nabla\rho|](\mathbf{r}) d^3r = \int_{\Omega} \rho(\mathbf{r}) \varepsilon_{\text{xc}}(\mathbf{r}, \rho(\mathbf{r}), |\nabla\rho(\mathbf{r})|) d^3r & , \text{GGA}, \end{cases}$$

$$\mu_{\text{xc}}(\mathbf{r}) = \frac{\delta E_{\text{xc}}[\rho]}{\delta \rho(\mathbf{r})} = \begin{cases} \frac{\partial}{\partial \rho(\mathbf{r})} \rho(\mathbf{r}) \varepsilon_{\text{xc}}(\mathbf{r}, \rho(\mathbf{r})) & , \text{LDA} \\ \frac{\partial}{\partial \rho(\mathbf{r})} \rho(\mathbf{r}) \varepsilon_{\text{xc}}(\mathbf{r}, \rho(\mathbf{r}), |\nabla\rho(\mathbf{r})|) \\ + \frac{\partial}{\partial |\nabla\rho(\mathbf{r})|} \rho(\mathbf{r}) \varepsilon_{\text{xc}}(\mathbf{r}, \rho(\mathbf{r}), |\nabla\rho(\mathbf{r})|) & , \text{GGA}, \end{cases}$$

muffin-tin and interstitial contributions can be calculated separately. However, as ε_{xc} and μ_{xc} depend on the density themselves in a more complicated fashion, the construction of those terms has to be executed in real space. Once finished, they are back-transformed into the standard FLAPW representation.

ε_{xc} and μ_{xc} in the muffin-tin spheres

The charge density is already given as a spherical/lattice harmonic expansion in the atomic spheres. The real space representation can thus be found on a mesh by multiplying the radial functions evaluated at a certain set of arguments $\{\mathbf{r}_i\}$ with the spherical/lattice harmonics at a certain set of angular positions $\{\hat{\mathbf{r}}_i = (\Theta_i, \phi_i)\}$ as

$$\rho(\mathbf{r}_i) = \sum_{lm} \rho_{lm}(r_i) Y_{lm}(\hat{\mathbf{r}}_i).$$

The absolute value of the gradient needed for the GGA method is constructed with the same set of $\{\mathbf{r}_i\}$.

After plugging the density (and possibly the gradient thereof) into the formulas for ε_{xc} and μ_{xc} , both are given on the same mesh. The choice of the mesh points should be made considering the back-transformation onto spherical/lattice harmonics. A good set of mesh points allows for the orthonormality conditions of the spherical harmonics to be used on it. The radial functions are given by

$$\varepsilon_{\text{xc},lm} \setminus \mu_{\text{xc},lm}(r_i) = \sum_{j:r_j=r_i} Y_{lm}^*(\hat{\mathbf{r}}_j) \varepsilon_{\text{xc}} \setminus \mu_{\text{xc}}(\mathbf{r}_j).$$

ε_{xc} and μ_{xc} in the interstitial

Stored as plane wave coefficients, a real space representation of the charge density in the interstitial can be constructed by multiplying them with a phase factor belonging to a grid point \mathbf{r}_i and summing them up over the reciprocal lattice vectors:

$$\rho(\mathbf{r}_i) = \sum_{\mathbf{G}} \rho(\mathbf{G}) e^{i\mathbf{G} \cdot \mathbf{r}_i}$$

3. Electronic structure methods

This can efficiently be done by a fast Fourier transformation. After computing ε_{xc} and μ_{xc} on each grid point, the inverse fast Fourier transformation provides their plane wave counterparts.

$$\rho(\mathbf{G}) \xrightarrow{\text{FFT}} \rho(\mathbf{r}_i) \longrightarrow \varepsilon_{xc} \setminus \mu_{xc}(\mathbf{r}_i) \xrightarrow{\text{FFT}^{-1}} \varepsilon_{xc} \setminus \mu_{xc}(\mathbf{G})$$

3.3.5. Construction of the Hamilton and overlap matrices

The description (3.6) of the Hamilton matrix and (3.7) of the overlap matrix can now be used to find the eigenvalues $\varepsilon_i(\mathbf{k})$ of the Kohn-Sham states. For that purpose, the occurring integrals are split into the muffin-tins and the interstitial region and evaluated separately. We will apply the notation used in the NIC summer school article about the FLEUR code [BB06].

Contribution of the muffin-tin spheres

We use the abbreviations

$$\varphi_{lm}^a(\mathbf{r}_a) = u_l^a(r_a) Y_{lm}(\hat{\mathbf{r}}_a) \text{ and} \quad (3.34a)$$

$$\dot{\varphi}_{lm}^a(\mathbf{r}_a) = \dot{u}_l^a(r_a) Y_{lm}(\hat{\mathbf{r}}_a) \quad (3.34b)$$

for part of the muffin-tin representation of the wave functions, noting that the spherical part of the muffin-tin Hamiltonian acts on it by construction as

$$\mathcal{H}_{\text{sph}}^a \varphi_{lm}^a = E_l^a \varphi_{lm}^a \quad (3.35a)$$

$$\mathcal{H}_{\text{sph}}^a \dot{\varphi}_{lm}^a = E_l^a \dot{\varphi}_{lm}^a + \varphi_{lm}^a. \quad (3.35b)$$

Plugged into the corresponding parts of the Hamilton matrix (3.6) and the overlap matrix (3.7), we get

$$\begin{aligned} H_{\text{MT}_a}^{\mathbf{G}'\mathbf{G}}(\mathbf{k}) &= \int_{B_{R_a}(\mathbf{0})} \left(\sum_{l'm'} a_{lm}^{ak\mathbf{G}'} \varphi_{l'm'}^a(\mathbf{r}_a) + b_{l'm'}^{ak\mathbf{G}'} \dot{\varphi}_{l'm'}^a(\mathbf{r}_a) \right)^* \\ &\quad \times \mathcal{H}_{\text{MT}_a} \left(\sum_{lm} a_{lm}^{ak\mathbf{G}} \varphi_{lm}^a(\mathbf{r}_a) + b_{lm}^{ak\mathbf{G}} \dot{\varphi}_{lm}^a(\mathbf{r}_a) \right) d^3r_a \text{ and} \end{aligned} \quad (3.36a)$$

$$\begin{aligned} S_{\text{MT}_a}^{\mathbf{G}'\mathbf{G}}(\mathbf{k}) &= \int_{B_{R_a}(\mathbf{0})} \left(\sum_{l'm'} a_{lm}^{ak\mathbf{G}'} \varphi_{l'm'}^a(\mathbf{r}_a) + b_{l'm'}^{ak\mathbf{G}'} \dot{\varphi}_{l'm'}^a(\mathbf{r}_a) \right)^* \\ &\quad \times \left(\sum_{lm} a_{lm}^{ak\mathbf{G}} \varphi_{lm}^a(\mathbf{r}_a) + b_{lm}^{ak\mathbf{G}} \dot{\varphi}_{lm}^a(\mathbf{r}_a) \right) d^3r_a. \end{aligned} \quad (3.36b)$$

In the evaluation of those terms, the spatial integrals can be executed independent of the reciprocal vectors \mathbf{k} and \mathbf{G} . Doing this in the form of

$$t_{L'L}^{a\varphi\varphi} = \int_{B_{R_a}(\mathbf{0})} \varphi_{L'}^{a*}(\mathbf{r}_a) \mathcal{H}_{\text{MT}_a} \varphi_L^a(\mathbf{r}_a) d^3 r_a, \quad (3.37a)$$

$$t_{L'L}^{a\varphi\dot{\varphi}} = \int_{B_{R_a}(\mathbf{0})} \varphi_{L'}^{a*}(\mathbf{r}_a) \mathcal{H}_{\text{MT}_a} \dot{\varphi}_L^a(\mathbf{r}_a) d^3 r_a, \quad (3.37b)$$

$$t_{L'L}^{a\dot{\varphi}\varphi} = \int_{B_{R_a}(\mathbf{0})} \dot{\varphi}_{L'}^{a*}(\mathbf{r}_a) \mathcal{H}_{\text{MT}_a} \varphi_L^a(\mathbf{r}_a) d^3 r_a, \quad (3.37c)$$

and

$$t_{L'L}^{a\dot{\varphi}\dot{\varphi}} = \int_{B_{R_a}(\mathbf{0})} \dot{\varphi}_{L'}^{a*}(\mathbf{r}_a) \mathcal{H}_{\text{MT}_a} \dot{\varphi}_L^a(\mathbf{r}_a) d^3 r_a \quad (3.37d)$$

saves a significant amount of computation time and lets us use the aforementioned eigenvalue properties of φ with respect to the spherical component of the Hamiltonian:

$$\langle \varphi_{L'}^a | \mathcal{H}_{\text{sph}}^a \varphi_L^a \rangle_{\text{MT}_a} = \delta_{ll'} \delta_{mm'} E_l^a \quad (3.38a)$$

$$\langle \varphi_{L'}^a | \mathcal{H}_{\text{sph}}^a \dot{\varphi}_L^a \rangle_{\text{MT}_a} = \delta_{ll'} \delta_{mm'} \quad (3.38b)$$

$$\langle \dot{\varphi}_{L'}^a | \mathcal{H}_{\text{sph}}^a \varphi_L^a \rangle_{\text{MT}_a} = 0 \quad (3.38c)$$

$$\langle \dot{\varphi}_{L'}^a | \mathcal{H}_{\text{sph}}^a \dot{\varphi}_L^a \rangle_{\text{MT}_a} = \delta_{ll'} \delta_{mm'} E_l^a \|\dot{\varphi}_L^a\|^2 \quad (3.38d)$$

Then, only the non-spherical part of the potential demands for an explicit computation to obtain the t matrices. Since the potential is expanded into lattice harmonics, the angular part of the integration collapses into Gaunt coefficients, leaving the radial integrals

$$I_{l'l'}^{a\varphi\varphi} = \int_0^{R_a} r_a^2 u_{l'}^a(r_a) u_l^a(r_a) V_{\text{eff}\nu}^a(r_a) dr_a, \quad (3.39a)$$

$$I_{l'l'}^{a\varphi\dot{\varphi}} = \int_0^{R_a} r_a^2 u_{l'}^a(r_a) \dot{u}_l^a(r_a) V_{\text{eff}\nu}^a(r_a) dr_a, \quad (3.39b)$$

$$I_{l'l'}^{a\dot{\varphi}\varphi} = \int_0^{R_a} r_a^2 \dot{u}_{l'}^a(r_a) u_l^a(r_a) V_{\text{eff}\nu}^a(r_a) dr_a, \quad (3.39c)$$

and

$$I_{l'l'}^{a\dot{\varphi}\dot{\varphi}} = \int_0^{R_a} r_a^2 \dot{u}_{l'}^a(r_a) \dot{u}_l^a(r_a) V_{\text{eff}\nu}^a(r_a) dr_a \quad (3.39d)$$

3. Electronic structure methods

to be calculated for $\nu \neq 0$. The t matrices consequently are

$$t_{L'L}^{a\varphi\varphi} = \sum_{\nu \neq 0} I_{l'l\nu}^{a\varphi\varphi} \sum_{m_\nu} c_{\nu m_\nu}^a G_{l'l\nu}^{m'mm_\nu} + \delta_{l'l'} \delta_{mm'} E_l^a, \quad (3.40a)$$

$$t_{L'L}^{a\varphi\dot{\varphi}} = \sum_{\nu \neq 0} I_{l'l\nu}^{a\varphi\dot{\varphi}} \sum_{m_\nu} c_{\nu m_\nu}^a G_{l'l\nu}^{m'mm_\nu} + \delta_{l'l'} \delta_{mm'}, \quad (3.40b)$$

$$t_{L'L}^{a\dot{\varphi}\varphi} = \sum_{\nu \neq 0} I_{l'l\nu}^{a\dot{\varphi}\varphi} \sum_{m_\nu} c_{\nu m_\nu}^a G_{l'l\nu}^{m'mm_\nu} \text{ and} \quad (3.40c)$$

$$t_{L'L}^{a\dot{\varphi}\dot{\varphi}} = \sum_{\nu \neq 0} I_{l'l\nu}^{a\dot{\varphi}\dot{\varphi}} \sum_{m_\nu} c_{\nu m_\nu}^a G_{l'l\nu}^{m'mm_\nu} + \delta_{l'l'} \delta_{mm'} E_l^a \|\dot{\varphi}_L^a\|^2. \quad (3.40d)$$

Finally, the Hamilton and overlap matrix elements are thus given by:

$$H_{\text{MT}_a}^{\mathbf{G}'\mathbf{G}}(\mathbf{k}) = \sum_{L'L} a_{L'}^{a\mathbf{k}\mathbf{G}'} t_{L'L}^{a\varphi\varphi} a_L^{a\mathbf{k}\mathbf{G}} + b_{L'}^{a\mathbf{k}\mathbf{G}'} t_{L'L}^{a\varphi\dot{\varphi}} b_L^{a\mathbf{k}\mathbf{G}} \\ + a_{L'}^{a\mathbf{k}\mathbf{G}'} t_{L'L}^{a\varphi\dot{\varphi}} b_L^{a\mathbf{k}\mathbf{G}} + b_{L'}^{a\mathbf{k}\mathbf{G}'} t_{L'L}^{a\dot{\varphi}\varphi} a_L^{a\mathbf{k}\mathbf{G}} \quad (3.41a)$$

$$S_{\text{MT}_a}^{\mathbf{G}'\mathbf{G}}(\mathbf{k}) = \sum_L a_L^{a\mathbf{k}\mathbf{G}'} a_L^{a\mathbf{k}\mathbf{G}} + b_L^{a\mathbf{k}\mathbf{G}'} b_L^{a\mathbf{k}\mathbf{G}} \|\dot{\varphi}_L^a\|^2 \quad (3.41b)$$

Contribution of the interstitial

The interstitial part of (3.6) and (3.7) can be found by multiplying the integrand with the unit step function corresponding to the unit cell without the muffin-tin spheres,

$$\Theta_{\text{IS}}(\mathbf{r}) = 1 - \sum_{a \in \Omega}^{\text{atoms}} \Theta(|\mathbf{r} - \boldsymbol{\tau}_a| \leq R_a). \quad (3.42)$$

It has the Fourier transform

$$\hat{\Theta}_{\text{IS}}(\mathbf{G}) = \delta_{\mathbf{G}\mathbf{0}} - \sum_{a \in \Omega}^{\text{atoms}} e^{-i\mathbf{G}\cdot\boldsymbol{\tau}_a} \frac{4\pi R_a^3 j_1(GR_a)}{\Omega GR_a}. \quad (3.43)$$

When the plane wave representation of the basis functions is inserted, we obtain

$$S_{\text{IS}}^{\mathbf{G}'\mathbf{G}} = \frac{1}{\Omega} \int_{\Omega} e^{-i(\mathbf{G}'-\mathbf{G})\cdot\mathbf{r}} \Theta_{\text{IS}}(\mathbf{r}) d^3r = \hat{\Theta}_{\text{IS}}(\mathbf{G}' - \mathbf{G}) \quad (3.44a)$$

$$H_{\text{IS}}^{\mathbf{G}'\mathbf{G}}(\mathbf{k}) = \frac{1}{2} |\mathbf{k} + \mathbf{G}'|^2 \hat{\Theta}_{\text{IS}}(\mathbf{G}' - \mathbf{G}) + (\widehat{V\Theta_{\text{IS}}})(\mathbf{G}' - \mathbf{G}) \quad (3.44b)$$

As each wave function is given in plane waves up to a G -cutoff of G_{max} , the Fourier transform of the unit step function and its product with the potential has to be given up to a cutoff twice as big. Unit step function and potential are then fast Fourier transformed into real space and multiplied with each other on a real space mesh. The product is then back-transformed into reciprocal space via another fast Fourier transformation.

3.4. Local orbitals

During our introduction to the LAPW basis set, we noted that one gets reasonable results in band structure calculations, if the energy parameters of the valence states are chosen in the middle of the bands one wishes to study. Furthermore we assumed that the core states are highly localized and low in energy so that the valence states are orthogonal to them. While this description gives a good conceptual understanding of the theory at hand, it lacks applicability with materials where core and valence states are not separated enough to support such assumptions. That kind of material features states which, while bound to the core of an atom and not participating at chemical bonds, noticeably extend into the interstitial region. Such states are called semicore states. Because they are not orthogonal to the LAPW basis, the interstitial part of them is sampled by the basis while the muffin-tin part of the basis lacks the flexibility for a proper description. The result of this deficiency are 'ghost-bands', artifacts in the band structure arising from the partial description of the semicore states, whose energies are off the mark of the valence energies.

A way to deal with this problem is the introduction of local orbitals, as done by Singh [Sin91]. Aiming at an even higher flexibility of the muffin-tin representation of the LAPW basis, he suggested to add to the basis valence like functions that vanish to first order at the muffin-tin boundary and thus do not meddle with the interstitial representation. This is done by including the radial solution of (3.9), \tilde{u}_l , to an energy parameter \tilde{E}_l^a that fits the semicore state energy to the u_l and \dot{u}_l functions. The conditions which define the local orbitals together with a normalization constraint yields the equations

$$a_{l,lo}^a u_{l,lo}^a(R_a, E_l^a) + b_{l,lo}^a \dot{u}_{l,lo}^a(R_a, E_l^a) + c_{l,lo}^a \tilde{u}_{l,lo}^a(R_a, \tilde{E}_l^a) = 0, \quad (3.45a)$$

$$a_{l,lo}^a \partial_r u_{l,lo}^a(R_a, E_l^a) + b_{l,lo}^a \partial_r \dot{u}_{l,lo}^a(R_a, E_l^a) + c_{l,lo}^a \partial_r \tilde{u}_{l,lo}^a(R_a, \tilde{E}_l^a) = 0, \text{ and } (3.45b)$$

$$\int_0^{R_a} \left(a_{l,lo}^a u_{l,lo}^a(r_a, E_l^a) + b_{l,lo}^a \dot{u}_{l,lo}^a(r_a, E_l^a) + c_{l,lo}^a \tilde{u}_{l,lo}^a(r_a, \tilde{E}_l^a) \right)^2 r_a^2 dr_a = 1. \quad (3.45c)$$

They are solved by choosing the matching parameters as

$$a_{l,lo}^a = K_{l,lo}^{a,1} c_{l,lo}^a, \quad (3.46a)$$

$$b_{l,lo}^a = K_{l,lo}^{a,2} c_{l,lo}^a, \text{ and } (3.46b)$$

$$c_{l,lo}^a = \left((K_{l,lo}^{a,1})^2 + (K_{l,lo}^{a,2})^2 (\dot{u}_{l,lo}^a, \dot{u}_{l,lo}^a) + 2(K_{l,lo}^{a,1})(u_{l,lo}^a, \tilde{u}_{l,lo}^a) + 2(K_{l,lo}^{a,2})(\dot{u}_{l,lo}^a, \tilde{u}_{l,lo}^a) \right)^{-\frac{1}{2}} \quad (3.46c)$$

with the scalar product $(f, g) = \int_0^{R_a} r^2 f g dr$ and the abbreviations

$$K_{l,lo}^{a,1} = \frac{1}{W_l^a(R_a, E_l^a)} (\tilde{u}_{l,lo}^a(R_a) \partial_r \dot{u}_{l,lo}^a(R_a) - \partial_r \tilde{u}_{l,lo}^a(R_a) \dot{u}_{l,lo}^a(R_a)), \quad (3.47a)$$

$$K_{l,lo}^{a,2} = -\frac{1}{W_l^a(R_a, E_l^a)} (\tilde{u}_{l,lo}^a(R_a) \partial_r u_{l,lo}^a(R_a) - \partial_r \tilde{u}_{l,lo}^a(R_a) u_{l,lo}^a(R_a)), \text{ and } (3.47b)$$

$$W_l^a(R_a, E_l^a) = \partial_r u_{l,lo}^a(R_a) \dot{u}_{l,lo}^a(R_a) - u_{l,lo}^a(R_a) \partial_r \dot{u}_{l,lo}^a(R_a). \quad (3.47c)$$

3. Electronic structure methods

Note that the local orbitals are not orthogonal to the LAPW basis even though they vanish to first order at the muffin-tin boundary. In contrast to the radial functions u_l and \dot{u}_l , which solve the Schrödinger equation for the energy parameter E_l , and the new radial function \tilde{u}_l , which solves the Schrödinger equation for a different energy parameter \tilde{E}_l , their sum is for that very reason not an eigenfunction of the same Hamiltonian. This was a critical condition of showing the orthogonality between the radial functions and the core states.

As they originate from plane waves, the valence states fulfill Bloch's theorem by construction. To rigorously include the local orbitals in the LAPW basis, they too have to respect the theorem. Therefore, they are coupled to virtual plane waves $\mathbf{k} + \mathbf{G}_{l_0}$ such that they become

$$\begin{aligned} & \phi_{\mathbf{k}\mathbf{G}_{l_0}}^{a,l_0}(\mathbf{r}_a) \\ &= \sum_m \left(A_{L,l_0}^{a\mathbf{k}\mathbf{G}_{l_0}} u_{l_0}^a(r_a, E_l^a) + B_{L,l_0}^{a\mathbf{k}\mathbf{G}_{l_0}} \dot{u}_{l_0}^a(r_a, E_l^a) + C_{L,l_0}^{a\mathbf{k}\mathbf{G}_{l_0}} \tilde{u}_{l_0}^a(r_a, \tilde{E}_l^a) \right) Y_L(\hat{\mathbf{r}}_a). \end{aligned} \quad (3.48)$$

The capital letter A , B and C coefficients are related to their small letter counterparts by

$$A \setminus B \setminus C_{L,l_0}^{a\mathbf{k}\mathbf{G}_{l_0}} = \frac{4\pi i^l}{W_l^a(R_a, E_l^a)} e^{i(\mathbf{k} + \mathbf{G}_{l_0}) \cdot \boldsymbol{\tau}_a} a \setminus b \setminus c_{l_0}^a Y_L^*(\widehat{\mathbf{k} + \mathbf{G}_{l_0}}). \quad (3.49)$$

Here, we also can introduce the index λ , which we defined as a switch between quantities belonging to the radial function and quantities belonging to its radial derivative. By letting $\lambda = 2$ indicate the quantities belonging to the radial solution \tilde{u} , we can write

$$\psi_{i\mathbf{k}}(\mathbf{r})|_{\mathbf{r} \in \text{MT}_a} = \sum_{\mathbf{G}} z_{i\mathbf{k}\mathbf{G}} \phi_{\mathbf{k}\mathbf{G}}(\mathbf{r})|_{\mathbf{r} \in \text{MT}_a} + \sum_{\mathbf{G}_{l_0}} z_{i\mathbf{k}\mathbf{G}_{l_0}}^a \phi_{\mathbf{k}\mathbf{G}_{l_0}}^{a,l_0}(\mathbf{r} - \boldsymbol{\tau}_a) \quad (3.50a)$$

$$= \sum_{\mathbf{G}} z_{i\mathbf{k}\mathbf{G}} \sum_{L\lambda} a_{L\lambda}^{a\mathbf{k}\mathbf{G}} u_{l\lambda}^a(r_a) Y_L(\hat{\mathbf{r}}_a) \quad (3.50b)$$

$$+ \sum_{\mathbf{G}_{l_0}} z_{i\mathbf{k}\mathbf{G}_{l_0}}^a \sum_{m\lambda} A_{L,l_0,\lambda}^{a\mathbf{k}\mathbf{G}_{l_0}} u_{l,\lambda}^a(r_a) Y_L(\hat{\mathbf{r}}_a) \quad (3.50c)$$

A great benefit of local orbitals is that they can be used situationally. It is possible to add a single local orbital of a certain angular momentum l to an atom when appropriate. Due to this, the basis grows reasonably with the selective addition of a few local orbitals. There are three blocks that have to be added to the Hamilton and overlap matrices, namely two contributions from the interplay between the regular basis and the local orbital addition and one contribution from the interplay of the local orbitals with themselves, leading to

$$\begin{pmatrix} H_{\mathbf{G}'\mathbf{G}}(\mathbf{k}) & H_{\mathbf{G}'\mathbf{G}_{l_0}}(\mathbf{k}) \\ H_{\mathbf{G}'_{l_0}\mathbf{G}}(\mathbf{k}) & H_{\mathbf{G}'_{l_0}\mathbf{G}_{l_0}}(\mathbf{k}) \end{pmatrix} \quad \text{and} \quad \begin{pmatrix} S_{\mathbf{G}'\mathbf{G}}(\mathbf{k}) & S_{\mathbf{G}'\mathbf{G}_{l_0}}(\mathbf{k}) \\ S_{\mathbf{G}'_{l_0}\mathbf{G}}(\mathbf{k}) & S_{\mathbf{G}'_{l_0}\mathbf{G}_{l_0}}(\mathbf{k}) \end{pmatrix}. \quad (3.51)$$

We will not delve further into the construction of these extended matrices, as it is similar to the construction of their first blocks.

3.5. Variational total energy for metals

Insulators and semiconductors are characterized by having their Fermi-energy separate the occupied and unoccupied energy bands altogether. This justifies to assume that the occupation numbers of the Kohn-Sham states are either zero or two (or one, if a spin resolved calculation is executed) and are thus insensitive to small strains.

Metals on the other hand possess partially occupied bands since their Fermi-energy cuts through one or more energy bands. Therefore, fractional occupation numbers have to be employed and integration over the Brillouin zone has to be executed with care. This is due to the integration method applied to Brillouin zone integrals. They are sampled as discrete sums over a mesh of \mathbf{k} -points and demand that the quantity to be integrated is smoothly varying over the integration zone. Then one can write for an integrand $f_i(\mathbf{k})$ depending on the band index i

$$\frac{1}{V_{\text{BZ}}} \int_{\text{BZ}} \sum_{i:\epsilon_i(\mathbf{k}) < E_F} f_i(\mathbf{k}) d^3k \longrightarrow \sum_{\mathbf{k}} \sum_{i:\epsilon_i(\mathbf{k}) < E_F} f_i(\mathbf{k}) w(\mathbf{k})$$

with the weights $w(\mathbf{k})$ containing the general occupation of a state at the corresponding \mathbf{k} -point. However, the condition of being smoothly varying is not fulfilled near the Fermi-edge because of the sharp transition from occupied to unoccupied states.

To provide applicability, the states are therefore smeared by a Fermi function to a parameter T that is chosen for good convergence.

$$\tilde{w}(\mathbf{k}, \epsilon_i(\mathbf{k}) - E_F) = w(\mathbf{k}) \frac{1}{e^{(\epsilon_i(\mathbf{k}) - E_F)/k_B T} + 1}$$

The determination of the Fermi energy and the construction of $\tilde{w}(\mathbf{k}, \epsilon_i(\mathbf{k}) - E_F)$ are achieved in two simple steps. First, the bands are occupied at each \mathbf{k} -point starting with the lowest one in energy until all electrons of the system are distributed:

$$N = \sum_{\mathbf{k}} \sum_i w(\mathbf{k})$$

Afterwards, the smearing is applied with the Fermi energy chosen such that the number of electrons is reproduced.

$$N = \sum_{\mathbf{k}} \sum_i \tilde{w}(\mathbf{k}, \epsilon_i(\mathbf{k}) - E_F)$$

As the Fermi function does only vary close to the Fermi-edge, lower lying bands do not experience an alteration of their weights and higher lying bands are still excluded from the summation as intended.

3. Electronic structure methods

Weinert and Davenport [WD92] proved that the total energy is no longer variational when fractional occupation numbers are part of the electronic structure calculation. They have shown that an electronic density which slightly differs from the ground state density results in a first order deviation of the energy functional from the ground state energy as given by

$$E[\rho_0 + \delta\rho] = E[\rho_0] + \sum_{\mathbf{k}} \sum_i \delta\tilde{w}(\mathbf{k}, \epsilon_i(\mathbf{k}) - E_F)\epsilon_i(\mathbf{k}) + \mathcal{O}(\delta^2).$$

To remedy this problem, they proposed the incorporation of an entropy like term

$$TS = k_B T \sum_{\mathbf{k}} \sum_i [\tilde{w}(\mathbf{k}, i) \ln(\tilde{w}(\mathbf{k}, i)) + (w(\mathbf{k}) - \tilde{w}(\mathbf{k}, i)) \ln(w(\mathbf{k}) - \tilde{w}(\mathbf{k}, i))]$$

into the energy functional, where $\tilde{w}(\mathbf{k}, i)$ is an abbreviation for $\tilde{w}(\mathbf{k}, \epsilon_i(\mathbf{k}) - E_F)$. The variation of this expression is exactly the necessary adjustment to the energy variation:

$$\begin{aligned} T\delta S &= k_B T \sum_{\mathbf{k}} \sum_i [\delta\tilde{w}(\mathbf{k}, i) \ln(\tilde{w}(\mathbf{k}, i)) + \delta\tilde{w}(\mathbf{k}, i) - \delta\tilde{w}(\mathbf{k}, i) \ln(w(\mathbf{k}) - \tilde{w}(\mathbf{k}, i)) - \delta\tilde{w}(\mathbf{k}, i)] \\ &= k_B T \sum_{\mathbf{k}} \sum_i \delta\tilde{w}(\mathbf{k}, i) \ln\left(\frac{\tilde{w}(\mathbf{k}, i)}{w(\mathbf{k}) - \tilde{w}(\mathbf{k}, i)}\right) \\ &= k_B T \sum_{\mathbf{k}} \sum_i \delta\tilde{w}(\mathbf{k}, i) \ln\left(\frac{1}{e^{(\epsilon_i(\mathbf{k}) - E_F)/k_B T} + 1 - 1}\right) = - \sum_{\mathbf{k}} \sum_i \delta\tilde{w}(\mathbf{k}, i)\epsilon_i(\mathbf{k}) \end{aligned}$$

The last equality holds as the number of electrons in the system is a constant, meaning that $\sum \delta\tilde{w}(\mathbf{k}, i)E_F$ is zero.

Using the same argumentation, an energy functional subject to fractional occupation numbers but corrected by the entropy like term is also variational with respect to a strain variation. Due to this circumstance, we will neglect changes in occupation numbers during the stress calculation, as they will cancel out.

To suit other publications, we will write $n_{i\mathbf{k}}$ for the occupation numbers $\tilde{w}(\mathbf{k}, i)$.

4. Forces from total energy calculations

Before we start with the derivation of the stress formula, we want to explain the calculation of atomic forces in the FLAPW method as formulated by Yu *et al.* [YSK91]. A good understanding of the contributions appearing in their derivation will help us to identify and characterize the corresponding terms appearing in the stress/strain formalism. Let us assume that we have given a self-consistent solution of a system with unit cell Ω and atoms placed at positions $\boldsymbol{\tau}_a$. We then want to find the force acting on a specific atom c at $\boldsymbol{\tau}_c$. To that end, we displace that atom by an infinitesimal vector $\delta\boldsymbol{\tau}_c$ and observe the changes in the total energy. We indicate quantities which are subject to variation due to the displacement by adding $[\delta\boldsymbol{\tau}_c]$ to them.

The total energy of the slightly altered system is given by

$$E[\delta\boldsymbol{\tau}_c] = \sum_{\mathbf{k}i} n_{i\mathbf{k}} \epsilon_i[\delta\boldsymbol{\tau}_c](\mathbf{k}) - \int_{\Omega} \rho[\delta\boldsymbol{\tau}_c](\mathbf{r}) V_{\text{eff}}[\delta\boldsymbol{\tau}_c](\mathbf{r}) d^3r + \int_{\Omega} \rho[\delta\boldsymbol{\tau}_c](\mathbf{r}) \epsilon_{\text{xc}}[\delta\boldsymbol{\tau}_c](\mathbf{r}) d^3r \quad (4.1a)$$

$$+ \frac{1}{2} \int_{\Omega} \rho[\delta\boldsymbol{\tau}_c](\mathbf{r}) \left\{ \int_{\mathbb{R}^3} \frac{\rho[\delta\boldsymbol{\tau}_c](\mathbf{s})}{|\mathbf{r} - \mathbf{s}|} d^3s - \sum_b^{\text{atoms}} \frac{Z_b}{|\mathbf{r} - \boldsymbol{\tau}_b[\delta\boldsymbol{\tau}_c]|} \right\} d^3r \quad (4.1b)$$

$$- \frac{1}{2} \sum_{a \in \Omega}^{\text{atoms}} Z_a \left\{ \int_{\Omega} \frac{\rho[\delta\boldsymbol{\tau}_c](\mathbf{s})}{|\boldsymbol{\tau}_a[\delta\boldsymbol{\tau}_c] - \mathbf{s}|} d^3s - \sum_{b \neq a}^{\text{atoms}} \frac{Z_b}{|\boldsymbol{\tau}_a[\delta\boldsymbol{\tau}_c] - \boldsymbol{\tau}_b[\delta\boldsymbol{\tau}_c]|} \right\}. \quad (4.1c)$$

The changes in the density $\rho[\delta\boldsymbol{\tau}_c](\mathbf{r})$ and the potential $V_{\text{eff}}[\delta\boldsymbol{\tau}_c](\mathbf{r})$ are largely unknown. Independent from the change in the shape of the potential, we can say however, that the contribution of the nucleus c and its core electrons to the original effective potential will have moved to $\boldsymbol{\tau}_c + \delta\boldsymbol{\tau}_c$ according to the atomic displacement. The atomic positions are displaced as $\boldsymbol{\tau}_a[\delta\boldsymbol{\tau}_c] = \boldsymbol{\tau}_a + \delta_{ac} \delta\boldsymbol{\tau}_c$. The eigenvalue sum also changes. We now want to calculate the linear change of the energy with respect to the infinitesimal vector $\delta\boldsymbol{\tau}_c$. Note that the variation in the density occurring in the integral which contains the density and the effective potential will cancel out exactly with the corresponding terms that appear in the integral containing the electronic density and the electrostatic potential (4.1b) as well as in the sum over the nuclei and the Madelung potential (4.1c). Furthermore, the integral over the exchange-correlation energy density will be handled according to $\mu_{\text{xc}}(\mathbf{r}) = \delta[\rho(\mathbf{r}) \epsilon_{\text{xc}}(\mathbf{r})] / \delta\rho(\mathbf{r})$ applying the chain-rule. Thus, it cancels the exchange-correlation potential part in the integral containing the density and the effective potential integral. We obtain

$$\delta E = \sum_{\mathbf{k}i} n_{i\mathbf{k}} \delta \epsilon_i[\delta\boldsymbol{\tau}_c](\mathbf{k}) - \int_{\Omega} \rho(\mathbf{r}) \delta V_{\text{eff}}[\delta\boldsymbol{\tau}_c](\mathbf{r}) d^3r - \mathbf{F}_{\text{HF}}^c \cdot \delta\boldsymbol{\tau}_c$$

4. Forces from total energy calculations

with \mathbf{F}_{HF}^c being the Hellmann-Feynman force, written as

$$\begin{aligned} \mathbf{F}_{\text{HF}}^c &= \sum_{a \in \Omega} Z_a \frac{\delta}{\delta \boldsymbol{\tau}_c} \left(\int_{\mathbb{R}^3} \frac{\rho(\mathbf{s})}{|\boldsymbol{\tau}_a[\delta \boldsymbol{\tau}_c] - \mathbf{s}|} d^3 s - \frac{1}{2} \sum_{b \neq a}^{\text{atoms}} \frac{Z_b}{|\boldsymbol{\tau}_a[\delta \boldsymbol{\tau}_c] - \boldsymbol{\tau}_b[\delta \boldsymbol{\tau}_c]|} \right) \\ &= Z_c \frac{\delta}{\delta \boldsymbol{\tau}_c} \left(\int_{\mathbb{R}^3} \frac{\rho(\mathbf{s})}{|\boldsymbol{\tau}_c + \delta \boldsymbol{\tau}_c - \mathbf{s}|} d^3 s - \sum_{b \neq c}^{\text{atoms}} \frac{Z_b}{|\boldsymbol{\tau}_c + \delta \boldsymbol{\tau}_c - \boldsymbol{\tau}_b|} \right), \end{aligned} \quad (4.2)$$

which is the variation of the Madelung potential of atom c . The force acting on that atom then becomes

$$\mathbf{F}^c = -\frac{\delta E}{\delta \boldsymbol{\tau}_c} = \mathbf{F}_{\text{HF}}^c - \frac{1}{\delta \boldsymbol{\tau}_c} \left(\sum_{\mathbf{k}i} n_{i\mathbf{k}} \delta \epsilon_i[\delta \boldsymbol{\tau}_c](\mathbf{k}) - \int_{\Omega} \rho(\mathbf{r}) \delta V_{\text{eff}}[\delta \boldsymbol{\tau}_c](\mathbf{r}) d^3 r \right). \quad (4.3)$$

There is no contribution from the electron-electron interaction in the Hellmann-Feynman force because, due to the cancellation of the density variation, the remaining expression $\rho(\mathbf{r})\rho(\mathbf{s})/|\mathbf{r} - \mathbf{s}|$ does not depend on atomic positions. This is clear as the Hellmann-Feynman force consists of all forces which act on the nucleus of atom c . The Hartree interaction mediates only between electrons. Also note that the Hellmann-Feynman force is composed of the electron-nuclei interaction as part of the remaining electron-charged particle interaction, which is the second term in the curly brackets in line (4.1b), as well as of the total nuclei-charged particle interaction, which is the first term in the curly brackets in the subsequent line (4.1c). This is a result of splitting the electron-ion interaction to equal parts to (4.1b) and (4.1c).

The additional term is the so-called Pulay correction for the force. If one used a complete basis set for the description of the Kohn-Sham system, this correction would vanish identically. However, in the FLAPW method the basis set is not sufficiently complete, which makes a careful handling of this term necessary. We will divide it in three parts so that

$$\mathbf{F}^c = \mathbf{F}_{\text{HF}}^c + \mathbf{F}_{\text{core}}^c + \mathbf{F}_{\text{val}}^c + \mathbf{F}_{\text{disc}}^c. \quad (4.4)$$

The core and valence corrections are a direct result of splitting the Pulay correction into core and valence states. They come in because the atomic displacement demands for an adjusted description of the Kohn-Sham states due to the new atomic location. Furthermore, the discontinuity correction is a result of matching the plane waves and the representation in the muffin-tin spheres to first order, only.

4.1. The Hellman-Feynman force

We noted earlier that the Hellmann-Feynman force is the variation of the Madelung potential of atom c , i.e., the Coulomb potential arising from all charges of the system except of the atomic nucleus at $\boldsymbol{\tau}_c$. We therefore are in the fortunate position to be able

to calculate it directly from the Dirichlet boundary value problem 3.31 without having to apply a variation to the interstitial potential. In the appendix section A.2, we give the detailed derivation, which results in the following expression for the Hellmann-Feynman force:

$$\mathbf{F}_{\text{HF}}^c = Z_c \sum_{m=-1}^1 \left\{ \frac{4\pi}{3} \int_0^{R_c} \rho_{1m}^c(\mathbf{r}) \left[1 - \left(\frac{r}{R_c} \right)^3 \right] dr + \frac{V_{C1m}^c(R_c)}{R_c} \right\} \nabla [rY_{1m}(\hat{\mathbf{r}})] \quad (4.5)$$

This formula is easy to implement in DFT codes based on the FLAPW method.

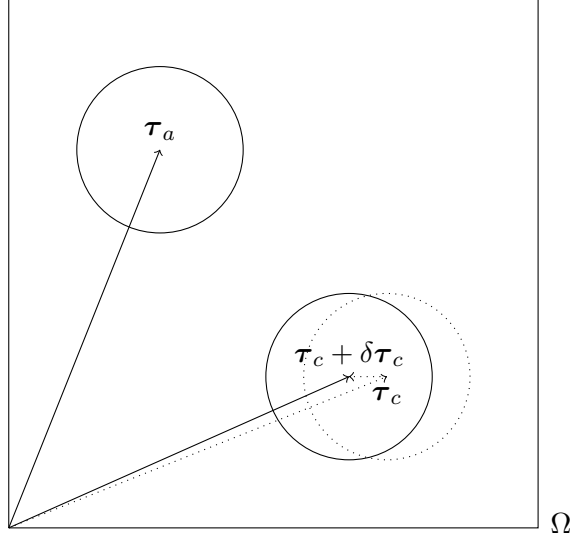


Figure 4.1.: Infinitesimal displacement of atom c at τ_c by $\delta\tau_c$.

4.2. The Pulay correction

Now we have to evaluate the additional term, the variation of the eigenvalue sum minus the integral containing the variation of the effective potential. As core and valence states are treated differently in the FLAPW method, we have to distinguish between them. Because the core electrons are direct solutions of a simple Schrödinger equation, they do not require a basis set. This makes their treatment fairly easy. However, the treatment of the valence states will be more involved. The wave functions are subject to change, and the variation of the wave functions cannot be expressed in terms of the basis.

4.2.1. Core correction

To obtain the change in the energy eigenvalue $\epsilon_i[\delta\tau_c]$ of a core state $\psi_i^c[\delta\tau_c]$ with respect to the atomic displacement $\delta\tau_c$, we can apply the Hellman-Feynman theorem. As was

4. Forces from total energy calculations

mentioned in the introduction of the total energy (4.1) of the system containing the displaced atom, from the perspective of the core states, they move along with the dominant part of the potential. Therefore we have

$$\frac{\delta}{\delta \boldsymbol{\tau}_c} \epsilon_i[\delta \boldsymbol{\tau}_c] = \frac{\delta}{\delta \boldsymbol{\tau}_c} \left\langle \psi_i^c[\delta \boldsymbol{\tau}_c] \left| \left[-\frac{1}{2} \nabla^2 + V_{\text{eff}}[\delta \boldsymbol{\tau}_c](\mathbf{r}) \right] \right| \psi_i^c[\delta \boldsymbol{\tau}_c] \right\rangle_{\text{MT}_c} \quad (4.6a)$$

$$= \left\langle \psi_i^c \left| \frac{\delta}{\delta \boldsymbol{\tau}_c} V_{\text{eff}}[\delta \boldsymbol{\tau}_c](\mathbf{r}) \right| \psi_i^c \right\rangle_{\text{MT}_c} \quad (4.6b)$$

$$= \int_{B_{R_c}(\mathbf{0})} \rho_i^c(\mathbf{r}_c) \left[\frac{\delta}{\delta \boldsymbol{\tau}_c} V_{\text{eff}}^c[\delta \boldsymbol{\tau}_c](\mathbf{r}_c) \right] d^3 r_c. \quad (4.6c)$$

In the core part of the double counting term, the last term in (4.3), we observe a different effect, since we only have given the variation of the potential times the original density as the integrand. Then, the dominant part of the potential is displaced by $\delta \boldsymbol{\tau}_c$ with respect to the core density. Thus, we obtain

$$\begin{aligned} & - \int_{B_{R_c}(\boldsymbol{\tau}_c)} \rho_i^c(\mathbf{r} - \boldsymbol{\tau}_c) \left[\frac{\delta}{\delta \boldsymbol{\tau}_c} V_{\text{eff}}^c[\delta \boldsymbol{\tau}_c](\mathbf{r} - [\boldsymbol{\tau}_c + \delta \boldsymbol{\tau}_c]) \right] d^3 r \\ &= - \int_{B_{R_c}(\mathbf{0})} \rho_i^c(\mathbf{r}_c) \left[\frac{\delta}{\delta \boldsymbol{\tau}_c} V_{\text{eff}}^c[\delta \boldsymbol{\tau}_c](\mathbf{r}_c) - \nabla V_{\text{eff}}^c(\mathbf{r}_c) \right] d^3 r_c \end{aligned} \quad (4.7)$$

By summing up (4.6c) and (4.7), it becomes apparent that the core states contribute to the Pulay correction a gradient of the effective potential,

$$\begin{aligned} \mathbf{F}_{\text{core}}^c &= - \frac{1}{\delta \boldsymbol{\tau}_c} \sum_{i \in \text{core}} \left(\delta \epsilon_i[\delta \boldsymbol{\tau}_c] - \int_{B_{R_c}(\mathbf{0})} \rho_i^c(\mathbf{r}_c) \delta V_{\text{eff}}^c[\delta \boldsymbol{\tau}_c](\mathbf{r}_c) d^3 r_c \right) \\ &= - \sum_{i \in \text{core}} \int_{B_{R_c}(\mathbf{0})} \rho_i^c(\mathbf{r}_c) \nabla V_{\text{eff}}^c(\mathbf{r}_c) d^3 r_c. \end{aligned} \quad (4.8)$$

The difference we have found here arises because the effective potential changes twofold when looked at from the perspective of the original core density of atom c : First, the potential is displaced by $\delta \boldsymbol{\tau}_c$. Second, the potential adjusts to the new crystal field. The latter part is the only change in the potential seen by the core states when shifted along with the atom. Thus, this latter part cancels out.

4.2.2. Valence correction

The valence states are not confined to a muffin-tin sphere. We therefore have to take into account the whole unit cell. The eigenvalues can be obtained through the Rayleigh coefficient. Let i denote a valence state, then we have:

$$\epsilon_i(\mathbf{k}) = \frac{\int_{\Omega} \psi_{i\mathbf{k}}^*(\mathbf{r}) \left[-\frac{1}{2} \nabla^2 + V_{\text{eff}}(\mathbf{r}) \right] \psi_{i\mathbf{k}}(\mathbf{r}) d^3 r}{\int_{\Omega} \psi_{i\mathbf{k}}^*(\mathbf{r}) \psi_{i\mathbf{k}}(\mathbf{r}) d^3 r}$$

The Kohn-Sham eigenvalue in the disturbed system is thus given by

$$\epsilon_i[\delta\boldsymbol{\tau}_c](\mathbf{k}) = \frac{\int_{\Omega} \psi_{i\mathbf{k}}^*[\delta\boldsymbol{\tau}_c](\mathbf{r}) \left[-\frac{1}{2}\nabla^2 + V_{\text{eff}}[\delta\boldsymbol{\tau}_c](\mathbf{r})\right] \psi_{i\mathbf{k}}[\delta\boldsymbol{\tau}_c](\mathbf{r}) d^3r}{\int_{\Omega} \psi_{i\mathbf{k}}^*[\delta\boldsymbol{\tau}_c](\mathbf{r}) \psi_{i\mathbf{k}}[\delta\boldsymbol{\tau}_c](\mathbf{r}) d^3r}. \quad (4.9)$$

Even though the FLAPW basis is constructed to give a good representation of the system one wishes to study, it lacks the flexibility to describe a perturbed system. Therefore, the derivative of the Kohn-Sham states with respect to the atomic displacement cannot fully be described by the same FLAPW basis. As a consequence, the Hellmann-Feynman theorem does not yield the complete atomic force. We now have to introduce the variation in the eigenfunctions of the Kohn-Sham system as well.

$$\begin{aligned} n_{i\mathbf{k}}\delta\epsilon_i[\delta\boldsymbol{\tau}_c](\mathbf{k}) &= n_{i\mathbf{k}} \int_{\Omega} \rho_{i\mathbf{k}}(\mathbf{r}) \delta V_{\text{eff}}[\delta\boldsymbol{\tau}_c](\mathbf{r}) d^3r \\ &\quad + 2n_{i\mathbf{k}} \text{Re} \left(\int_{\Omega} \delta\psi_{i\mathbf{k}}^*[\delta\boldsymbol{\tau}_c](\mathbf{r}) \left\{ -\frac{1}{2}\nabla^2 + V_{\text{eff}}(\mathbf{r}) - \epsilon_i(\mathbf{k}) \right\} \psi_{i\mathbf{k}}(\mathbf{r}) d^3r \right) \end{aligned}$$

We see that the first term cancels with the last expression in equation (4.3). The contribution to the Pulay correction coming from the valence electrons then becomes

$$\mathbf{F}_{\text{val}}^c = -2 \sum_{\mathbf{k}i \in \text{val}} n_{i\mathbf{k}} \text{Re} \left(\int_{\Omega} \frac{\delta\psi_{i\mathbf{k}}^*[\delta\boldsymbol{\tau}_c](\mathbf{r})}{\delta\boldsymbol{\tau}_c} \left\{ -\frac{1}{2}\nabla^2 + V_{\text{eff}}(\mathbf{r}) - \epsilon_i(\mathbf{k}) \right\} \psi_{i\mathbf{k}}(\mathbf{r}) d^3r \right).$$

If written in terms of operators,

$$\mathbf{F}_{\text{val}}^c = -2 \sum_{\mathbf{k}i \in \text{val}} n_{i\mathbf{k}} \text{Re} \left\langle \frac{\delta\psi_{i\mathbf{k}}[\delta\boldsymbol{\tau}_c]}{\delta\boldsymbol{\tau}_c} \left| \mathcal{H} - \epsilon_i(\mathbf{k}) \right| \psi_{i\mathbf{k}} \right\rangle,$$

one would be tempted to argue that this term should vanish. However, as was emphasized above, the FLAPW basis set, in which the eigenfunctions $\psi(\mathbf{r})$ are expressed, is incomplete. The variation of the eigenfunctions is not necessarily expandable in the same basis set, and as such it acts in a distributive manner on the Hilbert space available.

4.2.3. Discontinuity correction

There is an additional feature of the FLAPW basis that leads to a correction. While the basis functions are constructed to be continuous up to first order on the muffin-tin boundaries, the kinetic energy operator is a differential operator of second order. The rigorous distinction between interstitial region and muffin-tin spheres causes a surface contribution from the boundaries, as will be shown below.

4. Forces from total energy calculations

The basis functions and the Kohn-Sham eigenfunctions may be written with the idempotent projection function Θ (the unit step function) as:

$$\begin{aligned}\phi_{\mathbf{k}\mathbf{G}}(\mathbf{r}) &= \frac{1}{\sqrt{\Omega}} e^{i(\mathbf{k}+\mathbf{G})\cdot\mathbf{r}} \left(1 - \sum_{a \in \Omega} \Theta(\mathbf{r} \in B_{R_a}(\boldsymbol{\tau}_a)) \right) \\ &\quad + \sum_{a \in \Omega} \sum_{lm} \left(a_{lm}^{a\mathbf{k}\mathbf{G}} u_l(r) Y_{lm}(\hat{\mathbf{r}}) + b_{lm}^{a\mathbf{k}\mathbf{G}} \dot{u}_l(r) Y_{lm}(\hat{\mathbf{r}}) \right) \Theta(\mathbf{r} \in B_{R_a}(\boldsymbol{\tau}_a)) \\ \psi_{i\mathbf{k}}(\mathbf{r}) &= \sum_G z_{i\mathbf{k}\mathbf{G}} \phi_{\mathbf{k}\mathbf{G}}(\mathbf{r}) \left(1 - \sum_{a \in \Omega} \Theta(\mathbf{r} \in B_{R_a}(\boldsymbol{\tau}_a)) \right) \\ &\quad + \sum_{a \in \Omega} \sum_G z_{i\mathbf{k}\mathbf{G}} \phi_{\mathbf{k}\mathbf{G}}(\mathbf{r}) \Theta(\mathbf{r} \in B_{R_a}(\boldsymbol{\tau}_a))\end{aligned}$$

In the local frame of atom c , the unit step function translates to $\Theta(|\mathbf{r} - \boldsymbol{\tau}_c| \leq R_c)$, which becomes $\Theta(|\mathbf{r} - \boldsymbol{\tau}_c - \delta\boldsymbol{\tau}_c| \leq R_c)$ in the disturbed system. Applying the variation to this expression leads to

$$\frac{\delta}{\delta\boldsymbol{\tau}_c} \Theta(|\mathbf{r} - \boldsymbol{\tau}_c| \leq R_c) = -\frac{(\mathbf{r} - \boldsymbol{\tau}_c)}{|\mathbf{r} - \boldsymbol{\tau}_c|} \delta(|\mathbf{r} - \boldsymbol{\tau}_c| = R_c) = -\hat{\mathbf{r}}_c \delta(|\mathbf{r} - \boldsymbol{\tau}_c| = R_c),$$

the Dirac delta distribution weighted only on the muffin-tin boundary. Executing just this part of the variation to the altered wave functions in (4.9) (and remembering the idempotence of Θ), one obtains for the discontinuity correction:

$$\begin{aligned}\mathbf{F}_{\text{disc}}^c &= - \sum_{\mathbf{k}i} n_{i\mathbf{k}} \oint_{\partial B_{R_c}(\boldsymbol{\tau}_c)} \left[\psi_{i\mathbf{k}}^*(\mathbf{r}) \left(-\frac{1}{2} \nabla^2 \right) \psi_{i\mathbf{k}}(\mathbf{r}) \Big|_{\text{MT}_c} - \psi_{i\mathbf{k}}^*(\mathbf{r}) \left(-\frac{1}{2} \nabla^2 \right) \psi_{i\mathbf{k}}(\mathbf{r}) \Big|_{\text{IS}} \right] \hat{\mathbf{r}}_c dS_2\end{aligned}$$

Due to the continuity of the wave functions on the muffin-tin boundary, the terms $\psi_{i\mathbf{k}}^*(\mathbf{r}) [V_{\text{eff}}(\mathbf{r}) - \epsilon_i] \psi_{i\mathbf{k}}(\mathbf{r})$ are equal in muffin-tin and interstitial representation on the sphere shell. Thus, there are no additional contributions from them.

5. Stress from total energy calculations

Now that we followed through the steps presented in Yu's paper [YSK91] for the calculation of atomic forces, we proceed in a similar manner for the stress calculation. In order to obtain the stress tensor, we need to find a parametrization of the total energy with respect to strain. Since straining the system means a coordinated displacement of all atoms of the system instead of only one atom, we expect to find contributions that resemble those of the atomic force calculation. Furthermore, the unit cell volume can change. This will result in contributions in addition to those that we derived for the atomic force calculation. If we have self-consistently calculated the quantities of a certain configuration, we know its electronic density $\rho(\mathbf{r})$, its effective potential $V_{\text{eff}}(\mathbf{r})$ etc. Next, we imagine a set of quantities belonging to a configuration slightly strained by a tensor $\underline{\underline{\varepsilon}}$. Examples are the new electronic density $\rho[\underline{\underline{\varepsilon}}]$, the new effective potential $V_{\text{eff}}[\underline{\underline{\varepsilon}}]$ and the Kohn-Sham eigenvalues $\epsilon_i[\underline{\underline{\varepsilon}}]$. In the strained system, the atomic positions and spatial vectors have changed from $\boldsymbol{\tau}_a$ and \mathbf{r} to $\boldsymbol{\tau}_a[\underline{\underline{\varepsilon}}] = (\underline{\underline{1}} + \underline{\underline{\varepsilon}})\boldsymbol{\tau}_a$, and the volume has become $\Omega[\underline{\underline{\varepsilon}}]$, which is the triple product of the strained lattice vectors. Vectors in reciprocal space as well as the nabla operator will transform inversely, i.e., $\nabla_\varepsilon = (\underline{\underline{1}} - \underline{\underline{\varepsilon}})\nabla$. Letting \mathbf{r}_ε and \mathbf{s}_ε denote the integration variables and \mathbf{k}_ε the wave vectors in the strained system, we can write the total energy (2.8) of this system as

$$E[\underline{\underline{\varepsilon}}] = \sum_{\mathbf{k}_\varepsilon i} n_i \mathbf{k}_\varepsilon \epsilon_i[\underline{\underline{\varepsilon}}](\mathbf{k}_\varepsilon) - \int_{\Omega[\underline{\underline{\varepsilon}}]} \rho[\underline{\underline{\varepsilon}}](\mathbf{r}_\varepsilon) V_{\text{eff}}[\underline{\underline{\varepsilon}}](\mathbf{r}_\varepsilon) d^3 r_\varepsilon + \int_{\Omega[\underline{\underline{\varepsilon}}]} \rho[\underline{\underline{\varepsilon}}](\mathbf{r}_\varepsilon) \varepsilon_{\text{xc}}[\underline{\underline{\varepsilon}}](\mathbf{r}_\varepsilon) d^3 r_\varepsilon \quad (5.1a)$$

$$+ \frac{1}{2} \int_{\Omega[\underline{\underline{\varepsilon}}]} \rho[\underline{\underline{\varepsilon}}](\mathbf{r}_\varepsilon) \left\{ \int_{\mathbb{R}} \frac{\rho[\underline{\underline{\varepsilon}}](\mathbf{s}_\varepsilon)}{|\mathbf{r}_\varepsilon - \mathbf{s}_\varepsilon|} d^3 s_\varepsilon - \sum_b^{\text{atoms}} \frac{Z_b}{|\mathbf{r}_\varepsilon - \boldsymbol{\tau}_b[\underline{\underline{\varepsilon}}]|} \right\} d^3 r_\varepsilon \quad (5.1b)$$

$$- \frac{1}{2} \sum_{a \in \Omega[\underline{\underline{\varepsilon}}]}^{\text{atoms}} Z_a \left\{ \int_{\mathbb{R}} \frac{\rho[\underline{\underline{\varepsilon}}](\mathbf{s}_\varepsilon)}{|\boldsymbol{\tau}_a[\underline{\underline{\varepsilon}}] - \mathbf{s}_\varepsilon|} d^3 s_\varepsilon - \sum_{b \neq a}^{\text{atoms}} \frac{Z_b}{|\boldsymbol{\tau}_a[\underline{\underline{\varepsilon}}] - \boldsymbol{\tau}_b[\underline{\underline{\varepsilon}}]|} \right\}. \quad (5.1c)$$

by using a similar notation as with the atomic forces.

The ground-state valence density $\rho_v[\underline{\underline{\varepsilon}}](\mathbf{r}_\varepsilon)$ acquires a somewhat different shape due to the change in the new crystal field. The core density $\rho_c^a[\underline{\underline{\varepsilon}}](\mathbf{r}_\varepsilon - \boldsymbol{\tau}_a[\underline{\underline{\varepsilon}}])$ of an atom a , on the other hand, is defined in a new muffin-tin sphere of the same radius as in the unstrained system but centered at the new atomic position $\boldsymbol{\tau}_a[\underline{\underline{\varepsilon}}]$. It thus moves along with the atom in addition to a change in its shape.

The most obvious change of the energy formula to the one expressing an atomic displacement (4.1) is, as expected, the change in the volume of integration. Therefore,

5. Stress from total energy calculations

a variation in strain introduces terms coming from the surface of the unit cell.

However, to avoid those surface terms, we can back-transform the integration volume to the unstrained volume Ω by the substitution $\mathbf{r}_\varepsilon \rightarrow (\underline{1} + \underline{\varepsilon})\mathbf{r}$ when dealing with the Kohn-Sham states. This introduces a Jacobian $\det(\underline{1} + \underline{\varepsilon})$. We then can avoid the surface terms at the cost of an explicit dependence of the spatial vectors on the strain according to

$$\int_{\Omega[\underline{\varepsilon}]} f(\mathbf{r}_\varepsilon) d^3 r_\varepsilon = \det(\underline{1} + \underline{\varepsilon}) \int_{\Omega} f(\mathbf{r}[\underline{\varepsilon}]) d^3 r. \quad (5.2)$$

5.1. Recurring relations

In the derivation of the stress components, which will be performed in the order of their appearance in the total energy formula, there will be a certain amount of repetition. Some expressions will appear in many terms of the stress formula, and we want to provide some handy definitions and examples for the most common ones.

We will exploit the fact that the stress as well as the strain are symmetric tensors, i.e., $\underline{\varepsilon}^T = \underline{\varepsilon}$. For the variation in a strained vector \mathbf{v}_ε and its absolute, we have

$$\left. \frac{\delta}{\delta \varepsilon_{\alpha\beta}} (\underline{1} \pm \underline{\varepsilon}) \mathbf{v} \right|_{\underline{\varepsilon}=0} = \left. \frac{\delta}{\delta \varepsilon_{\alpha\beta}} \left(\delta_{ij} \pm \frac{\varepsilon_{ij} + \varepsilon_{ji}}{2} \right) v_j \hat{\mathbf{e}}_i \right|_{\underline{\varepsilon}=0} = \pm \frac{1}{2} (v_\alpha \hat{\mathbf{e}}_\beta + v_\beta \hat{\mathbf{e}}_\alpha), \quad (5.3)$$

$$\begin{aligned} \left. \frac{\delta}{\delta \varepsilon_{\alpha\beta}} |(\underline{1} \pm \underline{\varepsilon}) \mathbf{v}| \right|_{\underline{\varepsilon}=0} &= \left. \frac{\delta}{\delta \varepsilon_{\alpha\beta}} \left[(\delta_{ij} \pm \frac{\varepsilon_{ij} + \varepsilon_{ji}}{2}) v_j (\delta_{ik} \pm \frac{\varepsilon_{ik} + \varepsilon_{ki}}{2}) v_k \right]^{1/2} \right|_{\underline{\varepsilon}=0} \\ &= \pm \frac{v_\alpha v_\beta}{v}. \end{aligned} \quad (5.4)$$

Then the variation in the volume is

$$\left. \frac{\delta}{\delta \varepsilon_{\alpha\beta}} \Omega[\underline{\varepsilon}] \right|_{\underline{\varepsilon}=0} = \left. \frac{\delta}{\delta \varepsilon_{\alpha\beta}} \det((\underline{1} + \underline{\varepsilon})(\mathbf{abc})) \right|_{\underline{\varepsilon}=0} = \delta_{\alpha\beta} \det(\mathbf{abc}) = \delta_{\alpha\beta} \Omega. \quad (5.5)$$

In the muffin-tin spheres, all quantities are expanded into spherical harmonics. Therefore, we have to take a look at these, too.

We already used the Gaunt coefficients G , which are defined as integrals of products of three spherical harmonics over the unit sphere boundary,

$$G_{l'l''}^{mm'm''} = \oint_{B_1(\mathbf{0})} Y_{lm}^*(\hat{\mathbf{r}}) Y_{l'm'}(\hat{\mathbf{r}}) Y_{l''m''}(\hat{\mathbf{r}}) dS_2. \quad (5.6)$$

It is nonzero only for those combinations of arguments for which $m = m' + m''$ and $|l' - l''| \leq l \leq l' + l''$. Furthermore, $l + l' + l''$ has to be even.

We also define the unit vector expansion coefficient $c_{\alpha t}$ and the differential factor $c_\alpha^{st}(l, m)$.

5.1. Recurring relations

The unit vector expansion coefficient $c_{\alpha t}$ is the projection of the α -component of a unit vector along direction $\hat{\mathbf{r}}$ onto $Y_{1t}(\hat{\mathbf{r}})$:

$$c_{\alpha t} = \oint_{B_1(\mathbf{0})} \hat{r}_\alpha Y_{1t}^*(\hat{\mathbf{r}}) dS_2 \quad (5.7a)$$

As the components of a unit vector can also be expressed in spherical harmonics with $l = 1$, the unit vector expansion coefficients are exactly the necessary coefficients

$$\underline{c} = (c_{\alpha t})_{\alpha=1\dots 3}^{t=-1\dots 1} \begin{pmatrix} \sqrt{\frac{2\pi}{3}} & 0 & -\sqrt{\frac{2\pi}{3}} \\ -i\sqrt{\frac{2\pi}{3}} & 0 & -i\sqrt{\frac{2\pi}{3}} \\ 0 & \sqrt{\frac{4\pi}{3}} & 0 \end{pmatrix}. \quad (5.7b)$$

Finally, it is known that the derivative of a spherical harmonic along a direction α times the radius r is a linear combination of spherical harmonics with an l quantum number shifted by 1 and an m quantum number shifted at most by 1. The differential factors are the expansion coefficients of the derivative of a spherical harmonic in terms of spherical harmonics,

$$c_\alpha^{st}(l, m) = \oint_{B_1(\mathbf{0})} [r\partial_\alpha Y_{lm}(\hat{\mathbf{r}})] Y_{l+s, m+t}^*(\hat{\mathbf{r}}) dS_2. \quad (5.8)$$

These quantities become relevant because, according to (5.3), the variation in a spherical harmonic of a strained vector is

$$\begin{aligned} \left. \frac{\delta}{\delta\varepsilon_{\alpha\beta}} Y_{lm}(\widehat{(\underline{1} \pm \underline{\varepsilon})\mathbf{v}}) \right|_{\underline{\varepsilon}=0} &= \left[\frac{\delta}{\delta\varepsilon_{\alpha\beta}} (\underline{1} \pm \underline{\varepsilon})\mathbf{v} \right]_{\underline{\varepsilon}=0} \cdot \nabla Y_{lm}(\hat{\mathbf{v}}) \\ &= \pm \frac{1}{2} (v_\alpha \partial_\beta + v_\beta \partial_\alpha) Y_{lm}(\hat{\mathbf{v}}) = \pm \frac{1}{2} (\hat{v}_\alpha v \partial_\beta + \hat{v}_\beta v \partial_\alpha) Y_{lm}(\hat{\mathbf{v}}) \\ &= \pm \frac{1}{2} \sum_{t'=-1}^1 Y_{1t'}(\hat{\mathbf{v}}) (c_{\alpha t'} v \partial_\beta + c_{\beta t'} v \partial_\alpha) Y_{lm}(\hat{\mathbf{v}}) \\ &= \pm \frac{1}{2} \sum_{s=-1}^{1,2} \sum_{t,t'=-1}^1 Y_{1t'}(\hat{\mathbf{v}}) (c_{\alpha t'} c_\beta^{st}(l, m) + c_{\beta t'} c_\alpha^{st}(l, m)) Y_{l+s, m+t}(\hat{\mathbf{v}}) \\ &= \pm \frac{1}{2} \sum_{s=-1}^{1,2} \sum_{t,t'=-1}^1 (c_{\alpha t'} c_\beta^{st}(l, m) + c_{\beta t'} c_\alpha^{st}(l, m)) \sum_{s'=|l+s-1|}^{l+s+1,2} G_{s',1,l+s}^{m+t+t',t',m+t} Y_{s', m+t+t'}(\hat{\mathbf{v}}) \end{aligned} \quad (5.9)$$

The second number above the summation symbols denotes the increment to the summation variable. While we will stay with the last but one line (5.9) in our calculations, the last line shows explicitly that the strain derivative of a spherical harmonic Y_{lm} mixes the spherical harmonics with l quantum numbers $l-2$, l , and $l+2$. The mixing in the m quantum numbers ranges from $m-2$ to $m+2$. This behavior matches with that of a differential operator of second order, as should be expected for differentiating with

5. Stress from total energy calculations

respect to a tensor of rank 2.

Another simple expression that will occur mainly when dealing with the atomic phase factors is the scalar product of strained spatial and reciprocal vectors. As the latter transform inversely to their spatial counterparts, we have

$$\mathbf{k}_\varepsilon \cdot \mathbf{r}_\varepsilon = (\underline{\mathbf{1}} - \underline{\varepsilon}) \mathbf{k} \cdot (\underline{\mathbf{1}} + \underline{\varepsilon}) \mathbf{r} = \mathbf{k} \cdot (\underline{\mathbf{1}} - \underline{\varepsilon})^T (\underline{\mathbf{1}} + \underline{\varepsilon}) \mathbf{r} = \mathbf{k} \cdot \mathbf{r}. \quad (5.10)$$

Note that this equation holds exactly for $(\underline{\mathbf{1}} + \underline{\varepsilon})^{-1}$ instead of $(\underline{\mathbf{1}} - \underline{\varepsilon})$. Since we are interested in an infinitesimal strain only, we find the latter term as the linear Taylor expansion for the inverse strain.

Keeping those relations in mind, we proceed with the calculation of the stress components.

5.2. Variation of the kinetic energy

The first two terms of (5.1a) contributed to the atomic force calculation with the Pulay correction. In the case of a strained system, we will find similar terms, but also additional contributions. The differentiation of the Kohn-Sham eigenvalues will be split into core and valence states. However, the derivative of the double counting term is the same for the two cases. A back-transformation to the unstrained volume results in

$$\begin{aligned} \frac{\delta}{\delta \varepsilon_{\alpha\beta}} \int_{\Omega[\underline{\varepsilon}]} \rho[\underline{\varepsilon}](\mathbf{r}_\varepsilon) V_{\text{eff}}[\underline{\varepsilon}](\mathbf{r}_\varepsilon) d^3 r_\varepsilon \Big|_{\underline{\varepsilon}=0} &= \frac{\delta}{\delta \varepsilon_{\alpha\beta}} \int_{\Omega} \det(\underline{\mathbf{1}} + \underline{\varepsilon}) \rho[\underline{\varepsilon}](\mathbf{r}[\underline{\varepsilon}]) V_{\text{eff}}[\underline{\varepsilon}](\mathbf{r}[\underline{\varepsilon}]) d^3 r \Big|_{\underline{\varepsilon}=0} \\ &= \delta_{\alpha\beta} \int_{\Omega} \rho(\mathbf{r}) V_{\text{eff}}(\mathbf{r}) d^3 r \end{aligned} \quad (5.11a)$$

$$+ \int_{\Omega} \left[\frac{\delta}{\delta \varepsilon_{\alpha\beta}} \rho[\underline{\varepsilon}](\mathbf{r}[\underline{\varepsilon}]) \Big|_{\underline{\varepsilon}=0} \right] V_{\text{eff}}(\mathbf{r}) d^3 r \quad (5.11b)$$

$$+ \int_{\Omega} \rho(\mathbf{r}) \left[\frac{\delta}{\delta \varepsilon_{\alpha\beta}} V_{\text{eff}}[\underline{\varepsilon}](\mathbf{r}[\underline{\varepsilon}]) \Big|_{\underline{\varepsilon}=0} \right] d^3 r \quad (5.11c)$$

We already know an expression of the form (5.11c) from the calculation of the atomic forces. It is the variation of the potential due to the new atomic configuration. The term (5.11b) did not explicitly appear since a change in coordinates of the electronic density $\rho(\mathbf{r}[\underline{\varepsilon}])$ did not happen within the force calculation. It was shown that the variation in the shape of the density $\rho[\underline{\varepsilon}](\mathbf{r})$ would cancel with similar terms. We will see that this is also the case in the context of the stress calculation. The trace term (5.11a) comes from the change in the unit-cell volume and is thus one of the additional terms in the stress calculation.

5.2.1. Contribution of core electrons

We want to consider the change in the eigenvalues of the core states. We can apply the Hellman-Feynman theorem to the core states as we did in chapter 4.2.1. For a core state i of atom a , this gives us

$$\left. \frac{\delta}{\delta \varepsilon_{\alpha\beta}} \epsilon_i[\underline{\varepsilon}] \right|_{\underline{\varepsilon}=0} = \left. \frac{\delta}{\delta \varepsilon_{\alpha\beta}} \left\langle \psi_i^a[\underline{\varepsilon}] \left| \left[-\frac{1}{2} \nabla^2 + V_{\text{eff}}[\underline{\varepsilon}](\mathbf{r}) \right] \right| \psi_i^a[\underline{\varepsilon}] \right\rangle_{\text{MT}_a} \right|_{\underline{\varepsilon}=0} \quad (5.12a)$$

$$= \left\langle \psi_i^a \left| \frac{\delta}{\delta \varepsilon_{\alpha\beta}} V_{\text{eff}}[\underline{\varepsilon}](\mathbf{r}) \right| \psi_i^a \right\rangle_{\text{MT}_a} \Big|_{\underline{\varepsilon}=0} \quad (5.12b)$$

$$= \int_{B_{R_a}(\mathbf{0})} \rho_i^a(\mathbf{r}_a) \left[\frac{\delta}{\delta \varepsilon_{\alpha\beta}} V_{\text{eff}}^a[\underline{\varepsilon}](\mathbf{r}_a) \Big|_{\underline{\varepsilon}=0} \right] d^3 r_a. \quad (5.12c)$$

Since the double counting term is subtracted from the eigenvalue sum, the core part of (5.11c) cancels the term from the eigenvalue sum. The remaining expression summed up over all core states is the core correction to the stress,

$$\begin{aligned} \sigma_{\alpha\beta}^{\text{core}} &= -\frac{1}{\Omega} \sum_{a \in \Omega}^{\text{atoms}} \int_{B_{R_a}(\mathbf{0})} \rho_c^a(\mathbf{r}_a) \left[\frac{\delta}{\delta \varepsilon_{\alpha\beta}} V_{\text{eff}}^a(\mathbf{r}_a[\underline{\varepsilon}]) \Big|_{\underline{\varepsilon}=0} \right] d^3 r_a \\ &= -\frac{1}{\Omega} \sum_{a \in \Omega}^{\text{atoms}} \int_{B_{R_a}(\mathbf{0})} \rho_c^a(\mathbf{r}_a) r_{a\alpha} \partial_\beta V_{\text{eff}}^a(\mathbf{r}_a) d^3 r_a. \end{aligned} \quad (5.13)$$

As (4.8) within the atomic forces, this term stems from the twofold change in the effective potential from the perspective of the original core density, that is the change in the shape of the potential and its displacement to the shifted lattice position. Only the former contribution is seen in the variation of the core eigenvalues, as the core states are displaced along the atomic nucleus in this case. (4.8) is obtained by applying the gradient to the effective potential, while the corresponding stress term is found by acting on the effective potential with the stress operator $\mathbf{r} \otimes \nabla$.

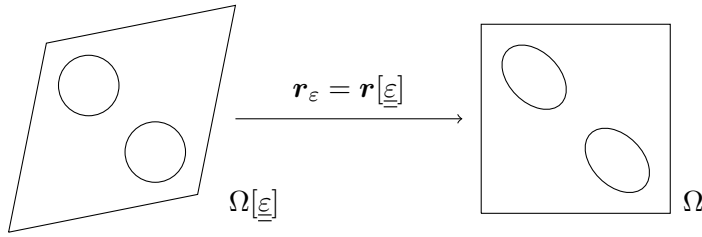


Figure 5.1.: The stress components from the valence states, the double counting term, and the exchange-correlation energy of the strained system are calculated using a back-transformation to the unstrained coordinates.

5. Stress from total energy calculations

5.2.2. Contribution of valence electrons

We will continue by evaluating the effect of the strain on the eigenvalues of the valence states. As the states extend over the whole lattice, the deformation of the unit cell yields surface terms. These will be avoided by back-transforming the strained volume to the original one. Using the Rayleigh quotient, we get

$$\begin{aligned} \left. \frac{\delta}{\delta \varepsilon_{\alpha\beta}} \epsilon_v[\underline{\underline{\varepsilon}}](\mathbf{k}_\varepsilon) \right|_{\underline{\underline{\varepsilon}}=0} &= \left. \frac{\delta}{\delta \varepsilon_{\alpha\beta}} \frac{\int_{\Omega[\underline{\underline{\varepsilon}}]} \psi_{v\mathbf{k}_\varepsilon}^*[\underline{\underline{\varepsilon}}](\mathbf{r}_\varepsilon) \left\{ -\frac{1}{2} \nabla_\varepsilon^2 + V_{\text{eff}}[\underline{\underline{\varepsilon}}](\mathbf{r}_\varepsilon) \right\} \psi_{v\mathbf{k}_\varepsilon}[\underline{\underline{\varepsilon}}](\mathbf{r}_\varepsilon) d^3 r_\varepsilon}{\int_{\Omega[\underline{\underline{\varepsilon}}]} \psi_{v\mathbf{k}_\varepsilon}^*[\underline{\underline{\varepsilon}}](\mathbf{r}_\varepsilon) \psi_{v\mathbf{k}_\varepsilon}[\underline{\underline{\varepsilon}}](\mathbf{r}_\varepsilon) d^3 r_\varepsilon} \right|_{\underline{\underline{\varepsilon}}=0} \\ &= \left. \frac{\delta}{\delta \varepsilon_{\alpha\beta}} \frac{\int_{\Omega} \psi_{v\mathbf{k}_\varepsilon}^*[\underline{\underline{\varepsilon}}](\mathbf{r}[\underline{\underline{\varepsilon}}]) \left\{ -\frac{1}{2} [(\underline{\underline{1}} - \underline{\underline{\varepsilon}}) \nabla]^2 + V_{\text{eff}}[\underline{\underline{\varepsilon}}](\mathbf{r}[\underline{\underline{\varepsilon}}]) \right\} \psi_{v\mathbf{k}_\varepsilon}[\underline{\underline{\varepsilon}}](\mathbf{r}[\underline{\underline{\varepsilon}}]) d^3 r}{\int_{\Omega} \psi_{v\mathbf{k}_\varepsilon}^*[\underline{\underline{\varepsilon}}](\mathbf{r}[\underline{\underline{\varepsilon}}]) \psi_{v\mathbf{k}_\varepsilon}[\underline{\underline{\varepsilon}}](\mathbf{r}[\underline{\underline{\varepsilon}}]) d^3 r} \right|_{\underline{\underline{\varepsilon}}=0} \\ &= 2 \operatorname{Re} \left(\int_{\Omega} \left[\left. \frac{\delta}{\delta \varepsilon_{\alpha\beta}} \psi_{v\mathbf{k}_\varepsilon}[\underline{\underline{\varepsilon}}](\mathbf{r}[\underline{\underline{\varepsilon}}]) \right|_{\underline{\underline{\varepsilon}}=0} \right]^* (\mathcal{H} - \epsilon_v(\mathbf{k})) \psi_{v\mathbf{k}}(\mathbf{r}) d^3 r \right) \end{aligned} \quad (5.14a)$$

$$\begin{aligned} &- \frac{1}{2} \sum_{a \in \Omega}^{\text{atoms}} R_a^3 \oint_{S_2} s_\alpha s_\beta \left\{ \psi_{v\mathbf{k}}^{\text{MT}a*}(R_a \mathbf{s}) \nabla^2 \psi_{v\mathbf{k}}^{\text{MT}a}(R_a \mathbf{s}) \right. \\ &\quad \left. - \psi_{v\mathbf{k}}^{\text{IS}*}(R_a \mathbf{s} + \boldsymbol{\tau}_a) \nabla^2 \psi_{v\mathbf{k}}^{\text{IS}}(R_a \mathbf{s} + \boldsymbol{\tau}_a) \right\} dS_2 \end{aligned} \quad (5.14b)$$

$$+ \frac{1}{2} \int_{\Omega} \psi_{v\mathbf{k}}^*(\mathbf{r}) (\partial_\alpha \partial_\beta + \partial_\beta \partial_\alpha) \psi_{v\mathbf{k}}(\mathbf{r}) d^3 r \quad (5.14c)$$

$$+ \int_{\Omega} |\psi_{v\mathbf{k}}(\mathbf{r})|^2 \left[\left. \frac{\delta}{\delta \varepsilon_{\alpha\beta}} V_{\text{eff}}[\underline{\underline{\varepsilon}}](\mathbf{r}[\underline{\underline{\varepsilon}}]) \right|_{\underline{\underline{\varepsilon}}=0} \right] d^3 r. \quad (5.14d)$$

The first two terms of this formula explicitly account for the incompleteness of the FLAPW basis and correspond to $\mathbf{F}_{\text{val}}^c$ and $\mathbf{F}_{\text{disc}}^c$. The discontinuity correction does not only take into account the displacement of the atoms but also the deformation of the muffin-tin spheres due to the back-transformation $B_{R_a}(\mathbf{0}) \rightarrow (\underline{\underline{1}} - \underline{\underline{\varepsilon}}) B_{R_a}(\mathbf{0})$. We thus define the Pulay contributions of the incomplete basis set and the surface term as:

$$\Omega \sigma_{\alpha\beta}^{\text{val}} = (5.14a) \quad (5.15a)$$

$$\Omega \sigma_{\alpha\beta}^{\text{disc}} = (5.14b) \quad (5.15b)$$

The last term (5.14d) cancels with the valence part of (5.11c). The remaining expression (5.14c) is a contribution from the variation in the kinetic energy of the valence states. Because the valence states have to adjust to the strained volume, they have a different bending. This is seen by the kinetic energy operator.

5.3. Exchange-correlation contribution

The stress contribution that stems from the change in the exchange correlation energy is best found if the total electronic density is back-transformed into the old system. In

the case of local approximations to the exchange-correlation functional like the LDA or GGA, this yields

$$\begin{aligned} & \left. \frac{\delta}{\delta \varepsilon_{\alpha\beta}} \int_{\Omega[\underline{\varepsilon}]} \rho[\underline{\varepsilon}](\mathbf{r}_\varepsilon) \varepsilon_{\text{xc}}[\underline{\varepsilon}](\mathbf{r}_\varepsilon) d^3 r_\varepsilon \right|_{\underline{\varepsilon}=0} \\ &= \frac{\delta}{\delta \varepsilon_{\alpha\beta}} \det(\mathbf{1} + \underline{\varepsilon}) \int_{\Omega} \rho[\underline{\varepsilon}](\mathbf{r}[\underline{\varepsilon}]) \varepsilon_{\text{xc}}[\underline{\varepsilon}](\mathbf{r}[\underline{\varepsilon}]) d^3 r \Big|_{\underline{\varepsilon}=0} \\ &= \delta_{\alpha\beta} \int_{\Omega} \rho(\mathbf{r}) \varepsilon_{\text{xc}}(\mathbf{r}) d^3 r \end{aligned} \quad (5.16a)$$

$$+ \int_{\Omega} \left[\frac{\delta}{\delta \varepsilon_{\alpha\beta}} \rho[\underline{\varepsilon}](\mathbf{r}[\underline{\varepsilon}]) \Big|_{\underline{\varepsilon}=0} \right] \mu_{\text{xc}}(\mathbf{r}) d^3 r. \quad (5.16b)$$

The variation of the density (5.16b) cancels with the exchange-correlation part of the corresponding expression in the stress contributions from the double counting term (5.11b). This leaves only the electrostatic potential as integrand for the strained density. The trace term (5.16b) is due to the change in volume.

In total, we obtain as the strain derivative of the first line (5.1a) of the total energy

$$\left. \frac{\delta}{\delta \varepsilon_{\alpha\beta}} \left\{ \sum_{\mathbf{k}_\varepsilon i} n_{i\mathbf{k}_\varepsilon} \varepsilon_i[\underline{\varepsilon}](\mathbf{k}_\varepsilon) - \int_{\Omega[\underline{\varepsilon}]} \rho[\underline{\varepsilon}](\mathbf{r}_\varepsilon) V_{\text{eff}}[\underline{\varepsilon}](\mathbf{r}_\varepsilon) d^3 r_\varepsilon + \int_{\Omega[\underline{\varepsilon}]} \rho[\underline{\varepsilon}](\mathbf{r}_\varepsilon) \varepsilon_{\text{xc}}[\underline{\varepsilon}](\mathbf{r}_\varepsilon) d^3 r_\varepsilon \right\} \right|_{\underline{\varepsilon}=0}$$

$$\begin{aligned} &= \Omega \sigma_{\alpha\beta}^{\text{core}} + \Omega \sigma_{\alpha\beta}^{\text{val}} + \Omega \sigma_{\alpha\beta}^{\text{disc}} \\ &+ \frac{1}{2} \sum_{\mathbf{k}v} n_{v\mathbf{k}} \int_{\Omega} \psi_{v\mathbf{k}}^*(\mathbf{r}) (\partial_\alpha \partial_\beta + \partial_\beta \partial_\alpha) \psi_{v\mathbf{k}}(\mathbf{r}) d^3 r \\ &+ \delta_{\alpha\beta} \int_{\Omega} \rho(\mathbf{r}) (\varepsilon_{\text{xc}}(\mathbf{r}) - V_{\text{eff}}(\mathbf{r})) d^3 r \end{aligned} \quad (5.17a)$$

$$- \int_{\Omega} \left[\frac{\delta}{\delta \varepsilon_{\alpha\beta}} \rho[\underline{\varepsilon}](\mathbf{r}[\underline{\varepsilon}]) \Big|_{\underline{\varepsilon}=0} \right] V_C(\mathbf{r}) d^3 r \quad (5.17b)$$

with $\sigma_{\alpha\beta}^{\text{core}}$, $\sigma_{\alpha\beta}^{\text{val}}$, and $\sigma_{\alpha\beta}^{\text{disc}}$ as in (5.13), (5.15a), and (5.15b), respectively.

5.4. Variation of the electrostatic energy

What remains to be calculated is the stress contribution coming from the electrostatic interaction between all electrons and nuclei, the derivatives of (5.1b) and (5.1c). Simply back-transforming the system to the unstrained volume would yield integrands of the form

$$\left. \frac{\delta}{\delta \varepsilon_{\alpha\beta}} \frac{1}{|\mathbf{r}[\underline{\varepsilon}] - \mathbf{s}[\underline{\varepsilon}]|} \right|_{\underline{\varepsilon}=0} = - \frac{(\mathbf{r} - \mathbf{s})_\alpha (\mathbf{r} - \mathbf{s})_\beta}{|\mathbf{r} - \mathbf{s}|^3}. \quad (5.18)$$

5. Stress from total energy calculations

To the knowledge of the author, these integrands cannot conveniently be integrated. Therefore, we want to refrain from back-transforming the coordinates. This will only be done to sort out the strain derivative of the charge density using

$$\begin{aligned}
\frac{\delta}{\delta\varepsilon_{\alpha\beta}} \int_{\Omega[\underline{\varepsilon}]} f[\underline{\varepsilon}](\mathbf{r}_\varepsilon) g[\underline{\varepsilon}](\mathbf{r}_\varepsilon) d^3 r_\varepsilon \Big|_{\underline{\varepsilon}=0} &= \frac{\delta}{\delta\varepsilon_{\alpha\beta}} \det(\underline{1} + \underline{\varepsilon}) \int_{\Omega} f[\underline{\varepsilon}](\mathbf{r}[\underline{\varepsilon}]) g[\underline{\varepsilon}](\mathbf{r}[\underline{\varepsilon}]) d^3 r \Big|_{\underline{\varepsilon}=0} \\
&= \int_{\Omega} \left[\frac{\delta}{\delta\varepsilon_{\alpha\beta}} f[\underline{\varepsilon}](\mathbf{r}[\underline{\varepsilon}]) \Big|_{\underline{\varepsilon}=0} \right] g(\mathbf{r}) d^3 r \\
&\quad + \frac{\delta}{\delta\varepsilon_{\alpha\beta}} \det(\underline{1} + \underline{\varepsilon}) \int_{\Omega} f(\mathbf{r}) g[\underline{\varepsilon}](\mathbf{r}[\underline{\varepsilon}]) d^3 r \Big|_{\underline{\varepsilon}=0} \\
&= \int_{\Omega} \left[\frac{\delta}{\delta\varepsilon_{\alpha\beta}} f[\underline{\varepsilon}](\mathbf{r}[\underline{\varepsilon}]) \Big|_{\underline{\varepsilon}=0} \right] g(\mathbf{r}) d^3 r \\
&\quad + \frac{\delta}{\delta\varepsilon_{\alpha\beta}} \int_{\Omega} f((\underline{1} - \underline{\varepsilon})\mathbf{r}_\varepsilon) g[\underline{\varepsilon}](\mathbf{r}_\varepsilon) d^3 r_\varepsilon \Big|_{\underline{\varepsilon}=0}. \quad (5.19)
\end{aligned}$$

Performing the differentiation of the electrostatic energy then gives for the electrostatic stress

$$\begin{aligned}
\Omega\sigma_{\alpha\beta}^{\text{es}} &= \frac{1}{2} \int_{\Omega} \left[\frac{\delta}{\delta\varepsilon_{\alpha\beta}} \rho[\underline{\varepsilon}](\mathbf{r}[\underline{\varepsilon}]) \Big|_{\underline{\varepsilon}=0} \right] V_C(\mathbf{r}) d^3 r \\
&\quad + \frac{1}{2} \int_{\Omega} \left[\frac{\delta}{\delta\varepsilon_{\alpha\beta}} \rho[\underline{\varepsilon}](\mathbf{r}[\underline{\varepsilon}]) \Big|_{\underline{\varepsilon}=0} \right] \left\{ \int_{\mathbb{R}^3} \frac{\rho(\mathbf{s})}{|\mathbf{r} - \mathbf{s}|} d^3 s - \sum_b^{\text{atoms}} \frac{Z_b}{|\mathbf{r} - \boldsymbol{\tau}_b|} \right\} d^3 r \\
&\quad + \frac{1}{2} \frac{\delta}{\delta\varepsilon_{\alpha\beta}} \int_{\Omega[\underline{\varepsilon}]} \rho((\underline{1} - \underline{\varepsilon})\mathbf{r}_\varepsilon) V_C[\underline{\varepsilon}](\mathbf{r}_\varepsilon) d^3 r_\varepsilon \Big|_{\underline{\varepsilon}=0} \quad (5.20a)
\end{aligned}$$

$$- \frac{1}{2} \sum_{a \in \Omega}^{\text{atoms}} Z_a \left[\frac{\delta}{\delta\varepsilon_{\alpha\beta}} V_M^a[\underline{\varepsilon}](\boldsymbol{\tau}_a[\underline{\varepsilon}]) \Big|_{\underline{\varepsilon}=0} \right], \quad (5.20b)$$

where the first two terms are identical and sum up to cancel (5.17b). They are written on two lines to emphasize their origin: The first line is a direct differentiation of the density in (5.1b) while to the second line the differentiation of the density in the electrostatic potential (5.1b) and the Madelung potential (5.1c) contributes. New alternative electrostatic and Madelung potentials are used in this equation. They are given as

$$V_C[\underline{\varepsilon}](\mathbf{r}_\varepsilon) = \int_{\mathbb{R}^3} \frac{\rho((\underline{1} - \underline{\varepsilon})\mathbf{s}_\varepsilon)}{|\mathbf{r}_\varepsilon - \mathbf{s}_\varepsilon|} d^3 s_\varepsilon - \sum_b^{\text{atoms}} \frac{Z_b}{|\mathbf{r}_\varepsilon - \boldsymbol{\tau}_b[\underline{\varepsilon}]|} \quad \text{and} \quad (5.21)$$

$$V_M^a[\underline{\varepsilon}](\boldsymbol{\tau}_a[\underline{\varepsilon}]) = \int_{\mathbb{R}^3} \frac{\rho((\underline{1} - \underline{\varepsilon})\mathbf{s}_\varepsilon)}{|\boldsymbol{\tau}_a[\underline{\varepsilon}] - \mathbf{s}_\varepsilon|} d^3 s_\varepsilon - \sum_{b \neq a}^{\text{atoms}} \frac{Z_b}{|\boldsymbol{\tau}_a[\underline{\varepsilon}] - \boldsymbol{\tau}_b[\underline{\varepsilon}]|}. \quad (5.22)$$

In contrast to the actual electrostatic and Madelung potential of the strained system, these equations define the alternative potentials as coming from known quantities: The valence density of the unstrained system smeared over the strained lattice and the core density of the unstrained system, moved along with the nuclei to the positions of the nuclei in the strained lattice and smeared over the ellipsoids $(\underline{1} - \underline{\varepsilon})B_R(\boldsymbol{\tau}[\underline{\varepsilon}])$. Consequently, the whole charge density is smeared over the lattice. Thus, the density generating these potentials, which can be plugged into (3.22b) and (3.23), is

$$n[\underline{\varepsilon}](\mathbf{r}_\varepsilon) = \rho((\underline{1} - \underline{\varepsilon})\mathbf{r}_\varepsilon) - \sum_{b \in \mathbb{R}^3} Z_b \delta(\mathbf{r}_\varepsilon - \boldsymbol{\tau}_b[\underline{\varepsilon}]). \quad (5.23)$$

5.4.1. Electrostatic pressure formulas

The introduction of an alternative electrostatic and Madelung potential is necessary to avoid terms of the form

$$\frac{\delta}{\delta \varepsilon_{\alpha\beta}} \frac{1}{|\mathbf{r}[\underline{\varepsilon}] - \mathbf{s}[\underline{\varepsilon}]|} \Big|_{\underline{\varepsilon}=0} = - \frac{(\mathbf{r} - \mathbf{s})_\alpha (\mathbf{r} - \mathbf{s})_\beta}{|\mathbf{r} - \mathbf{s}|^3}, \quad (5.24)$$

which would give rise to integrals that cannot be evaluated analytically. However, the pressure, which corresponds to the negative trace of the stress, preserves the $1/r$ form of the electrostatic potential. Therefore, we have with the pressure formula a decent check for the implementation of the electrostatic stress. The trace of the derivatives of (5.20a) and (5.20b) is given by

$$\begin{aligned} & \frac{1}{2} \sum_{\alpha=1}^3 \frac{\delta}{\delta \varepsilon_{\alpha\alpha}} \left[\int_{\Omega[\underline{\varepsilon}]} \rho((\underline{1} - \underline{\varepsilon})\mathbf{r}_\varepsilon) V_C[\underline{\varepsilon}](\mathbf{r}_\varepsilon) d^3 r_\varepsilon \right] \Big|_{\underline{\varepsilon}=0} \\ &= \frac{1}{2} \sum_{\alpha=1}^3 \frac{\delta}{\delta \varepsilon_{\alpha\alpha}} \left[\int_{\Omega} \rho(\mathbf{r}) \left\{ \int_{\mathbb{R}^3} \frac{\det^2(\underline{1} + \underline{\varepsilon}) \rho(\mathbf{s})}{|\mathbf{r}[\underline{\varepsilon}] - \mathbf{s}[\underline{\varepsilon}]|} d^3 s - \sum_b^{\text{atoms}} \frac{\det(\underline{1} + \underline{\varepsilon}) Z_b}{|\mathbf{r}[\underline{\varepsilon}] - \boldsymbol{\tau}_b[\underline{\varepsilon}]|} \right\} d^3 r \right] \Big|_{\underline{\varepsilon}=0} \\ &= \int_{\Omega} \rho(\mathbf{r}) V_C(\mathbf{r}) d^3 r + \frac{3}{2} \int_{\Omega} \rho(\mathbf{r}) \int_{\mathbb{R}^3} \frac{\rho(\mathbf{s})}{|\mathbf{r} - \mathbf{s}|} d^3 s d^3 r \end{aligned}$$

and

$$\begin{aligned} & - \frac{1}{2} \sum_{a \in \Omega}^{\text{atoms}} Z_a \sum_{\alpha=1}^3 \frac{\delta}{\delta \varepsilon_{\alpha\alpha}} V_M^a[\underline{\varepsilon}](\boldsymbol{\tau}_a[\underline{\varepsilon}]) \Big|_{\underline{\varepsilon}=0} \\ &= - \frac{1}{2} \sum_{a \in \Omega}^{\text{atoms}} Z_a \sum_{\alpha=1}^3 \frac{\delta}{\delta \varepsilon_{\alpha\alpha}} \left\{ \det(\underline{1} + \underline{\varepsilon}) \int_{\mathbb{R}^3} \frac{\rho(\mathbf{s})}{|\mathbf{r}[\underline{\varepsilon}] - \mathbf{s}[\underline{\varepsilon}]|} d^3 s - \sum_{b \neq a}^{\text{atoms}} \frac{Z_b}{|\mathbf{r}[\underline{\varepsilon}] - \boldsymbol{\tau}_b[\underline{\varepsilon}]|} \right\} \Big|_{\underline{\varepsilon}=0} \\ &= - \frac{3}{2} \int_{\Omega} \rho(\mathbf{r}) \sum_b^{\text{atoms}} \frac{Z_b}{|\mathbf{r} - \boldsymbol{\tau}_b|} d^3 r + \frac{1}{2} \sum_{a \in \Omega}^{\text{atoms}} Z_a V_M^a(\boldsymbol{\tau}_a). \end{aligned}$$

5. Stress from total energy calculations

Summed up, we obtain as a control formula for the electrostatic part of the pressure

$$-3P_{\text{es}}\Omega = \frac{5}{2} \int_{\Omega} \rho(\mathbf{r}) V_C(\mathbf{r}) d^3r + \frac{1}{2} \sum_{a \in \Omega}^{\text{atoms}} Z_a V_M^a(\boldsymbol{\tau}_a). \quad (5.25)$$

5.4.2. Variation of the alternative electrostatic potential

As they were constructed in (5.21) and (5.22), the alternative electrostatic and Madelung potential contain the electronic density of the unstrained system, with the core and valence parts being smeared over the strained lattice and the core part being displaced along with the nuclei. The latter part will result in a simplification of our calculations, as inside a muffin-tin sphere no change in the potential risen by the nucleus will be seen. Therefore, a nucleus will reproduce the same multipole moments as in the unstrained case and the only differences are the smeared charge density and the multipoles of the atoms outside of the muffin-tin sphere at their strained locations. This explicitly means that the strain variation of the alternative electrostatic and Madelung potential should be the same at an atomic position.

We have already explained Weinert's method in chapter 3.3.3 in the general context of a parametrized density $n[\underline{\varepsilon}](\mathbf{r}_{\varepsilon})$ and are now prepared to insert the alternative total charge density (5.23) into the formalism to obtain the strain variation in the electrostatic potential.

Multipole and pseudo-charge variation

According to (3.23), the multipole moments and their derivatives take the form

$$q_{lm}^a[\underline{\varepsilon}] = \int_0^{R_a} r_a^{l+2} \rho_{lm}^a(|(\underline{1} - \underline{\varepsilon})\mathbf{r}_a|) dr_a - \sqrt{4\pi} Z_a \delta_{l0}, \quad (5.26)$$

$$\left. \frac{\delta}{\delta \varepsilon_{\alpha\beta}} q_{lm}^a[\underline{\varepsilon}] \right|_{\underline{\varepsilon}=0} = \int_0^{R_a} r_a^{l+2} \left[\left. \frac{\delta}{\delta \varepsilon_{\alpha\beta}} \rho_{lm}^a(|(\underline{1} - \underline{\varepsilon})\mathbf{r}_a|) \right|_{\underline{\varepsilon}=0} \right] dr_a \quad \text{and} \quad (5.27)$$

$$\begin{aligned} \left. \frac{\delta}{\delta \varepsilon_{\alpha\beta}} \rho_{lm}^a(|(\underline{1} - \underline{\varepsilon})\mathbf{r}_a|) \right|_{\underline{\varepsilon}=0} &= \oint_{S_2} Y_{lm}^*(\hat{\mathbf{r}}_a) \left[\left. \frac{\delta}{\delta \varepsilon_{\alpha\beta}} \rho^a(|(\underline{1} - \underline{\varepsilon})\mathbf{r}_a|) \right|_{\underline{\varepsilon}=0} \right] dS_2 \\ &= - \sum_{l'm'} \sum_{t,t'=-1}^1 \left\{ r_a \partial_r \rho_{l'm'}^a(r_a) c_{\alpha t} c_{\beta t'} \sum_{s=0}^{2,2} G_{l,s,l'}^{m,t+t',m'} G_{s,1,1}^{t+t',t,t'} \right. \\ &\quad \left. + \frac{1}{2} \rho_{l'm'}^a(r_a) \sum_{s=-1}^{1,2} (c_{\alpha t'} c_{\beta}^{st}(l', m') + c_{\beta t'} c_{\alpha}^{st}(l', m')) G_{l,1,l'+m}^{m,t',m'+t} \right\}. \quad (5.28) \end{aligned}$$

The spherical harmonics expansion of the strained density is calculated according to (5.28) in the routine `st_cdn2.f`.

5.4. Variation of the electrostatic energy

Calculating the strained plane-wave density inside the muffin-tin spheres demands for the Fourier transform of the interstitial density to be known. In a finite volume, the Fourier transform is given as

$$\hat{n}[\underline{\underline{\varepsilon}}](\mathbf{G}_\varepsilon) = \frac{1}{\Omega[\underline{\underline{\varepsilon}}]} \int_{\Omega[\underline{\underline{\varepsilon}}]} \rho_{\text{PW}}((\underline{1} - \underline{\underline{\varepsilon}})\mathbf{r}_\varepsilon) e^{-i\mathbf{G}_\varepsilon \cdot \mathbf{r}_\varepsilon} d^3r_\varepsilon \quad (5.29a)$$

$$= \frac{1}{\Omega} \int_{\Omega} \rho_{\text{PW}}(\mathbf{r}) e^{i\mathbf{G} \cdot \mathbf{r}} d^3r = \hat{\rho}_v(\mathbf{G}). \quad (5.29b)$$

Then, the strain derivative of the plane wave multipole moments (3.24) is

$$\begin{aligned} \left. \frac{\delta}{\delta \varepsilon_{\alpha\beta}} q_{lm}^{a,\text{PW}}[\underline{\underline{\varepsilon}}] \right|_{\underline{\underline{\varepsilon}}=0} &= 4\pi i^l \sum_{\mathbf{G} \neq \mathbf{0}} \hat{\rho}_{\text{PW}}(\mathbf{G}) e^{i\mathbf{G} \cdot \boldsymbol{\tau}_a} \left[\left. \frac{\delta}{\delta \varepsilon_{\alpha\beta}} Y_{lm}^*(\hat{\mathbf{G}}_\varepsilon) \frac{R_a^{l+3} j_{l+1}(G_\varepsilon R_a)}{G_\varepsilon R_a} \right|_{\underline{\underline{\varepsilon}}=0} \right] \\ &= 4\pi i^l \sum_{\mathbf{G} \neq \mathbf{0}} \hat{\rho}_{\text{PW}}(\mathbf{G}) e^{i\mathbf{G} \cdot \boldsymbol{\tau}_a} R_a^{l+3} \left[Y_{lm}^*(\hat{\mathbf{G}}) \frac{G_\alpha G_\beta}{G^2} \left(\frac{j_{l+1}(GR_a)}{GR_a} - j'_{l+1}(GR_a) \right) \right. \\ &\quad \left. - \frac{j_{l+1}(GR_a)}{2GR_a} \sum_{s=-1}^{1,2} \sum_{t=-1}^1 \left(\frac{G_\alpha}{G} c_\beta^{st}(l, m) + \frac{G_\beta}{G} c_\alpha^{st}(l, m) \right) Y_{l+s, m+t}^*(\hat{\mathbf{G}}) \right]. \quad (5.30) \end{aligned}$$

By subtracting (5.30) from (5.27), the variation of the total multipole moments $\delta \tilde{q}_{lm}^a[\underline{\underline{\varepsilon}}]$ can be obtained. This is done in the routine `st_mpmom2.f`.

For the variation of the Fourier transform of the pseudo-charge, we are now able to find with (3.28a) and (3.28b):

$$\begin{aligned} \left. \frac{\delta}{\delta \varepsilon_{\alpha\beta}} \hat{n}_{\text{ps}}[\underline{\underline{\varepsilon}}](\mathbf{G}_\varepsilon) \right|_{\underline{\underline{\varepsilon}}=0} &= \left. \frac{\delta}{\delta \varepsilon_{\alpha\beta}} \left(\hat{\rho}_{\text{PW}}(\mathbf{G}) + \hat{n}_{\text{ps}}[\underline{\underline{\varepsilon}}](\mathbf{G}_\varepsilon) \right) \right|_{\underline{\underline{\varepsilon}}=0} \\ &= -\delta_{\alpha\beta} \hat{n}_{\text{ps}}(\mathbf{G}) + \frac{4\pi}{\Omega} \sum_{lma} \frac{(-i)^l (2l + 2N + 3)!!}{(2l + 1)!! R_a^l} e^{i\mathbf{G} \cdot \boldsymbol{\tau}_a} \\ &\quad \times \left\{ \frac{j_{l+N+1}(GR_a)}{(GR_a)^{N+1}} Y_{lm}(\hat{\mathbf{G}}) \left[\left. \frac{\delta}{\delta \varepsilon_{\alpha\beta}} \tilde{q}_{lm}^a[\underline{\underline{\varepsilon}}] \right|_{\underline{\underline{\varepsilon}}=0} \right] + \tilde{q}_{lm}^a \right. \\ &\quad \times \left[Y_{lm}(\hat{\mathbf{G}}) \frac{G_\alpha G_\beta}{G^2 (GR_a)^{N+1}} \left((N + 1) j_{l+N+1}(GR_a) - GR_a j'_{l+N+1}(GR_a) \right) \right. \\ &\quad \left. \left. - \frac{j_{l+N+1}(GR_a)}{2(GR_a)^{N+1}} \sum_{s=-1}^{1,2} \sum_{t=-1}^1 \left(\frac{G_\alpha}{G} c_\beta^{st}(l, m) + \frac{G_\beta}{G} c_\alpha^{st}(l, m) \right) Y_{l+s, m+t}(\hat{\mathbf{G}}) \right] \right\} \quad (5.31a) \end{aligned}$$

$$\left. \frac{\delta}{\delta \varepsilon_{\alpha\beta}} \hat{n}_{\text{ps}}[\underline{\underline{\varepsilon}}](\mathbf{0}) \right|_{\underline{\underline{\varepsilon}}=0} = -\delta_{\alpha\beta} \hat{n}_{\text{ps}}(\mathbf{0}) + \frac{\sqrt{4\pi}}{\Omega} \sum_{a \in \Omega}^{\text{atoms}} \left[\left. \frac{\delta}{\delta \varepsilon_{\alpha\beta}} \tilde{q}_{00}^a \right|_{\underline{\underline{\varepsilon}}=0} \right] \quad (5.31b)$$

In the routine `st_psqpw2.f`, the variation of the pseudo-charge presented in this section is calculated. There we make use of $\hat{n}_{\text{ps}}(\mathbf{G}) = \hat{n}_{\text{ps}}(\mathbf{G}) - \hat{\rho}_{\text{PW}}(\mathbf{G})$.

5. Stress from total energy calculations

Variation of interstitial potential

With (3.29), we already know how the interstitial potential is made up of the pseudo-charge. Its variation takes the form

$$\begin{aligned}
\left. \frac{\delta}{\delta \varepsilon_{\alpha\beta}} V_C[\underline{\varepsilon}](\mathbf{r}_\varepsilon) \right|_{\underline{\varepsilon}=0} &= \sum_{\mathbf{G} \neq \mathbf{0}} \left[\left. \frac{\delta}{\delta \varepsilon_{\alpha\beta}} \hat{V}_C[\underline{\varepsilon}](\mathbf{G}_\varepsilon) \right|_{\underline{\varepsilon}=0} \right] e^{i\mathbf{G} \cdot \mathbf{r}} \\
&= \sum_{\mathbf{G} \neq \mathbf{0}} 4\pi \left[\left. \frac{\delta}{\delta \varepsilon_{\alpha\beta}} \frac{\hat{n}_{\text{ps}}[\underline{\varepsilon}](\mathbf{G}_\varepsilon)}{G_\varepsilon^2} \right|_{\underline{\varepsilon}=0} \right] e^{i\mathbf{G} \cdot \mathbf{r}} \\
&= \sum_{\mathbf{G} \neq \mathbf{0}} \frac{4\pi}{G^2} \left[2G_\alpha G_\beta \frac{\hat{n}_{\text{ps}}(\mathbf{G})}{G^2} + \left[\left. \frac{\delta}{\delta \varepsilon_{\alpha\beta}} \hat{n}_{\text{ps}}[\underline{\varepsilon}](\mathbf{G}_\varepsilon) \right|_{\underline{\varepsilon}=0} \right] \right] e^{i\mathbf{G} \cdot \mathbf{r}}. \quad (5.32)
\end{aligned}$$

The expansion coefficients of the strained interstitial potential are calculated in the routine `st_hf_coulpot.F` by the name `st_vpw`. Additionally, we need the variation on the muffin-tin boundaries to obtain the potential variation inside the spheres.

$$\begin{aligned}
\left. \frac{\delta}{\delta \varepsilon_{\alpha\beta}} V_C[\underline{\varepsilon}](\mathbf{R}_a + \boldsymbol{\tau}_a[\underline{\varepsilon}]) \right|_{\underline{\varepsilon}=0} &= \sum_{\mathbf{G} \neq \mathbf{0}} 4\pi \left[\left. \frac{\delta}{\delta \varepsilon_{\alpha\beta}} \frac{\hat{n}_{\text{ps}}[\underline{\varepsilon}](\mathbf{G}_\varepsilon)}{G_\varepsilon^2} e^{i\mathbf{G}_\varepsilon \cdot \mathbf{R}_a} \right|_{\underline{\varepsilon}=0} \right] e^{i\mathbf{G} \cdot \boldsymbol{\tau}_a} \\
&= \sum_{\mathbf{G} \neq \mathbf{0}} \left[\left. \frac{\delta}{\delta \varepsilon_{\alpha\beta}} \hat{V}_C[\underline{\varepsilon}](\mathbf{G}_\varepsilon) \right|_{\underline{\varepsilon}=0} \right] e^{i\mathbf{G} \cdot (\mathbf{R}_a + \boldsymbol{\tau}_a)} \\
&\quad - \frac{i}{2} \sum_{\mathbf{G} \neq \mathbf{0}} \hat{V}_C(\mathbf{G}) e^{i\mathbf{G} \cdot (\mathbf{R}_a + \boldsymbol{\tau}_a)} \sum_{t=-1}^1 (G_\alpha R_a c_{\beta t} + G_\beta R_a c_{\alpha t}) Y_{1t}(\hat{\mathbf{R}}_a) \quad (5.33)
\end{aligned}$$

The second term, coming from the variation in the exponential, will have to be taken care of separately in further calculations as a correction to the boundary values.

Variation of muffin-tin and Madelung potential

First, we want to recall the particular difference between the electrostatic and Madelung potential inside the muffin-tin spheres: The Coulomb potential arises from all charged particles in the lattice while the Madelung potential of a certain atom arises from all charged particles other than that atom. To take this difference into account while calculating (3.31), the density can be adjusted to exclude the nuclear charge of an atom, while the boundary values are corrected by adding Z_a/R_a to them. The potentials are then given by

$$\begin{aligned}
V_C[\underline{\varepsilon}](\mathbf{r}_a + \boldsymbol{\tau}_a[\underline{\varepsilon}]) &= \int_{B_{R_a}(\mathbf{0})} \rho^a((\underline{\mathbf{1}} - \underline{\varepsilon})\mathbf{s}_a) G(\mathbf{r}_a, \mathbf{s}_a) d^3 s_a - Z_a \frac{1}{r_a} \left[1 - \frac{r_a}{R_a} \right] \\
&\quad - \frac{R_a^2}{4\pi} \oint_{\partial B_1(\mathbf{0})} V_C[\underline{\varepsilon}](R_a \mathbf{s} + \boldsymbol{\tau}_a[\underline{\varepsilon}]) \partial_s G(\mathbf{r}_a, \mathbf{s}) dS_2 \quad (5.34)
\end{aligned}$$

and

$$\begin{aligned}
 V_M^a[\underline{\varepsilon}](\boldsymbol{\tau}_a[\underline{\varepsilon}]) &= \int_{B_{R_a}(\mathbf{0})} \rho^a((\underline{1} - \underline{\varepsilon})\mathbf{s}_a) G(\mathbf{0}, \mathbf{s}_a) d^3 s_a \\
 &\quad - \frac{R_a^2}{4\pi} \oint_{\partial B_1(\mathbf{0})} \left(V_C[\underline{\varepsilon}](R_a \mathbf{s} + \boldsymbol{\tau}_a[\underline{\varepsilon}]) + \frac{Z_a}{R_a} \right) \partial_s G(\mathbf{0}, \mathbf{s}) dS_2. \quad (5.35)
 \end{aligned}$$

One can see clearly now that the difference between both potentials evaluated at an atomic site $\mathbf{r}_a = \mathbf{0}$ is independent of the strain, as was anticipated earlier. Therefore, the variation of both quantities can be found via (3.33) as

$$\begin{aligned}
 &\left. \frac{\delta}{\delta \varepsilon_{\alpha\beta}} V_C[\underline{\varepsilon}](\mathbf{r}_a + \boldsymbol{\tau}_a[\underline{\varepsilon}]) \right|_{\underline{\varepsilon}=\mathbf{0}} \\
 &= \sum_{lm} Y_{lm}(\hat{\mathbf{r}}_a) \frac{4\pi}{2l+1} \int_0^{R_a} s_a^2 \left[\left. \frac{\delta}{\delta \varepsilon_{\alpha\beta}} \rho_{lm}^a(|(\underline{1} - \underline{\varepsilon})\mathbf{s}_a|) \right|_{\underline{\varepsilon}=\mathbf{0}} \right] \frac{r_{<}^l}{r_{>}^{l+1}} \left[1 - \left(\frac{r_{>}}{R_a} \right)^{2l+1} \right] ds_a \\
 &\quad + \sum_{lm} Y_{lm}(\hat{\mathbf{r}}_a) \left(\frac{r_a}{R_a} \right)^l \sum_{\mathbf{G} \neq \mathbf{0}} e^{i\mathbf{G} \cdot \boldsymbol{\tau}_a} \left[\left. \frac{\delta}{\delta \varepsilon_{\alpha\beta}} \hat{V}_C[\underline{\varepsilon}](\mathbf{G}_\varepsilon) \right|_{\underline{\varepsilon}=\mathbf{0}} \right] \oint_{B_1(\mathbf{0})} e^{i\mathbf{G} \cdot R_a \mathbf{s}} Y_{lm}^*(\hat{\mathbf{s}}) dS_2 \\
 &\quad - \frac{i}{2} \sum_{lm} Y_{lm}(\hat{\mathbf{r}}_a) \left(\frac{r_a}{R_a} \right)^l \sum_{\mathbf{G} \neq \mathbf{0}} e^{i\mathbf{G} \cdot \boldsymbol{\tau}_a} \hat{V}_C(\mathbf{G}) \\
 &\quad \times \sum_{t=-1}^1 (G_\alpha R_a c_{\beta t} + G_\beta R_a c_{\alpha t}) \oint_{B_1(\mathbf{0})} e^{i\mathbf{G} \cdot R_a \mathbf{s}} Y_{1t}(\hat{\mathbf{s}}) Y_{lm}^*(\hat{\mathbf{s}}) dS_2, \quad (5.36)
 \end{aligned}$$

with the density and potential variation given by (5.28) and (5.32). Excluding the last term, which is the aforementioned correction to the variation of the boundary values of the potential, the variable `st_vr` stores the variation of the electrostatic potential in the muffin-tin spheres. The Rayleigh formula enables us to evaluate the surface integrals:

$$\begin{aligned}
 \oint_{B_1(\mathbf{0})} e^{i\mathbf{G} \cdot R_a \mathbf{s}} Y_{lm}^*(\hat{\mathbf{s}}) dS_2 &= 4\pi i^l Y_{lm}^*(\hat{\mathbf{G}}) j_l(GR_a) \\
 \oint_{B_1(\mathbf{0})} e^{i\mathbf{G} \cdot R_a \mathbf{s}} Y_{1t}(\hat{\mathbf{s}}) Y_{lm}^*(\hat{\mathbf{s}}) dS_2 &= \sum_{l'm'} 4\pi i^{l'} Y_{l'm'}^*(\hat{\mathbf{G}}) j_{l'}(GR_a) G_{11l'}^{mtm'}
 \end{aligned}$$

Since the evaluation of the potential variation at an atomic site sends r_a towards zero, only the angular momentum quantum number $l = 0$ contributes to the variation in the Madelung potential in the routine `st_hf_coulpot.F`. Therefore, we obtain for the stress arising from the interaction between the nuclei of a unit cell with all other charged

5. Stress from total energy calculations

particles

$$\begin{aligned}
& -\frac{1}{2} \sum_{a \in \Omega}^{\text{atoms}} Z_a \left[\frac{\delta}{\delta \varepsilon_{\alpha\beta}} V_M^a[\underline{\varepsilon}](\boldsymbol{\tau}_a[\underline{\varepsilon}]) \Big|_{\underline{\varepsilon}=0} \right] \\
& = -\frac{\sqrt{4\pi}}{2} \sum_{a \in \Omega}^{\text{atoms}} Z_a \int_0^{R_a} \left[\frac{\delta}{\delta \varepsilon_{\alpha\beta}} \rho_{00}^a(|(\underline{1} - \underline{\varepsilon})\mathbf{s}_a|) \Big|_{\underline{\varepsilon}=0} \right] s_a \left[1 - \frac{s_a}{R_a} \right] ds_a \\
& \quad - \frac{1}{2} \sum_{a \in \Omega}^{\text{atoms}} Z_a \sum_{\mathbf{G} \neq \mathbf{0}} e^{i\mathbf{G} \cdot \boldsymbol{\tau}_a} \left[\frac{\delta}{\delta \varepsilon_{\alpha\beta}} \hat{V}_C[\underline{\varepsilon}](\mathbf{G}_\varepsilon) \Big|_{\underline{\varepsilon}=0} \right] j_0(GR_a) \\
& \quad - \frac{1}{2} \sum_{a \in \Omega}^{\text{atoms}} Z_a \sum_{\mathbf{G} \neq \mathbf{0}} e^{i\mathbf{G} \cdot \boldsymbol{\tau}_a} \hat{V}_C(\mathbf{G}) \frac{G_\alpha G_\beta}{G^2} GR_a j_1(GR_a). \tag{5.37}
\end{aligned}$$

The routine containing this contribution is `st_hf_coulpot.F`. The integral containing the variation of the density is named `st_ZV1` while the Fourier sums are collected in `st_ZV2`. We thus know how to calculate (5.22).

Stress contribution from electron charged-particle interaction

We will now proceed with the derivation of (5.20a). By using the unit step function of the strained system, we can split the term into its interstitial and muffin-tin representation. The latter gives

$$\begin{aligned}
& \frac{1}{2} \sum_{a \in \Omega}^{\text{atoms}} \int_{B_{R_a}(\mathbf{0})} \left[\frac{\delta}{\delta \varepsilon_{\alpha\beta}} \int_{B_{R_a}(\mathbf{0})} \rho^a((\underline{1} - \underline{\varepsilon})\mathbf{r}_a) V_C[\underline{\varepsilon}](\mathbf{r}_a + \boldsymbol{\tau}_a[\underline{\varepsilon}]) d^3r_a \Big|_{\underline{\varepsilon}=0} \right] \\
& = \frac{1}{2} \sum_{a \in \Omega}^{\text{atoms}} \int_{B_{R_a}(\mathbf{0})} \left[\frac{\delta}{\delta \varepsilon_{\alpha\beta}} \rho^a((\underline{1} - \underline{\varepsilon})\mathbf{r}_a) \Big|_{\underline{\varepsilon}=0} \right] V_C^a(\mathbf{r}_a) d^3r_a \\
& \quad + \frac{1}{2} \sum_{a \in \Omega}^{\text{atoms}} \int_{B_{R_a}(\mathbf{0})} \rho^a(\mathbf{r}_a) \left[\frac{\delta}{\delta \varepsilon_{\alpha\beta}} V_C[\underline{\varepsilon}](\mathbf{r}_a + \boldsymbol{\tau}_a[\underline{\varepsilon}]) \Big|_{\underline{\varepsilon}=0} \right] d^3r_a. \tag{5.38}
\end{aligned}$$

The quantity described by the last line is evaluated in the variable `st_nV6` in the routine `st_hf_coulpot.F`. Additionally, the correction to the boundary variation, which was motivated in (5.33), is calculated as `st_nV5`. The first line, on the other hand, can be calculated by expanding the density variation and the potential into spherical harmonics, the former with respect to (5.28). The variable containing this part is `st_nV3`.

This leaves us with the interstitial part of (5.20a):

$$\begin{aligned}
& \Omega \sigma_{\alpha\beta}^{\text{nV}} \\
& := \frac{1}{2} \left[\frac{\delta}{\delta \varepsilon_{\alpha\beta}} \int_{\Omega[\underline{\varepsilon}]} \left(1 - \sum_{a \in \Omega}^{\text{atoms}} \Theta(|\mathbf{r}_\varepsilon - \boldsymbol{\tau}_a[\underline{\varepsilon}]| \leq R_a) \right) \rho((\underline{1} - \underline{\varepsilon})\mathbf{r}_\varepsilon) V_C[\underline{\varepsilon}](\mathbf{r}_\varepsilon) d^3r_\varepsilon \Big|_{\underline{\varepsilon}=0} \right]
\end{aligned}$$

5.4. Variation of the electrostatic energy

We want to use the Fourier representation of the quantities involved in this integral. However, we do not know the Fourier transform of the unit step function in the strained system. We do now the Fourier transform of the unstrained unit step function, though. Using (5.19), we can apply the strain variation just to this part and we find

$$\begin{aligned} \Omega\sigma_{\alpha\beta}^{\text{nV}} = & -\frac{1}{2} \sum_{a \in \Omega} R_a^3 \sum_{t,t'=-1}^1 c_{\alpha t} c_{\beta t'} \oint_{\partial B_1(\mathbf{0})} Y_{1t}(\hat{\mathbf{s}}) Y_{1t'}(\hat{\mathbf{s}}) \rho^a(R_a \mathbf{s}) V_C^a(R_a \mathbf{s}) dS_2 \\ & + \frac{1}{2} \left[\frac{\delta}{\delta \varepsilon_{\alpha\beta}} \int_{\Omega[\underline{\varepsilon}]} \Theta_{\text{IS}}((\underline{1} - \underline{\varepsilon}) \mathbf{r}_\varepsilon) \rho((\underline{1} - \underline{\varepsilon}) \mathbf{r}_\varepsilon) V_C[\underline{\varepsilon}](\mathbf{r}_\varepsilon) d^3 r_\varepsilon \Big|_{\underline{\varepsilon}=0} \right] \end{aligned}$$

By inserting the Fourier transforms of the strained density (which has the same expansion coefficients as in the unstrained case) and the potential (5.32), we get

$$\begin{aligned} \Omega\sigma_{\alpha\beta}^{\text{nV}} = & -\frac{1}{2} \sum_{a \in \Omega} R_a^3 \sum_{t,t'=-1}^1 c_{\alpha t} c_{\beta t'} \sum_{s=0}^{2,2} G_{s,1,1}^{t+t',t,t'} \sum_{lm} \sum_{l'm'} \rho_{lm}^{a*}(R_a) V_{Cl'm'}^a(R_a) G_{l,s,l'}^{m,t+t',m'} \\ & + \frac{1}{2} \left[\frac{\delta}{\delta \varepsilon_{\alpha\beta}} \sum_{\mathbf{G}} \sum_{\mathbf{G}' \neq \mathbf{0}} \hat{\rho}^*(\mathbf{G}) \hat{V}_C[\underline{\varepsilon}](\mathbf{G}_\varepsilon) \frac{\Omega[\underline{\varepsilon}]}{\Omega[\underline{\varepsilon}]} \int_{\Omega[\underline{\varepsilon}]} \Theta_{\text{IS}}((\underline{1} - \underline{\varepsilon}) \mathbf{r}_\varepsilon) e^{-i(\mathbf{G}_\varepsilon - \mathbf{G}') \cdot \mathbf{r}_\varepsilon} d^3 r_\varepsilon \Big|_{\underline{\varepsilon}=0} \right]. \end{aligned}$$

Parallel to (5.29b), the integral is the Fourier transform of its integrand in the unstrained case. Thus, we find

$$\begin{aligned} \Omega\sigma_{\alpha\beta}^{\text{nV}} = & -\frac{1}{2} \sum_{a \in \Omega} R_a^3 \sum_{t,t'=-1}^1 c_{\alpha t} c_{\beta t'} \sum_{s=0}^{2,2} G_{s,1,1}^{t+t',t,t'} \sum_{lm} \sum_{l'm'} \rho_{lm}^{a*}(R_a) V_{Cl'm'}^a(R_a) G_{l,s,l'}^{m,t+t',m'} \\ & + \frac{1}{2} \left[\frac{\delta}{\delta \varepsilon_{\alpha\beta}} \sum_{\mathbf{G}} \sum_{\mathbf{G}' \neq \mathbf{0}} \hat{\rho}^*(\mathbf{G}) \hat{V}_C[\underline{\varepsilon}](\mathbf{G}_\varepsilon) \Omega[\underline{\varepsilon}] \hat{\Theta}_{\text{IS}}(\mathbf{G} - \mathbf{G}') \Big|_{\underline{\varepsilon}=0} \right] \\ = & -\frac{1}{2} \sum_{a \in \Omega} R_a^3 \sum_{t,t'=-1}^1 c_{\alpha t} c_{\beta t'} \sum_{s=0}^{2,2} G_{s,1,1}^{t+t',t,t'} \sum_{lm} \sum_{l'm'} \rho_{lm}^{a*}(R_a) V_{Cl'm'}^a(R_a) G_{l,s,l'}^{m,t+t',m'} \\ & + \frac{1}{2} \sum_{\mathbf{G}} \sum_{\mathbf{G}' \neq \mathbf{0}} \hat{\rho}^*(\mathbf{G}) \left[\frac{\delta}{\delta \varepsilon_{\alpha\beta}} \hat{V}_C[\underline{\varepsilon}](\mathbf{G}_\varepsilon) \Big|_{\underline{\varepsilon}=0} \right] \Omega \hat{\Theta}_{\text{IS}}(\mathbf{G} - \mathbf{G}') \\ & + \frac{1}{2} \delta_{\alpha\beta} \sum_{\mathbf{G}} \sum_{\mathbf{G}' \neq \mathbf{0}} \hat{\rho}^*(\mathbf{G}) \hat{V}_C(\mathbf{G}) \Omega \hat{\Theta}_{\text{IS}}(\mathbf{G} - \mathbf{G}'). \end{aligned} \tag{5.39}$$

The surface term (first line) goes by the name of `st_nV4` in the routine `st_hf_coulpot.F`. The trace term (last line) is calculated as `st_nV2` and coincides with the interstitial part of the energy contribution of the electrons interacting with all charged particles to the

5. Stress from total energy calculations

total energy. The middle term is summed up in the variable `st_nV1`.

In contrast to the discontinuity correction derived in chapter 5.2.2, the surface term found in this chapter does not arise from a discontinuity of the wave functions or the density. Instead, it is necessary due to the use of the unit step function and its back-transformation. Because no back-transformation is performed during the calculation of the contribution to the stress tensor due to the muffin-tin spheres, the surface term does not cancel.

This concludes the formalism to obtain the electrostatic stress.

5.5. The Hellmann-Feynman stress

We are now able to summarize the stress formula in terms of the physical Hellmann-Feynman stress and the Pulay corrections, which are necessary due to our choice in describing the wave functions. The stress tensor is given by

$$\Omega\sigma_{\alpha\beta} = \frac{1}{2} \sum_{\mathbf{k}v} n_{v\mathbf{k}} \int_{\Omega} \psi_{v\mathbf{k}}^*(\mathbf{r}) (\partial_{\alpha}\partial_{\beta} + \partial_{\beta}\partial_{\alpha}) \psi_{v\mathbf{k}}(\mathbf{r}) d^3r \quad (5.40a)$$

$$+ \delta_{\alpha\beta} \int_{\Omega} \rho(\mathbf{r}) (\varepsilon_{xc}(\mathbf{r}) - V_{\text{eff}}(\mathbf{r})) d^3r \quad (5.40b)$$

$$+ \frac{1}{2} \left[\frac{\delta}{\delta\varepsilon_{\alpha\beta}} \int_{\Omega[\underline{\varepsilon}]} \rho((1 - \underline{\varepsilon})\mathbf{r}_{\varepsilon}) V_C[\underline{\varepsilon}](\mathbf{r}_{\varepsilon}) d^3r_{\varepsilon} \Big|_{\underline{\varepsilon}=0} \right] \quad (5.40c)$$

$$- \frac{1}{2} \sum_{a \in \Omega}^{\text{atoms}} Z_a \left[\frac{\delta}{\delta\varepsilon_{\alpha\beta}} V_M^a[\underline{\varepsilon}](\boldsymbol{\tau}_a[\underline{\varepsilon}]) \Big|_{\underline{\varepsilon}=0} \right] \quad (5.40d)$$

$$+ 2 \sum_{\mathbf{k}v} n_{v\mathbf{k}} \text{Re} \left(\int_{\Omega} \left[\frac{\delta}{\delta\varepsilon_{\alpha\beta}} \psi_{v\mathbf{k}_{\varepsilon}}[\underline{\varepsilon}](\mathbf{r}[\underline{\varepsilon}]) \Big|_{\underline{\varepsilon}=0} \right]^* (\mathcal{H} - \epsilon_v(\mathbf{k})) \psi_{v\mathbf{k}}(\mathbf{r}) d^3r \right) \quad (5.40e)$$

$$- \frac{1}{2} \sum_{a \in \Omega}^{\text{atoms}} R_a^3 \sum_{\mathbf{k}v} n_{v\mathbf{k}} \oint_{S_2} s_{\alpha} s_{\beta} \{ \psi_{v\mathbf{k}}^{\text{MT}a*}(R_a\mathbf{s}) \nabla^2 \psi_{v\mathbf{k}}^{\text{MT}a}(R_a\mathbf{s}) - \psi_{v\mathbf{k}}^{\text{IS}*}(R_a\mathbf{s} + \boldsymbol{\tau}_a) \nabla^2 \psi_{v\mathbf{k}}^{\text{IS}}(R_a\mathbf{s} + \boldsymbol{\tau}_a) \} dS_2 \quad (5.40f)$$

$$- \frac{1}{2} \sum_{a \in \Omega}^{\text{atoms}} \int_{B_{R_a}(\mathbf{0})} \rho_c^a(\mathbf{r}_a) r_{a\alpha} \partial_{\beta} V_{\text{eff}}^a(\mathbf{r}_a) d^3r_a. \quad (5.40g)$$

The lines (5.40a) to (5.40d) form the Hellmann-Feynman stress. The remaining lines constitute the Pulay correction.

Note that the contribution (5.40a) to the stress tensor contains the valence states only, since we have shown that the core electrons do not contribute a component to the

kinetic stress. However, Janak [Jan74] found a connection between (5.40g) and a term containing the core states that is similar to the expression we have found for the kinetic stress of the valence states, (5.40a). We will briefly sketch this connection, making use of our assumption that the core states and their derivatives vanish at the muffin-tin boundaries. We use the Schrödinger equation and its complex conjugate for the core states:

$$\left[-\frac{1}{2}\nabla^2 + V_{\text{eff}0}^a \right] \psi_c^a = \epsilon_c^a \psi_c^a \quad (5.41a)$$

$$\left[-\frac{1}{2}\nabla^2 + V_{\text{eff}0}^a \right] \psi_c^{a*} = \epsilon_c^a \psi_c^{a*} \quad (5.41b)$$

Operate on the first equation with $\int_{B_{R_a}(\mathbf{0})} \psi_c^{a*} [r_\alpha \partial_\beta \cdot] d^3r$ and on the second equation with $\int_{B_{R_a}(\mathbf{0})} \cdot [r_\alpha \partial_\beta \psi_c^a] d^3r$:

$$\begin{aligned} & \int_{B_{R_a}(\mathbf{0})} \psi_c^{a*} \left(r_\alpha \partial_\beta \left[-\frac{1}{2}\nabla^2 + V_{\text{eff}0}^a \right] \psi_c^a \right) d^3r \\ &= -\frac{1}{2} \int_{B_{R_a}(\mathbf{0})} \psi_c^{a*} r_\alpha \partial_\beta \partial_i \partial_i \psi_c^a d^3r + \int_{B_{R_a}(\mathbf{0})} \psi_c^{a*} [r_\alpha \partial_\beta V_{\text{eff}0}^a] \psi_c^a d^3r \\ & \quad + \int_{B_{R_a}(\mathbf{0})} \psi_c^{a*} V_{\text{eff}0}^a [r_\alpha \partial_\beta \psi_c^a] d^3r \\ &= \epsilon_c^a \int_{B_{R_a}(\mathbf{0})} \psi_c^{a*} [r_\alpha \partial_\beta \psi_c^a] d^3r \\ &= \int_{B_{R_a}(\mathbf{0})} \left(\left[-\frac{1}{2}\nabla^2 + V_{\text{eff}0}^a \right] \psi_c^{a*} \right) [r_\alpha \partial_\beta \psi_c^a] d^3r \\ &= -\frac{1}{2} \int_{B_{R_a}(\mathbf{0})} [\partial_i \partial_i \psi_c^{a*}] [r_\alpha \partial_\beta \psi_c^a] d^3r + \int_{B_{R_a}(\mathbf{0})} \psi_c^{a*} V_{\text{eff}0}^a [r_\alpha \partial_\beta \psi_c^a] d^3r \end{aligned}$$

Since both formulas are manipulated to give the same result, we can subtract them from each other and get:

$$\begin{aligned} - \int_{B_{R_a}(\mathbf{0})} \rho_c^a [r_\alpha \partial_\beta V_{\text{eff}0}^a] d^3r &= \frac{1}{2} \int_{B_{R_a}(\mathbf{0})} [\partial_i \partial_i \psi_c^{a*}] [r_\alpha \partial_\beta \psi_c^a] - \psi_c^{a*} r_\alpha \partial_\beta \partial_i \partial_i \psi_c^a d^3r \\ &= \frac{1}{2} \oint_{\partial B_{R_a}(\mathbf{0})} \hat{i} [\partial_i \psi_c^{a*}] [r_\alpha \partial_\beta \psi_c^a] - \psi_c^{a*} r_\alpha \hat{i} \partial_\beta \partial_i \psi_c^a dS_2 \\ & \quad - \frac{1}{2} \int_{B_{R_a}(\mathbf{0})} \left\{ [\partial_i \psi_c^{a*}] \delta_{\alpha i} [\partial_\beta \psi_c^a] + [\partial_i \psi_c^{a*}] [r_\alpha \partial_i \partial_\beta \psi_c^a] \right. \\ & \quad \left. - \delta_{\alpha i} \psi_c^{a*} [\partial_\beta \partial_i \psi_c^a] - [\partial_i \psi_c^{a*}] [r_\alpha \partial_\beta \partial_i \psi_c^a] \right\} d^3r \\ &= + \frac{1}{2} \int_{B_{R_a}(\mathbf{0})} \psi_c^{a*} (\partial_\alpha \partial_\beta + \partial_\beta \partial_\alpha) \psi_c^a d^3r \quad (5.42) \end{aligned}$$

5. Stress from total energy calculations

Therefore, the core correction (5.40g) can be ignored when the sum in line (5.40a) is extended to include the core states.

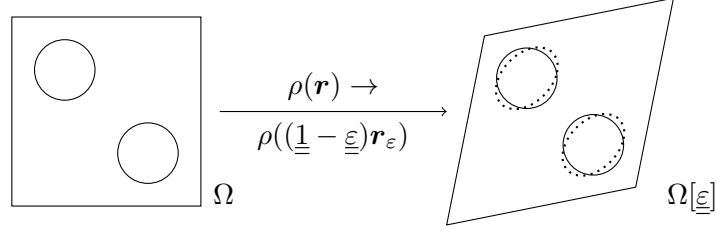


Figure 5.2.: The stress components from the electrostatic energy of the strained system are calculated in strained coordinates. They are evaluated using the original density smeared over the strained lattice.

5.6. Computational details

Since we already had to give a rather exhaustive overview over the electrostatic stress and its implementation in chapter 5.4, we want to follow up by providing formulas for the other stress contributions with the same degree of detail. We also want to provide other partial pressure formulas with which to compare the trace of our results. The exchange-correlation energy $\int \rho \varepsilon_{xc} d^3 r$ and the integral containing the effective potential $\int \rho V_{\text{eff}} d^3 r$ appearing in (5.40b) should already be part of FLAPW codes, so the corresponding trace term can be taken directly from an electronic structure calculation. This, however, makes comparison with a pressure formula redundant. The other parts of this formula need a more thorough analysis, though.

5.6.1. Kinetic stress formula

As the wave functions are expanded into plane waves in the interstitial, (5.40a) is straightforward to calculate in the interstitial region:

$$\begin{aligned}
 & \frac{1}{2} \sum_{\mathbf{k}v} n_{v\mathbf{k}} \int_{\Omega} \Theta(\mathbf{r} \in \text{IS}) \psi_{v\mathbf{k}}^*(\mathbf{r}) (\partial_{\alpha} \partial_{\beta} + \partial_{\beta} \partial_{\alpha}) \psi_{v\mathbf{k}}(\mathbf{r}) d^3 r \\
 &= \sum_{\mathbf{k}v} n_{v\mathbf{k}} \sum_{\mathbf{G}\mathbf{G}'} z_{v\mathbf{k}\mathbf{G}}^* z_{v\mathbf{k}\mathbf{G}'} (-\mathbf{k} + \mathbf{G}')_{\alpha} (\mathbf{k} + \mathbf{G}')_{\beta} \frac{1}{\Omega} \int_{\Omega} \Theta(\mathbf{r} \in \text{IS}) e^{-i(\mathbf{G}-\mathbf{G}') \cdot \mathbf{r}} d^3 r \\
 &= - \sum_{\mathbf{k}v} n_{v\mathbf{k}} \sum_{\mathbf{G}\mathbf{G}'} z_{v\mathbf{k}\mathbf{G}}^* z_{v\mathbf{k}\mathbf{G}'} (\mathbf{k} + \mathbf{G}')_{\alpha} (\mathbf{k} + \mathbf{G}')_{\beta} \hat{\Theta}_{\text{IS}}(\mathbf{G} - \mathbf{G}')
 \end{aligned}$$

This formula is implemented in the first part of `stkin.F` in the FLEUR-code. In the second part of this routine, the muffin-tin representation of the basis functions is

differentiated twice, which gives after a summation over all atoms

$$\begin{aligned}
 & \frac{1}{2} \sum_{\mathbf{k}v} n_{v\mathbf{k}} \sum_{a \in \Omega}^{\text{atoms}} \int_{B_{R_a}(\mathbf{0})} \psi_{v\mathbf{k}}^{a*}(\mathbf{r}) (\partial_\alpha \partial_\beta + \partial_\beta \partial_\alpha) \psi_{v\mathbf{k}}^a(\mathbf{r}) d^3r \\
 &= \sum_{\mathbf{k}v} n_{v\mathbf{k}} \sum_{a \in \Omega}^{\text{atoms}} \sum_l \sum_{l'=l-2}^{l+2} \sum_{\lambda\lambda'} \left\{ \delta_{\alpha\beta} \int_0^{R_a} r u_{l\lambda}^a(r) \partial_r u_{l'\lambda'}^a(r) dr \sum_{m'} A_{L'\lambda}^{av\mathbf{k}*} A_{L'\lambda'}^{av\mathbf{k}} \delta_{ll'} \delta_{mm'} \right. \\
 &+ \int_0^{R_a} r u_{l\lambda}^a(r) (r \partial_r^2 u_{l'\lambda'}^a(r) - \partial_r u_{l'\lambda'}^a(r)) dr \sum_{s=0}^{2,2} \sum_{t,t'=-1}^1 \sum_{m'} A_{l,m'+t+t',\lambda}^{av\mathbf{k}*} A_{L'\lambda'}^{av\mathbf{k}} \\
 &\quad \times c_{\alpha t} c_{\beta t'} G_{s,1,1}^{t+t',t,t'} G_{l,s,l'}^{m'+t+t',t+t',m'} \\
 &+ \frac{1}{2} \int_0^{R_a} u_{l\lambda}^a(r) (2r \partial_r u_{l'\lambda'}^a(r) - u_{l'\lambda'}^a(r)) dr \sum_{s=-1}^{1,2} \sum_{t,t'=-1}^1 \sum_{m'} A_{l,m'+t+t',\lambda}^{av\mathbf{k}*} A_{L'\lambda'}^{av\mathbf{k}} \\
 &\quad \times (c_{\alpha t'} c_{\beta}^{st}(l', m') + c_{\beta t'} c_{\alpha}^{st}(l', m')) G_{l,1,l'+s}^{m'+t+t',t',m'+t} \\
 &+ \frac{1}{2} \int_0^{R_a} u_{l\lambda}^a(r) u_{l'\lambda'}^a(r) dr \sum_{s=-1}^{1,2} \sum_{t,t'=-1}^1 \sum_{m'} A_{l,m'+t+t',\lambda}^{av\mathbf{k}*} A_{L'\lambda'}^{av\mathbf{k}} \sum_{s'=-1}^{1,2} \delta_{l,l'+s+s'} \delta_{m,m'+t+t'} \\
 &\quad \left. \times \left(c_{\alpha}^{s't'}(l'+s, m'+t) c_{\beta}^{st}(l', m') + c_{\beta}^{s't'}(l'+s, m'+t) c_{\alpha}^{st}(l', m') \right) \right\}. \quad (5.43)
 \end{aligned}$$

The restriction on possible values for l' and m' are given by the Kronecker symbols and the Gaunt coefficients. An additional restriction to the values of l' is that it only can have values from 0 to a maximal value l_{\max} . Therefore, the values $l-2$ and $l+2$ do not contribute if they are out of said interval.

Kinetic pressure

If the trace of the kinetic stress is considered, the resulting term becomes familiar. It is the negative double of the kinetic energy and can be obtained as an eigenvalue sum minus the effective potential integral regarding only the valence states

$$3P_{\text{kin}}\Omega = \sum_{\mathbf{k}v} n_{v\mathbf{k}} \int_{\Omega} \psi_{v\mathbf{k}}^*(\mathbf{r}) \nabla^2 \psi_{v\mathbf{k}}(\mathbf{r}) d^3r = -2E_{\text{kin}}^{\text{val}}. \quad (5.44)$$

5.6.2. Discontinuity correction

Since the FLAPW basis functions are continuous up to first order on the muffin-tin boundary, we will start by finding the second derivative of the interstitial basis functions. Differentiation will reproduce them because they are plane waves. Afterwards, they can

5. Stress from total energy calculations

be expressed by their muffin-tin representation

$$\begin{aligned}
& - \oint_{B_1(\mathbf{0})} s_\alpha s_\beta \psi_{v\mathbf{k}}^{\text{IS}*}(R_a \mathbf{s} + \boldsymbol{\tau}_a) \nabla^2 \psi_{v\mathbf{k}}^{\text{IS}}(R_a \mathbf{s} + \boldsymbol{\tau}_a) dS_2 \\
& = - \sum_{\mathbf{G}\mathbf{G}'} z_{v\mathbf{k}\mathbf{G}}^* z_{v\mathbf{k}\mathbf{G}'} \oint_{B_1(\mathbf{0})} s_\alpha s_\beta \phi_{\mathbf{k}\mathbf{G}}^{\text{IS}*}(R_a \mathbf{s} + \boldsymbol{\tau}_a) \nabla^2 \phi_{\mathbf{k}\mathbf{G}'}^{\text{IS}}(R_a \mathbf{s} + \boldsymbol{\tau}_a) dS_2 \\
& = \sum_{\mathbf{G}\mathbf{G}'} z_{v\mathbf{k}\mathbf{G}}^* z_{v\mathbf{k}\mathbf{G}'} |\mathbf{k} + \mathbf{G}'|^2 \oint_{B_1(\mathbf{0})} s_\alpha s_\beta \phi_{\mathbf{k}\mathbf{G}}^{\text{MT}^a*}(R_a \mathbf{s}) \phi_{\mathbf{k}\mathbf{G}'}^{\text{MT}^a}(R_a \mathbf{s}) dS_2. \tag{5.45}
\end{aligned}$$

We name $\sum_{\mathbf{G}'} z_{v\mathbf{k}\mathbf{G}'} |\mathbf{k} + \mathbf{G}'|^2 a_{L'\lambda'}^{a\mathbf{k}\mathbf{G}'}$ as $F_{L\lambda}^{av\mathbf{k}}$, mimicking the A and B coefficients. Then, the formula for the surface correction is

$$\begin{aligned}
\Omega \sigma_{\alpha\beta}^{\text{sur}} & = - \frac{1}{2} \sum_{\mathbf{k}v} n_{v\mathbf{k}} \sum_{a \in \Omega}^{\text{atoms}} R_a^3 \oint_{B_1(\mathbf{0})} s_\alpha s_\beta \{ \psi_{v\mathbf{k}}^{\text{MT}^a*}(R_a \mathbf{s}) \nabla^2 \psi_{v\mathbf{k}}^{\text{MT}^a}(R_a \mathbf{s}) \\
& \quad - \psi_{v\mathbf{k}}^{\text{IS}*}(R_a \mathbf{s} + \boldsymbol{\tau}_a) \nabla^2 \psi_{v\mathbf{k}}^{\text{IS}}(R_a \mathbf{s} + \boldsymbol{\tau}_a) \} dS_2 \\
& = - \frac{1}{2} \sum_{\mathbf{k}v} n_{v\mathbf{k}} \sum_{a \in \Omega}^{\text{atoms}} R_a^3 \sum_{L\lambda} \sum_{L'\lambda'} A_{L\lambda}^{av\mathbf{k}*} \\
& \quad \times \left\{ u_{l\lambda}^a(R_a) \left[A_{L'\lambda'}^{av\mathbf{k}} \left(\frac{2}{R_a} \partial_r u_{l'\lambda'}^a(R_a) + \partial_r^2 u_{l'\lambda'}^a(R_a) \right) + F_{L'\lambda'}^{av\mathbf{k}} u_{l'\lambda'}^a(R_a) \right] \right. \\
& \quad \times \sum_{s=0}^{2,2} \sum_{t,t'=-1}^1 c_{\alpha t} c_{\beta t'} G_{s,1,1}^{t+t',t,t'} G_{l,s,l'}^{m,t+t',m'} \\
& \quad + A_{L'\lambda'}^{av\mathbf{k}} u_{l\lambda}(R_a) \left(\frac{2}{R_a} \partial_r u_{l'\lambda'}^a(R_a) - \frac{1}{R_a^2} u_{l'\lambda'}^a(R_a) \right) \\
& \quad \times \sum_{s=0}^{2,2} \sum_{t,t'=-1}^1 c_{\alpha t} c_{\beta t'} G_{s,1,1}^{t+t',t,t'} \sum_{p=-1}^{1,2} \sum_{q,q'=-1}^1 \sum_{p'=|l'+p-1|}^{l'+p+1,2} G_{p',1,l'+p}^{m'+q+q',q',m'+q} \\
& \quad \times G_{l,s,p'}^{m,t+t',m'+q+q'} \sum_{j=1}^3 c_{jt'} c_j^{pq}(l',m') \\
& \quad + A_{L'\lambda'}^{av\mathbf{k}} \frac{1}{R_a^2} u_{l\lambda}(R_a) u_{l'\lambda'}(R_a) \\
& \quad \times \sum_{s=0}^{2,2} \sum_{t,t'=-1}^1 c_{\alpha t} c_{\beta t'} G_{s,1,1}^{t+t',t,t'} \sum_{p,p'=-1}^{1,2} \sum_{q,q'=-1}^1 G_{l,s,l'+p+p'}^{m,t+t',m'+q+q'} \\
& \quad \left. \times \sum_{j=1}^3 c_j^{pq}(l',m') c_j^{p'q'}(l'+p,m'+q) \right\}. \tag{5.46}
\end{aligned}$$

The indices s , t , and t' are reserved for handling the $s_\alpha s_\beta$ expression in spherical harmonics while the context of p , p' , q , and q' is that of the kinetic energy operator.

An expression similar to $F_{L'\lambda'}^{av\mathbf{k}}$ is already obtained during the force calculation. According to [YSK91] we write

$$E_{L'\lambda'}^{av\mathbf{k}} = \sum_{\mathbf{G}} z_{v\mathbf{k}\mathbf{G}} \left[\frac{1}{2} |\mathbf{k} + \mathbf{G}|^2 - \epsilon_v(\mathbf{k}) \right] a_{L'\lambda'}^{a\mathbf{k}\mathbf{G}} = \frac{1}{2} F_{L'\lambda'}^{av\mathbf{k}} - \epsilon_v(\mathbf{k}) A_{L'\lambda'}^{av\mathbf{k}}, \text{ giving}$$

$$F_{L'\lambda'}^{av\mathbf{k}} = 2(E_{L'\lambda'}^{av\mathbf{k}} + \epsilon_v(\mathbf{k}) A_{L'\lambda'}^{av\mathbf{k}}).$$

The implementation of (5.46) is provided in the `st_pulay_sur2.f` routine.

Pressure from discontinuity correction

The dependence of (5.46) on the strain component manifests itself only through the factor $s_\alpha s_\beta$ in the surface integral. The trace of this factor is 1 as \mathbf{s} is a vector on the unit sphere. Then, the pressure formula can be obtained by replacing $\sum_s \sum_{t,t'} c_{\alpha t} c_{\beta t'} G_{s,1,1}^{t+t',t,t'}$ with $\sqrt{4\pi}$ and s , t , and t' with zero in the remaining Gaunt coefficients. Unfortunately, the resulting expression cannot easily be obtained by means of known quantities from a previous electronic structure calculation but has to be computed via (5.46) with the aforementioned substitutions. This makes the pressure formula unsuitable as a check of the discontinuity correction.

5.6.3. Valence correction

Before we derive a detailed formula for the contribution of (5.40e) to the stress, we make an important observation regarding the strain derivative of the wave function ψ :

$$\begin{aligned} \left. \frac{\delta}{\delta \varepsilon_{\alpha\beta}} \psi_{v\mathbf{k}_\varepsilon}[\underline{\varepsilon}](\mathbf{r}[\underline{\varepsilon}]) \right|_{\underline{\varepsilon}=0} &= \frac{\delta}{\delta \varepsilon_{\alpha\beta}} \sum_{\mathbf{G}} z_{v\mathbf{k}_\varepsilon \mathbf{G}_\varepsilon} \phi_{\mathbf{k}_\varepsilon \mathbf{G}_\varepsilon}[\underline{\varepsilon}](\mathbf{r}[\underline{\varepsilon}]) \Big|_{\underline{\varepsilon}=0} \\ &= \sum_{\mathbf{G}} \left(\left[\left. \frac{\delta}{\delta \varepsilon_{\alpha\beta}} \frac{z_{v\mathbf{k}_\varepsilon \mathbf{G}_\varepsilon}}{\sqrt{\Omega[\underline{\varepsilon}]}} \right|_{\underline{\varepsilon}=0} \right] \sqrt{\Omega} \phi_{\mathbf{k}\mathbf{G}}(\mathbf{r}) + \frac{z_{v\mathbf{k}\mathbf{G}}}{\sqrt{\Omega}} \left[\left. \frac{\delta}{\delta \varepsilon_{\alpha\beta}} \sqrt{\Omega[\underline{\varepsilon}]} \phi_{\mathbf{k}_\varepsilon \mathbf{G}_\varepsilon}[\underline{\varepsilon}](\mathbf{r}[\underline{\varepsilon}]) \right|_{\underline{\varepsilon}=0} \right] \right) \end{aligned} \quad (5.47)$$

Here, the unit cell volume Ω is explicitly considered to be a prefactor, so $\sqrt{\Omega} \phi_{\mathbf{k}\mathbf{G}}(\mathbf{r})$ is an unweighted plane wave in the interstitial. Then, according to (5.10), the strained plane wave $\sqrt{\Omega[\underline{\varepsilon}]} \phi_{\mathbf{k}_\varepsilon \mathbf{G}_\varepsilon}[\underline{\varepsilon}](\mathbf{r}[\underline{\varepsilon}])$ coincides with the unstrained one, and its derivative vanishes. Since the first term of the sum is given in terms of the LAPW basis, it does not contribute to the Pulay stress. This leaves us with the second term of the sum evaluated inside the muffin-tin spheres and the Pulay stress arising only from the muffin-tin spheres.

Expanding the basis functions into spherical harmonics, we then have

$$\left. \frac{\delta}{\delta \varepsilon_{\alpha\beta}} \phi_{\mathbf{k}_\varepsilon \mathbf{G}_\varepsilon}[\underline{\varepsilon}](\mathbf{r}_a[\underline{\varepsilon}]) \right|_{\underline{\varepsilon}=0} = \frac{\delta}{\delta \varepsilon_{\alpha\beta}} \sum_{lm\lambda} a_{lm\lambda}^{a\mathbf{k}_\varepsilon \mathbf{G}_\varepsilon}[\underline{\varepsilon}] u_{l\lambda}^a[\underline{\varepsilon}](r_a[\underline{\varepsilon}]) Y_{lm}(\hat{\mathbf{r}}_a[\underline{\varepsilon}]) \Big|_{\underline{\varepsilon}=0}, \quad (5.48)$$

5. Stress from total energy calculations

which can be handled by the product rule. The derivative of the spherical harmonic is given by (5.9). Differentiating the other two gives

$$\left. \frac{\delta}{\delta \varepsilon_{\alpha\beta}} u_{l\lambda}^a[\underline{\underline{\varepsilon}}](r_a[\underline{\underline{\varepsilon}}]) \right|_{\underline{\underline{\varepsilon}}=0} = \frac{r_{a\alpha} r_{a\beta}}{r_a} \partial_{r_a} u_{l\lambda}^a(r_a) + \left. \frac{\delta}{\delta \varepsilon_{\alpha\beta}} u_{l\lambda}^a[\underline{\underline{\varepsilon}}](r_a) \right|_{\underline{\underline{\varepsilon}}=0}$$

and

$$\begin{aligned} \left. \frac{\delta}{\delta \varepsilon_{\alpha\beta}} \begin{pmatrix} a_{lm\lambda}^{a\mathbf{k}_\varepsilon \mathbf{G}_\varepsilon}[\underline{\underline{\varepsilon}}] \\ b_{lm\lambda}^{a\mathbf{k}_\varepsilon \mathbf{G}_\varepsilon}[\underline{\underline{\varepsilon}}] \end{pmatrix} \right|_{\underline{\underline{\varepsilon}}=0} &= \frac{4\pi i^l}{\sqrt{\Omega}} e^{i(\mathbf{k}+\mathbf{G})\cdot\boldsymbol{\tau}_a} \\ &\times \left. \frac{\delta}{\delta \varepsilon_{\alpha\beta}} Y_{lm}^*((\widehat{\mathbf{k}_\varepsilon + \mathbf{G}_\varepsilon})) \underline{\underline{U}}[\underline{\underline{\varepsilon}}]^{-1} \begin{pmatrix} j_l(|\mathbf{k}_\varepsilon + \mathbf{G}_\varepsilon| R_a) \\ |\mathbf{k}_\varepsilon + \mathbf{G}_\varepsilon| j'_l(|\mathbf{k}_\varepsilon + \mathbf{G}_\varepsilon| R_a) \end{pmatrix} \right|_{\underline{\underline{\varepsilon}}=0}. \end{aligned}$$

We recall that for vectors in reciprocal space, the strain transformation is $\mathbf{k}_\varepsilon = (\underline{\underline{1}} - \underline{\underline{\varepsilon}})\mathbf{k}$. Thus we can use (5.9) again. We also know the derivative of the absolutes (5.4), resulting in the evaluation of the vector as

$$\begin{aligned} &\left. \frac{\delta}{\delta \varepsilon_{\alpha\beta}} \begin{pmatrix} j_l(|\mathbf{k}_\varepsilon + \mathbf{G}_\varepsilon| R_a) \\ |\mathbf{k}_\varepsilon + \mathbf{G}_\varepsilon| j'_l(|\mathbf{k}_\varepsilon + \mathbf{G}_\varepsilon| R_a) \end{pmatrix} \right|_{\underline{\underline{\varepsilon}}=0} \\ &= -\frac{(\mathbf{k} + \mathbf{G})_\alpha (\mathbf{k} + \mathbf{G})_\beta}{|\mathbf{k} + \mathbf{G}|^2} \begin{pmatrix} |\mathbf{k} + \mathbf{G}| R_a j'_l(|\mathbf{k} + \mathbf{G}| R_a) \\ |\mathbf{k} + \mathbf{G}| j'_l(|\mathbf{k} + \mathbf{G}| R_a) + |\mathbf{k} + \mathbf{G}|^2 R_a j''_l(|\mathbf{k} + \mathbf{G}| R_a) \end{pmatrix}. \end{aligned}$$

The second term in the derivative of the radial functions u as well as the derivative of the matrix $\underline{\underline{U}}^{-1}$ features the change in the radial functions due to a strain in the system and goes beyond a simple modification in the muffin-tin coordinates. In principle, those functions would have to be adjusted to the real potential of the arbitrarily strained system (in contrast to the alternative potential used for obtaining the electrostatic stress). A guide to such a procedure is contained in the PhD thesis of Betzinger [Bet11], but in the context of the work at hand, we refrain from following it. Instead, Thonhauser *et al.* [TADS02] and Nagasako and Oguchi [NO11] suggested to neglect the corresponding terms, arguing that they should be comparatively small corrections. This is in parallel with the force calculation of Yu *et al.* [YSK91], where the change in the potential landscape, seen by the shifted atom, should make an adjustment of the radial functions necessary. In literature, this course of action is called the frozen augmentation approximation, since the augmentation of the plane waves is kept fix despite the changing potential.

Note that the variation in the unit cell volume is provided by the earlier split of the wave function into expansion coefficients by volume and volume times basis functions. The remaining variation in the a and b coefficients is calculated in the routine `dabcof.F`, where they are multiplied by the expansion coefficients and summed up over the reciprocal lattice vectors to form $\left. \frac{\delta}{\delta \varepsilon_{\alpha\beta}} A_{lm}^{av\mathbf{k}_\varepsilon}[\underline{\underline{\varepsilon}}] \right|_{\underline{\underline{\varepsilon}}=0}$.

We now can commence to formulate the valence contribution to the Pulay correction from the muffin-tin integrals

$$I_{\alpha\beta}^{av}(\mathbf{k}) = \int_{B_{R_a}(\mathbf{0})} \left[\frac{\delta}{\delta\varepsilon_{\alpha\beta}} \psi_{v\mathbf{k}}[\underline{\varepsilon}](\mathbf{r}_a[\underline{\varepsilon}]) \Big|_{\underline{\varepsilon}=0} \right]^* (\mathcal{H} - \epsilon_v(\mathbf{k})) \psi_{v\mathbf{k}}(\mathbf{r}_a) d^3r_a. \quad (5.49)$$

Similar to the calculation of the Hamilton and overlap matrices in chapter 3.3.5, we divide the expression into parts that are for the most part independent of the reciprocal vectors. To keep the formulas readable, we use the index λ , which we introduced in chapter 3.2 to switch between the radial function u and its energy derivative \dot{u} or their spatial counterparts $\varphi_L = u_l Y_L$ and $\dot{\varphi}_L = \dot{u}_l Y_L$. Then, the Pulay contribution takes the form

$$I_{\alpha\beta}^{av}(\mathbf{k}) = \sum_{L\lambda} \sum_{L'\lambda'} \left\{ \left[\frac{\delta}{\delta\varepsilon_{\alpha\beta}} A_{L\lambda}^{av\mathbf{k}\varepsilon}[\underline{\varepsilon}] \Big|_{\underline{\varepsilon}=0} \right] t_{LL'\alpha\beta}^{a\lambda\lambda'v}(\mathbf{k}) A_{L'\lambda'}^{av\mathbf{k}} + A_{L\lambda}^{av\mathbf{k}*} t_{LL'\alpha\beta}^{ad\lambda\lambda'v}(\mathbf{k}) A_{L'\lambda'}^{av\mathbf{k}} \right\}. \quad (5.50)$$

According to our convention, the factors $t_{LL'\alpha\beta}^{a\lambda\lambda'v}(\mathbf{k})$ correspond to the four factors $t_{LL'}^{a\varphi\varphi}$ to $t_{LL'}^{a\dot{\varphi}\dot{\varphi}}$, (3.40a) to (3.40d), with the energies E_l^a shifted down by $\epsilon_v(\mathbf{k})$. Therefore, we already know the left-hand sum. The factors $t_{LL'\alpha\beta}^{ad\lambda\lambda'v}(\mathbf{k})$ refer to the integrals containing the variation in $\varphi(\mathbf{r}[\underline{\varepsilon}])$,

$$t_{LL'\alpha\beta}^{ad\lambda\lambda'v}(\mathbf{k}) = \int_{B_{R_a}(\mathbf{0})} \left[\frac{\delta}{\delta\varepsilon_{\alpha\beta}} u_{l\lambda}^a(r[\underline{\varepsilon}]) Y_L(\widehat{\mathbf{r}[\underline{\varepsilon}]}) \Big|_{\underline{\varepsilon}=0} \right]^* \{\mathcal{H} - \epsilon_v(\mathbf{k})\} \varphi_{L'\lambda'}^a(\mathbf{r}) d^3r. \quad (5.51)$$

We split this expression according to the chain rule in a term containing the variation in the radial function and a term containing the variation in the spherical harmonic. This results in

$$t_{LL'\alpha\beta 1}^{ad\lambda\lambda'v}(\mathbf{k}) = (E_{l'}^a - \epsilon_v(\mathbf{k})) I_{ll'1}^{ad\lambda\lambda'} F_{LL'1}^{\alpha\beta} + \delta_{1\lambda'} I_{ll'1}^{ad\lambda 0} F_{LL'1}^{\alpha\beta} + \sum_{\nu>0} I_{l\nu l'1}^{ad\lambda\lambda'} F_{L\nu L'1}^{\alpha\beta} \quad \text{and} \quad (5.52a)$$

$$t_{LL'\alpha\beta 2}^{ad\lambda\lambda'v}(\mathbf{k}) = (E_{l'}^a - \epsilon_v(\mathbf{k})) I_{ll'2}^{ad\lambda\lambda'} F_{LL'2}^{\alpha\beta} + \delta_{1\lambda'} I_{ll'2}^{ad\lambda 0} F_{LL'2}^{\alpha\beta} + \sum_{\nu>0} I_{l\nu l'2}^{ad\lambda\lambda'} F_{L\nu L'2}^{\alpha\beta}. \quad (5.52b)$$

The radial integrals are given by

$$I_{ll'1}^{ad\lambda\lambda'} = \int_0^{R_a} r^3 \partial_r u_{l\lambda}^a(r) u_{l'\lambda'}^a(r) dr, \quad (5.53a)$$

$$I_{l\nu l'1}^{ad\lambda\lambda'} = \int_0^{R_a} r^3 \partial_r u_{l\lambda}^a(r) V_{\text{eff}\nu}^a(r) u_{l'\lambda'}^a(r) dr, \quad (5.53b)$$

$$I_{ll'2}^{ad\lambda\lambda'} = \int_0^{R_a} r^2 u_{l\lambda}^a(r) u_{l'\lambda'}^a(r) dr, \quad (5.53c)$$

and

$$I_{l\nu l'2}^{ad\lambda\lambda'} = \int_0^{R_a} r^2 u_{l\lambda}^a(r) V_{\text{eff}\nu}^a(r) u_{l'\lambda'}^a(r) dr, \quad (5.53d)$$

5. Stress from total energy calculations

while the factors

$$F_{LL'1}^{\alpha\beta} = \sum_{t,t'=-1}^1 c_{\alpha t} c_{\beta t'} \sum_{s=0}^{2,2} G_{s,1,1}^{t+t',t,t'} G_{l,s,l'}^{m,t+t',m'}, \quad (5.54a)$$

$$F_{L\nu L'1}^{\alpha\beta} = \sum_{t,t'=-1}^1 c_{\alpha t} c_{\beta t'} \sum_{s=0}^{2,2} G_{s,1,1}^{t+t',t,t'} \sum_{m_\nu} c_{\nu m_\nu}^a \sum_{s'=|l_\nu-l'|}^{l_\nu+l',2} G_{s',l_\nu,l'}^{m_\nu+m',m_\nu,m'} G_{l,s,s'}^{m,t+t',m_\nu+m'}, \quad (5.54b)$$

$$F_{LL'2}^{\alpha\beta} = \frac{1}{2} \sum_{s=-1}^{1,2} \sum_{t,t'=-1}^1 (c_{\alpha t'} c_{\beta}^{st*}(l, m) + c_{\beta t'} c_{\alpha}^{st*}(l, m)) G_{l+s,1,l'}^{m+t,t',m'}, \quad (5.54c)$$

and

$$F_{L\nu L'2}^{\alpha\beta} = \frac{1}{2} \sum_{s=-1}^{1,2} \sum_{t,t'=-1}^1 (c_{\alpha t'} c_{\beta}^{st*}(l, m) + c_{\beta t'} c_{\alpha}^{st*}(l, m)) \times \sum_{m_\nu} c_{\nu m_\nu}^a \sum_{s'=|l_\nu-l'|}^{l_\nu+l',2} G_{s',l_\nu,l'}^{m_\nu+m',m_\nu,m'} G_{l+s,1,s'}^{m+t,t',m_\nu+m'} \quad (5.54d)$$

contain the angular integrals resulting in Gaunt coefficients.

The dependence of (5.52a) and (5.52b) on the band index and the \mathbf{k} point expresses itself only through the eigenvalue of the band at the \mathbf{k} point. Storing the appropriate factors I and F beforehand allows to calculate these quantities on the fly when needed.

The Pulay stress is calculated in the routine `st_pulay_val2.f`, while the integrals and coefficients are set up in the subroutines `setintegrals` and `setcoefficients` of the same routine.

Again, a pressure calculation is not easily obtained by known quantities. Instead, the Pulay pressure should correct all other contributions with respect to the pressure zero, making it agree with the total energy minimum.

5.6.4. Core correction

In order to calculate the change in the energy eigenvalues of the core states, the term

$$\Omega \sigma_{\alpha\beta}^{\text{core}} = -\frac{1}{2} \sum_{a \in \Omega}^{\text{atoms}} \int_{B_{R_a}(\mathbf{0})} \rho_c^a(\mathbf{r}_a) (r_{a\alpha} \partial_\beta + r_{a\beta} \partial_\alpha) V_{\text{eff}}^a(\mathbf{r}_a) d^3 r_a \quad (5.55)$$

has to be evaluated. Remembering that the core density is already spherical, this leads to the formula

$$\begin{aligned}
 \Omega \sigma_{\alpha\beta}^{\text{core}} = & - \sum_{a \in \Omega} \sum_{\nu} I_{1\nu}^a \sum_{m_\nu} c_{\nu m_\nu}^{a*} \sum_{t,t'=-1}^1 c_{\alpha t} c_{\beta t'} G_{l_\nu, 1, 1}^{m_\nu, t, t'} \\
 & - \sum_{a \in \Omega} \sum_{\nu} I_{2\nu}^a \sum_{m_\nu} c_{\nu m_\nu}^{a*} \sum_{s=-1}^{1,2} \delta_{1, l_\nu + s} \\
 & \times \sum_{t,t'=-1}^1 (c_{\alpha t'} c_{\beta}^{st}(l_\nu, m_\nu) + c_{\beta t'} c_{\alpha}^{st}(l_\nu, m_\nu)) \delta_{t', m_\nu + t} \quad (5.56)
 \end{aligned}$$

with the radial integrals

$$I_{1\nu}^a = \int_0^{R_a} r^3 \rho_c^a(r) \partial_r V_{\text{eff}\nu}^a(r) dr \quad \text{and} \quad (5.57a)$$

$$I_{2\nu}^a = \int_0^{R_a} r^2 \rho_c^a(r) V_{\text{eff}\nu}^a(r) dr. \quad (5.57b)$$

This formula is contained in the routine `st_pulay_cor.f`.

Core Pressure

While the pressure arising from the core electrons also needs to be calculated separately, its simple form allows to use it as a test for accuracy. The trace of the core stress gives

$$\begin{aligned}
 3P_{\text{core}}\Omega = & \sum_{a \in \Omega} \int_{B_{R_a}(\mathbf{0})} \rho_c^a(\mathbf{r}_a) \mathbf{r}_a \cdot \nabla V_{\text{eff}}^a(\mathbf{r}_a) d^3 r_a \\
 = & \sqrt{4\pi} \sum_{a \in \Omega} \int_0^{R_a} r_a^2 \rho_c^a(r_a) \partial_{r_a} V_{\text{eff}0}^a(r_a) dr_a \quad (5.58)
 \end{aligned}$$

since the trace of $r_\alpha \partial_\beta$ is just a radial derivative.

The trace of (5.42) yields as a second test for the core correction

$$\sum_{a \in \Omega} \int_{B_{R_a}(\mathbf{0})} \rho_c^a(\mathbf{r}_a) \mathbf{r}_a \cdot \nabla V_{\text{eff}}^a(\mathbf{r}_a) d^3 r_a = 2E_{\text{kin}}^{\text{core}}. \quad (5.59)$$

The second term is easily obtained from the total kinetic energy by subtracting from it the kinetic energy of the valence states. In this way, the differentiation of the core states is avoided.

5.7. Stress from local orbitals

We now know how to proceed in the construction of the stress tensor in the standard FLAPW method using the frozen core and frozen augmentation approximation. We want to add the local orbital extension in the same framework as well. Recall (3.48), the definition of a local orbital as

$$\phi_{\mathbf{k}\mathbf{G}_{l_0}}^{a,l_0}(\mathbf{r}_a) = \sum_{m\lambda} A_{L,l_0,\lambda}^{a\mathbf{k}\mathbf{G}_{l_0}} u_{l,l_0,\lambda}^a(r_a) Y_L(\hat{\mathbf{r}}_a). \quad (5.60)$$

An expansion into the basis functions happened on three occasions of the stress calculation: The calculation of the kinetic stress (5.43), the correction of the stress from the surface terms (5.46) forming the discontinuity correction and the valence correction due to the incompleteness of the FLAPW basis set (5.49).

The implementation of this expression to the stress contribution coming from the kinetic energy (5.43) is straightforward. Let λ and λ' go from 0 to 2 and include the A , B , and C coefficients of the local orbitals in the factors $A_{L\lambda}^{av\mathbf{k}}$. The latter is the standard procedure of handling the A , B , and C coefficients in FLEUR. Since the dependence of the formula on \mathbf{G} or \mathbf{G}_{l_0} is only by these coefficients, no further adjustments have to be made to the kinetic stress formula.

Since the local orbitals are constructed to vanish at the muffin-tin boundary, they do not contribute to the discontinuity correction (5.46). Therefore, the remark in the previous paragraph about the matching coefficients already containing their counterparts from the local orbital extension is irrelevant in this context. One could subtract the A , B , and C coefficients from the factors $A_{L\lambda}^{av\mathbf{k}}$, but this would result in unnecessary computation time.

Then, only the adjustment of the Pulay stress (5.49) due to the local orbitals is left to be calculated. Herein, we back-transformed the coordinates to the unstrained system. We have thus to find the variation of

$$\psi_{\mathbf{k}\mathbf{G}_{l_0}}^{a,l_0}[\underline{\underline{\varepsilon}}](\mathbf{r}_a) = \sum_{m\lambda} A_{L,l_0,\lambda}^{a\mathbf{k}\varepsilon\mathbf{G}_{l_0\varepsilon}}[\underline{\underline{\varepsilon}}] u_{l,l_0,\lambda}^a(r_a[\underline{\underline{\varepsilon}}]) Y_L(\widehat{\mathbf{r}}_a[\underline{\underline{\varepsilon}}]) \quad (5.61)$$

The matrix elements (5.51) can handle the variation of the unmatched muffin-tin functions $\varphi_{L,l_0,\lambda}^a(\mathbf{r}_a) = u_{l,l_0,\lambda}^a(r_a[\underline{\underline{\varepsilon}}]) Y_L(\widehat{\mathbf{r}}_a[\underline{\underline{\varepsilon}}])$ in the case of local orbitals, too, by allowing for $\lambda = 2$. Since the $A_{L\lambda}^{av\mathbf{k}}$ of FLEUR already contain the A , B , and C coefficients of the local-orbital extension, we only need to find the variation of the matching coefficients of the local orbitals to also construct the left term of the sum in (5.50). With the frozen augmentation approximation and $\mathbf{K}_{l_0} = \mathbf{k} + \mathbf{G}_{l_0}$, the matching coefficients (3.49) of the strained system have the form

$$A_{L,l_0,\lambda}^{a\mathbf{k}\mathbf{G}_{l_0}}[\underline{\underline{\varepsilon}}] = \frac{4\pi i^l}{W_l^a(R_a, E_l^a)} e^{i\mathbf{K}_{l_0} \cdot \boldsymbol{\tau}_a} a_{l,l_0,\lambda}^a Y_L^*(\widehat{\mathbf{K}}_{l_0}[\underline{\underline{\varepsilon}}]), \quad (5.62)$$

since the lower case a , b , and c coefficients (3.46a) to (3.46c) are constructed only from radial functions evaluated at the muffin-tin boundary. Thus, the strain variation results in a contribution from the spherical harmonics, only. It is given by

$$\begin{aligned} \left. \frac{\delta}{\delta \varepsilon_{\alpha\beta}} A_{L,lo,\lambda}^{a\mathbf{k}\mathbf{G}_{lo}}[\underline{\varepsilon}] \right|_{\underline{\varepsilon}=0} &= \frac{4\pi i^l}{W_l^a(R_a, E_l^a)} e^{i\mathbf{K}_{lo}\cdot\boldsymbol{\tau}_a} a_{l,lo,\lambda}^a \\ &\times \frac{K_{lo\alpha}}{K_{lo}} \sum_{s=-1}^{1,2} \sum_{t=-1}^1 c_{\beta}^{st}(l, m) Y_{l+s, m+t}^*(\hat{\mathbf{K}}_{lo}). \end{aligned} \quad (5.63)$$

We can then add the product of the expansion coefficients $z_{v\mathbf{k}\mathbf{G}_{lo}}^a$ and the variation of the capital case factor $A_{L,lo,\lambda}^{a\mathbf{k}\mathbf{G}_{lo}}$ to the FLAPW matching coefficients and evaluate Eq. (5.49).

The local orbital extension is not yet implemented into the calculation of the stress tensor in the FLEUR code.

5.8. A simple pressure formula

We can sum up all checks for accuracy to obtain a simple formula for the pressure. By using the expressions (5.13), (5.14a), (5.14b), (5.14c), (5.17a) and (5.25), we find

$$\begin{aligned} -3P\Omega &= \sum_{\alpha=1}^3 \left. \frac{\delta}{\delta \varepsilon_{\alpha\alpha}} E[\underline{\varepsilon}] \right|_{\underline{\varepsilon}=0} \\ &= -2E_{kin}^{val} + \frac{5}{2} \int_{\Omega} \rho(\mathbf{r}) V_C(\mathbf{r}) d^3r + \frac{1}{2} \sum_{a \in \Omega}^{atoms} Z_a V_M^a(\boldsymbol{\tau}_a) + 3 \int_{\Omega} \rho(\mathbf{r}) (\varepsilon_{xc}(\mathbf{r}) - V_{eff}(\mathbf{r})) d^3r \\ &\quad + \sum_{a \in \Omega}^{atoms} \int_{B_{R_a}(\mathbf{0})} \rho_c^a(\mathbf{r}_a) \mathbf{r}_a \cdot \nabla V_{eff}^a(\mathbf{r}_a) d^3r_a + \sum_{\alpha=1}^3 (\sigma_{\alpha\alpha}^{val} + \sigma_{\alpha\alpha}^{disc}), \end{aligned} \quad (5.64a)$$

or, reformulating the core correction as in (5.42) and merging the second term of this equation with the one containing the exchange-correlation energy density

$$\begin{aligned} -3P\Omega &= -2E_{kin} - \frac{1}{2} \int_{\Omega} \rho V_C d^3r + \frac{1}{2} \sum_{a \in \Omega}^{atoms} Z_a V_M^a(\boldsymbol{\tau}_a) + 3 \int_{\Omega} \rho (\varepsilon_{xc} - \mu_{xc}) d^3r \\ &\quad + \sum_{\alpha=1}^3 (\sigma_{\alpha\alpha}^{val} + \sigma_{\alpha\alpha}^{disc}). \end{aligned} \quad (5.64b)$$

The simple pressure formula coincides with the one in [TADS02] found by Thonhauser *et al.* The first line can easily be obtained from quantities available in a FLAPW code for the total energy calculation. The second line makes use of (5.46) and (5.50).

6. Discussion

We want to draw a comparison between this work and the prior publications of Nielsen and Martin [NM85a], Thonhauser *et al.* and Nagasako and Oguchi [NO11].

Nielsen and Martin as well as Thonhauser *et al.* suggested that the wave functions and density change under strain by an inner variation only,

$$\psi[\underline{\underline{\varepsilon}}](\mathbf{r}_\varepsilon) = \frac{1}{\sqrt{\det(\underline{\underline{1}} + \underline{\underline{\varepsilon}})}} \psi(\mathbf{r}) \quad \text{and} \quad (6.1)$$

$$\rho[\underline{\underline{\varepsilon}}](\mathbf{r}_\varepsilon) = \frac{1}{\det(\underline{\underline{1}} + \underline{\underline{\varepsilon}})} \rho(\mathbf{r}). \quad (6.2)$$

This corresponds to the smearing of the density over the strained lattice which we found while deriving the electrostatic stress formula. Nielsen and Martin did not take into account the effects of a finite LAPW basis because they presented a general deduction in the DFT formalism. Therefore, they were able to apply the Hellmann-Feynman theorem to all states. Our equations less the discontinuity correction (5.15b) and the valence correction (5.15a) coincide with (30a) - (30e) of [NM85a] conceptually, with the electrostatic and Madelung stress split into the stress from ion-ion, ion-electron and electron-electron energies, respectively. Note though that we obtain the stress component from the kinetic energy of the core electrons from the core correction via (5.42). In the FLAPW method, the core charge is assumed to be spherical both in the strained and in the unstrained system and both systems are initially set up with muffin-tin spheres, not ellipsoids. Therefore, the core density of an atom can roughly be assumed to be displaced along with the atom without further changes, particularly in the kinetic energy.

Thonhauser *et al.* also included a contribution from the core electrons to their kinetic stress formula. As does this thesis, they worked in the context of the FLAPW method. Their corrections (30) and (31) in [TADS02] coincide with (5.15b) and (5.15a). They also present with their Eq. (21) the same core correction as we do in Eq. (5.13) of this thesis, but with a different sign. However, they reason that the trace term vanishes in the case of pure pressure. Following Janak [Jan74] we have shown that the core correction can either be accounted for directly by (5.13) or as a contribution to the kinetic stress (5.42), but not both. Hence we believe that Eq. (21) in [TADS02] is redundant. Since they present pressure calculations only, they could neither check the validity of their sign nor the necessity of their additional core correction.

A further sign that in the FLAPW method, the core correction does not initially stem from a change in the kinetic energy of the core electrons is provided in Eq. (4.8), its appearance in the force formalism. From this formula, no connection to a kinetic energy

6. Discussion

term can be drawn. In the FLAPW method, the special form of the stress operator, $\mathbf{r} \otimes \nabla$, is necessary to allow for a connection between the core correction and a term that can be linked to the kinetic energy by partial integration of the kinetic energy operator.

To return to the discussion of the strained density, we allowed for an arbitrary change of the electronic density in the strained lattice. The assumption that the density should only vary by a smearing seemed unphysical to the author, since the tightly bound core states should not be affected much by a small change in the lattice configuration, as we pointed out before. The fact that the variation of the form of the density does cancel during the calculation backs up the choice of Thonhauser *et al.* to assume the strained density as an inner variation of the original one.

In [TADS02], the authors already suggested that the "usual LAPW machinery for the Coulomb potential can be used" to obtain the variation in the electrostatic potential by plugging in the variation of the density in the Weinert method. However, they provide no formulas to which we can compare our equations to. Since the formulation of the variation of the electrostatic potential is elaborate and takes up a great part of this work, they might have skipped it for a better legibility of their publication. Note that they seem to have included only the variation of the $1/r$ potential in their calculation of the variation of the electrostatic potential, whereas we include the change in the volume as well. This results in a difference between our term (5.17a) and their Eq. (19) in $\delta_{\alpha\beta} \int \rho V_C d^3r$. The difference is the contribution from the change in volume of the integral containing the electrostatic potential. As we emphasized, the use of integral kernels of the form $(r_\alpha - s_\alpha)(r_\beta - s_\beta)/|\mathbf{r} - \mathbf{s}|^2$ is inconvenient in the FLAPW method due to their non-locality. Thus we suggested to calculate the alternative electrostatic and Madelung potential (5.21) and (5.22) in the strained system beforehand and perform the variation with respect to the strain afterwards.

While the formula for the discontinuity correction (5.15b) is provided by Thonhauser *et al.*, they use the Slater form of the kinetic energy operator in their computations, i.e. they integrate $(\nabla\psi)^*(\nabla\psi)$ instead of $-\psi^*\nabla^2\psi$. The LAPW basis is continuous up to first order at the muffin-tin boundaries. Therefore, the Slater form does not imply the discontinuity correction.

Nagasako and Oguchi also state that their derivation of the stress tensor does not contain any surface terms. The reason for the absence of the surface terms is the special basis set of Soler and Williams used in [NO11]: Without going into much detail, the basis set proposed by Soler and Williams is roughly described as plane waves plus local orbitals. A plane wave basis is used not only in the interstitial space, but extended over the whole unit cell. On top of those plane waves, in the muffin-tin spheres a special SW-LAPW basis is formed that is composed of a regular LAPW basis set from which the excess plane-wave states are subtracted again. Thus, the basis set of Soler and Williams does resemble the course of action taken with the Weinert method. The spherical Bessel functions that appear during this process replace the radial functions \tilde{u}_l that we use in our local orbital extension. Since the LAPW basis in the muffin-tin spheres is matched to the plane wave description of the interstitial region on the muffin-tin boundary, the

muffin-tin specific basis functions of the Soler and Williams basis set vanish at the sphere boundary. With this knowledge, the absence of a discontinuity correction or other surface terms becomes understandable: The plane waves are smooth in the whole unit cell and the basis functions restricted to the muffin-tin spheres are zero at the boundary of those spheres.

The discussion on the topic of the existence of surface integrals in the FLAPW method already occurred at the introduction of atomic forces to the FLAPW method by Yu *et al.* [YSK91] using the regular LAPW basis set and by Soler and Williams [SW89] using their SW-LAPW basis. The equivalence between both force formalisms was shown eventually by Soler and Williams [SW93].

Regarding the stress calculation, the modified LAPW basis set allows the description of a strained system by smearing the plane waves over the lattice and moving the muffin-tin spheres to the strained atomic positions. The kinetic stress of the plane wave basis, Eq. (33) in [NO11], corresponds well to our formula describing the interstitial kinetic stress, while they find for the variation of the muffin-tin basis functions Eq. (35) an expression that resembles the kinetic part of the valence correction (5.15a). Nagasako and Oguchi motivate the lack of a contribution to the kinetic stress from the core electrons by the frozen core approximation. They do not explicitly point out a core correction in their formulas. We believe however, that the last terms in Eqs. (47) and (58) within their calculation of the electrostatic and exchange-correlation stress correspond to the correction. This can be motivated by replacing the variation with respect to the strain by $r_\alpha \partial_\beta$ and performing an integration by parts. For an exact study, more insight into the construction of the core electronic density within the SW-LAPW basis would be necessary. Still, the deduction of Nielsen and Martin holds in the general context of DFT and implies a contribution to the kinetic stress from all states.

Nagasako and Oguchi find the contribution of the variation of the electrostatic potential to the valence correction in the two terms above the core correction in Eq. (47), where they also provide a formula for the actual stress contribution from the electrostatic energy. Finally, Eq. (56) and the first term in Eq. (58) complete their formula for the valence correction by adding its contribution containing the exchange-correlation potential.

7. Application of the stress formalism to aluminum

Aluminum is experimentally found to be a face-centered cubic system with an unit-cell volume of 66.42\AA^3 or $112.1a_0^3$ [Coo62].

To check the implementation of the stress formalism, we calculate an aluminum bulk. Values for pressure are given at four unit-cell volumes by Thonhauser *et al.* [TADS02], to which we can compare our results.

We calculate total energies, the components of the stress tensor, and the pressure formulas we have found for unit-cell volumes of $104.2a_0^3$, $106.4a_0^3$, $110.0a_0^3$, and $114.9a_0^3$ for comparison as well as intermediate volumes of $105.3a_0^3$, $108.2a_0^3$, $111.6a_0^3$, and $113.3a_0^3$. The calculations are set up with cut-off parameters of $g_{\max} = 3.8$ Htr and $l_{\max} = 10$ as provided by the input-file generator of FLEUR. Furthermore, the muffin-tin radius of the aluminum atoms is $R_{\text{Al}} = 2.59a_0$. The radial functions are sampled over 623 grid points with a logarithmic increment of 0.018. We use a $12 \times 12 \times 12$ \mathbf{k} -point mesh that includes the Γ -point for the first Brillouin zone. The exchange-correlation functional is chosen to be the LDA functional of Perdew and Zunger [PZ81]. Those settings are shared by all calculations.

In table 7.1, we give the parameters found by performing a least squares fit of the Birch-Murnaghan equation of states [Bir47]

$$E(\Omega) = E_0 + \frac{9\Omega_0 B_0}{16} \left\{ \left[\left(\frac{\Omega_0}{\Omega} \right)^{\frac{2}{3}} - 1 \right]^3 B'_0 + \left[\left(\frac{\Omega_0}{\Omega} \right)^{\frac{2}{3}} - 1 \right]^2 \left[6 - 4 \left(\frac{\Omega_0}{\Omega} \right)^{\frac{2}{3}} \right] \right\} \quad (7.1)$$

to the results of the calculation (see fig. 7.1 on the next page). The negative derivative of the Birch-Murnaghan formula with respect to the unit-cell volume provides the pressure $P = -dE(\Omega)/d\Omega$.

Parameters	Result
Minimal energy E_0 (Htr)	-241.9182166
Equilibrium volume Ω_0 (a_0^3)	107.106
Bulk modulus B_0 (Htr/ a_0^3)	$2.986 \cdot 10^{-3}$
Derivative B'_0 (dim.less)	4.774

Table 7.1.: Birch-Murnaghan fit to DFT data of aluminum

7. Application of the stress formalism to aluminum

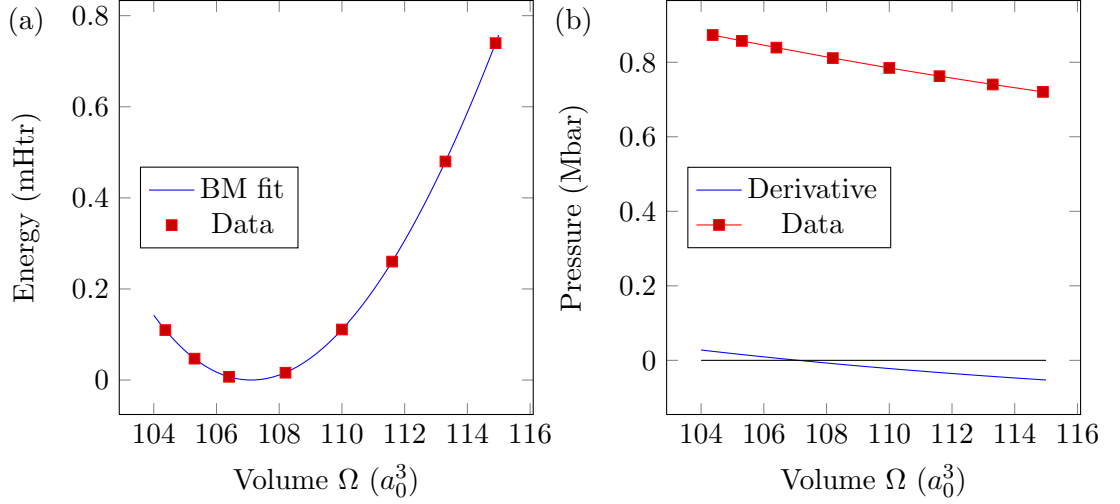


Figure 7.1.: (a) Birch-Murnaghan fit to total-energy data of aluminum, shifted by E_0 . (b) Negative derivative of the Birch-Murnaghan fit and pressure data without Pulay correction.

The equilibrium volume obtained from the total-energy calculation deviates by less than one percent from $106.519a_0^3$, the value found by Thonhauser *et al.* [TADS02]. This deviation can be explained by a different setup of the calculations. The size of the \mathbf{k} -point mesh, the cut-off parameters, and the choice of the exchange-correlation functional all influence the outcome of the calculation. The publication of Thonhauser *et al.* does not give details on their setup. Furthermore, LDA is known to underestimate lattice constants [KSU95], which explains the difference to the experimental value of $112.1a_0^3$.

Figure 7.2 shows the total values of stress and pressure in (a). Neither stress nor pressure exhibit a zero-crossing. Therefore, none of the quantities indicate an equilibrium volume of aluminum in the range of $104.2a_0^3$ to $114.9a_0^3$. This contradicts the existence of an energy minimum at a volume of $107.106a_0^3$. Furthermore, stress and pressure do not coincide. Even though at first glance the deviation seems to be caused by an error in sign, this is not the case, as the remaining figures demonstrate:

The components of stress and pressure from the kinetic energy of the valence states (5.40a) and (5.44), shown in figure (b), deviate by less than 0.1 percent from each other. In figure (c), the contributions of the core correction (5.40g) and the test term (5.42) agree within 0.3 percent. The remaining Pulay correction consisting of the valence term (5.40e) and the surface term (5.40f) is shown in figure (f). The correction is added to the stress as well as to the pressure. In figure (e), the contribution (5.40b) from the change in volume of the unit cell is depicted. This contribution is calculated identically within the stress and pressure computation, so there is no deviation by construction. Instead the deviation in figure (a) is a consequence of the systematic deviation between the stress and pressure components from the electrostatic energy derivation, as shown in figure (c).

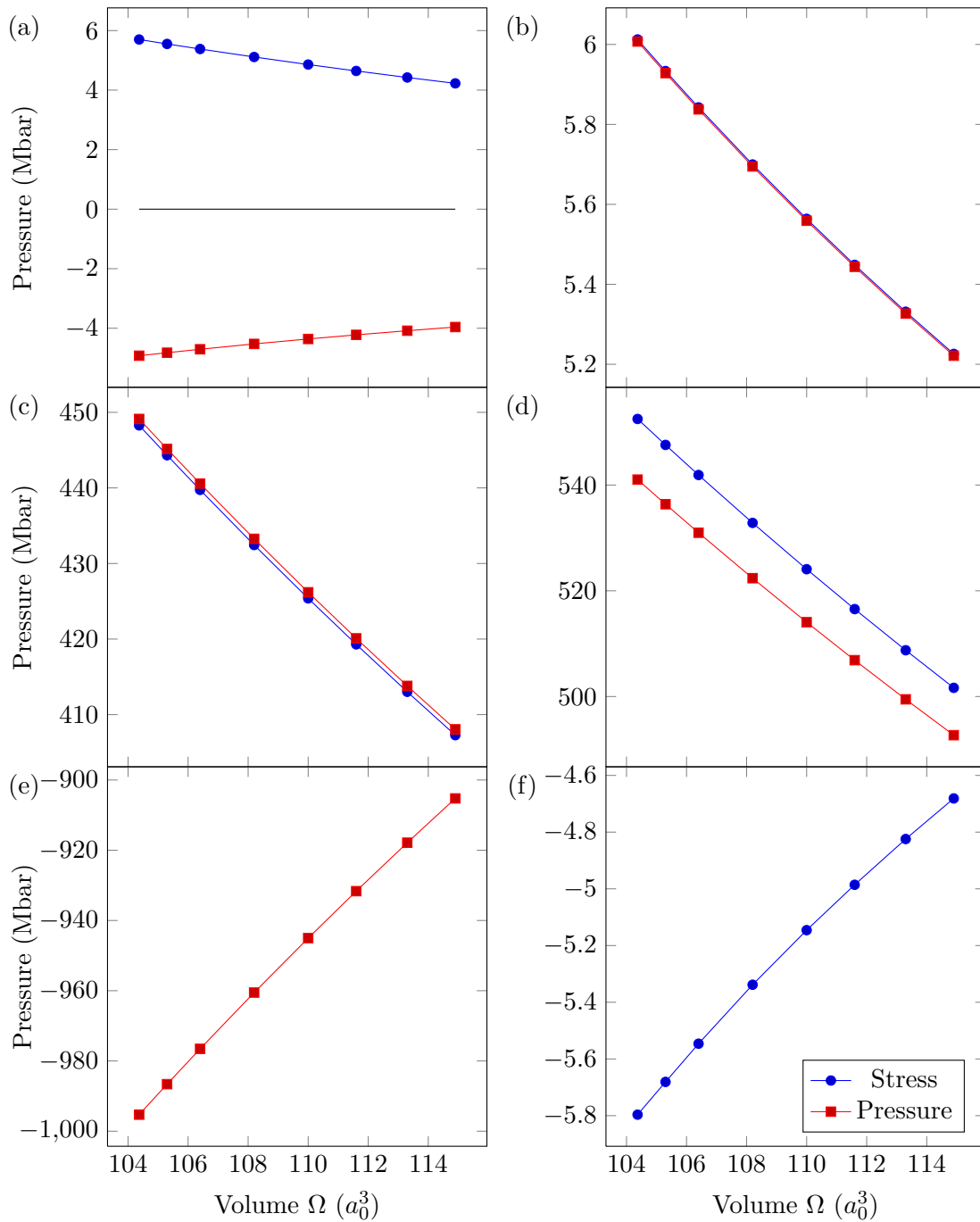


Figure 7.2.: Calculated results of the trace of the stress tensor and the pressure formulas. (a) shows the total stress and pressure, including the valence and discontinuity correction. (b) shows the kinetic stress and pressure of the valence states. (c) shows the core correction and the kinetic pressure of the core states. (d) shows the electrostatic stress and pressure. (e) shows the exchange-correlation stress (5.40b). It coincides with pressure by construction. (f) shows the Pulay correction without the core correction.

7. Application of the stress formalism to aluminum

The differences between the stress and pressure components are plotted in figure 7.3. It becomes apparent that the deviation between total stress and pressure is dominated by the deviation of the electrostatic components of both quantities.

Two conclusions have to be drawn from our results:

First, the calculation of the electrostatic stress components is erroneous. The simple pressure formula (5.64b) contains simple terms obtainable from any DFT total-energy calculation. It agrees to the formula derived by Thonhauser *et al.* and the earlier formula of Janak [Jan74]. Therefore, we assume that the stress components are wrong, not the pressure components. In addition, we present in table 7.2 a comparison between our calculations and the results presented by Thonhauser *et al.* The origin of this error has to be traced very vigilantly. The electrostatic stress component comprises of 8 different contributions. Not all of them can be tested separately by applying the stress formalism to realistic systems. Hence, the construction of convenient test cases is assumed to help with the correction of the electrostatic stress. The qualitatively similar form of the electrostatic stress curve compared to the pressure curve indicates a systematic error. Maybe the implementation of one or more of the 8 contributions misses a factor.

Another source of error is the special method, in which the iterations to find the self-consistent electronic density proceed. In order to find the ground state density, the density from the previous iteration is used as an input to construct the electrostatic potential. Then the Kohn-Sham states are calculated and the new density is formed as an output of the current iteration. However, a clever mixing of the input and output density can help to achieve a faster convergence. The formulas derived in this thesis are found under the assumption that the charge density is given self-consistently, meaning that the mixed input and output densities are assumed to coincide. While the calculations presented in this chapter are converged by the standards of a total-energy calculation, it is unclear, how sensitive the stress calculation is to differences between input and output density.

Second, the sum of valence and discontinuity correction is too large. Note that if the total pressure is shifted up by the Pulay correction, its curve progresses just above zero pressure (see fig. 7.1(b)). A smaller correction would then generate a zero-crossing. The comparison between our results and the results given by Thonhauser *et al.*, provided in table 7.2, shows that they obtained only a small contribution from the valence correction. In their publication, Thonhauser *et al.* comment that the valence correction should include a contribution from the interstitial region. We have proved in chapter 5.6.3, that our valence correction only comprises of terms that have their origin in the muffin-tin spheres. We therefore believe that the implementation of the Pulay correction in the FLEUR code is incorrect, not its analytic derivation. The construction of test cases that focus on the Pulay correction will help to pinpoint the error.

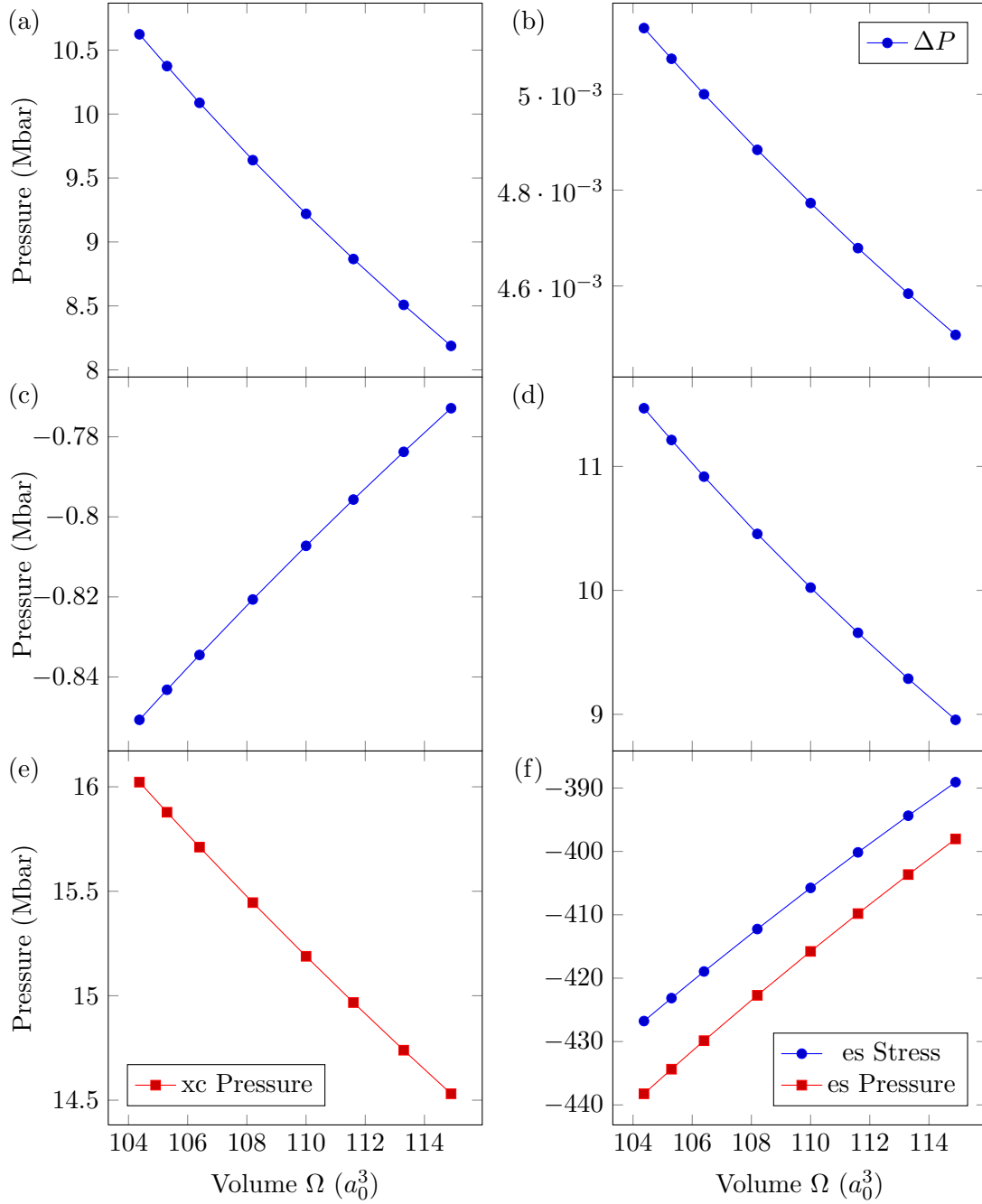


Figure 7.3.: Difference between stress and pressure. (a) shows the total difference. (b) and (c) show the difference between the kinetic stress and pressure components of the valence and core states, respectively. (d) shows the difference between electrostatic stress and pressure. This contribution dominates the difference between total stress and pressure. (e) and (f) correspond to figures 7.2(e) and (d). $6 \int \rho V_C d^3r$ is transferred from the exchange-correlation term to the electrostatic term. Thonhauser *et al.* use this convention.

7. Application of the stress formalism to aluminum

Volume (a_0^3)	104.2	106.4	110.0	114.9
Contribution	Pressure (kbar)			
Electrostatic	-437027.2	-427961.4	-414112.3	-396302.8
Pressure	-438236.9	-429861.6	-415775.6	-398024.5
Stress	-426767.7	-418944.3	-405753.5	-389068.9
Kinetic valence	5981.1	5797.8	5525.5	5189.3
Pressure	6007.3	5837.5	5559.0	5221.4
Stress	6012.4	5842.5	5563.8	5225.9
Kinetic core	447059.0	437820.8	423703.5	405540.6
Pressure	449125.0	440574.7	426190.2	408054.3
Stress	448274.3	439740.2	425383.0	407281.4
E_{xc} part	-16002.4	-15665.2	-15150.5	-14489.3
Pressure	-16022.3	-15711.3	-15188.7	-14530.7
Pulay correction	7.5	7.3	7.0	6.9
Stress	-5796.4	-5546.2	-5145.8	-4681.1

Table 7.2.: Results of the stress calculation of Thonhauser *et al.* [TADS02] (bold rows) and of the pressure and stress calculation of this thesis (indented lines below). Note that the variation in the unit-cell volume is part of the variation of the electrostatic potential in this thesis, but not in the publication of Thonhauser *et al.* There it cancels with the electrostatic contribution in the term containing the exchange-correlation density (5.40b). We have adjusted our results to provide comparability.

Thonhauser *et al.* note that in order to calculate the stress, similar large numbers have to be subtracted from each other. We recognize the problem this poses for the accuracy of the stress formalism. Once the electrostatic stress and the Pulay correction are implemented correctly in the FLEUR code, we are able to perform checks on the numerical accuracy of the stress tensor.

8. Conclusion & Outlook

In this thesis, we have derived the stress tensor from the total-energy expression of density-functional theory within the FLAPW method. We found several terms that are related to corresponding terms in the atomic-force formalism by Yu *et al.* [YSK91]. These include the Pulay corrections that are necessary due to the use of an insufficiently complete set of basis functions. Since the valence states are constructed using a finite basis, their derivation by strain cannot be expressed in terms of the same basis. Therefore, the valence correction occurs. Also, the valence states are constructed to match in value and radial derivative on the muffin-tin boundaries. The kinetic energy operator is a differential operator of second order. Hence it is sensible to the discontinuity of the valence states on the sphere shell, which moves to the new atomic position and deforms in the strained lattice. This explains the need for the discontinuity correction. The core correction has to be considered because the core density is always assumed to be spherical, in the original system as well as in the strained system. However, the (local) crystal potential in the strained lattice differs from the potential in the unstrained case, which affects the construction of the core states. This is accounted for in the core correction. The correction terms are conceptually of the same form as their counterparts in the force formalism. However, we have presented a relation between the core correction and a term that has the same form of the kinetic stress component of the valence states, but evaluated with the core states. This relation was proved by Janak [Jan74].

We also derived the Hellmann-Feynman stress, which is the variation of the Hamiltonian by stress. In contrast to the calculation of atomic forces, where the Hellmann-Feynman term was given exclusively by the variation in the Madelung potential, the HF stress includes also a contribution from the interaction of the electrons with all charged particles. In addition, the change of volume generated by strain gives rise to additional volume terms. We also derived a stress contribution from the kinetic energy of the valence states (and of the core states, if the core correction is allocated at this place and not with the corrections). The latter two are easy formulas, partly because we have chosen to stay with the local density and generalized gradient approximations. The derivation of the electrostatic stress is the most elaborate part of this thesis, though. As space is partitioned into the muffin-tin spheres and the interstitial region, the non-local nature of the electrostatic and Madelung potential poses a challenge to calculate their respective energy contributions. The calculation of stress is even more challenging, since the space is deformed in a strained system. Therefore, we have chosen to calculate an auxiliary alternative electrostatic potential in the strained lattice, using the strained coordinates but the original electronic density smeared over the strained lattice. Doing so, we are able to use the method to construct the electrostatic potential presented by Weinert [Wei81] prior to the variation by strain.

8. Conclusion & Outlook

First practical steps of an implementation have been taken. A rough agreement to data provided by Thonhauser *et al.* [TADS02] indicates that the implementation has to be revised. While most stress components are in good agreement to the pressure formulas that we provided for test purposes, the contribution to the stress from the electrostatic energy shows a systematic deviation from the pressure values. Also, the sum of the valence and discontinuity correction does not behave as expected. Both contributions, the electrostatic stress and the sum of the correction terms, are composed of several terms in our implementation. Hence, they are very susceptible for errors in the code.

As soon as the stress formulas are implemented more rigorously in the FLEUR-code, we are confident to have a tool at hand that allows for structural optimization of materials beyond atomic forces. The subsequent implementation of symmetry relations of stress components from related \mathbf{k} and \mathbf{G} vectors or spatial coordinates is expected to produce a considerable speed-up in the computing time.

By relaxing a system not with respect to $\underline{\underline{\sigma}} = \underline{\underline{0}}$, but to another value of the stress tensor, one should be able to perform a lattice relaxation for systems subject to external stress. Also, local minima of the energy surface with respect to the lattice configuration can be found, if the initial parameters are chosen accordingly. Thus, the existence of different phases of materials depending on pressure can be probed.

The addition of collinear magnetism to the formalism should present not much of a problem, since many of the formulas can simply be rewritten to include different spin channels. Doing so, data on magnetic anisotropy and magnetization axes should be accessible. Also, the effects of magnetic fields on the shape of systems can be obtained in this case. The implementation of magnetism into the calculation is of interested for finding materials usable in transformers or dynamos, for example. The iron cores often used in these devices periodically deform in a rotating magnetic field. Therefore, they consume energy and heat up. The periodic deformations are the origin of the characteristic humming one hears next to a transformer. Other materials which deform less than iron in a magnetic field, can improve the efficiency of those devices.

Since the development of more sophisticated exchange-correlation functionals goes on and has helped the accuracy of DFT calculations, their inclusion into the stress formalism seems to be asked for. Due to the non-locality of the newer attempts at the exchange-correlation functional, we predict their inclusion into the stress formalism to be a challenging endeavor, though.

A. Appendix

A.1. Proof of (3.27)

To make our introduction to Weinert's method to calculate the electrostatic potential sound, we have to show the equality

$$\sum_{\eta=0}^N \frac{(-1)^\eta}{2l + 2\eta + 3} \binom{N}{\eta} = \frac{2^N N!(2l + 1)!!}{(2l + 2N + 3)!!}.$$

In order to prove this equation, we borrow the beta and gamma functions from calculus [Abr65].

$$B(x, y) = \int_0^1 t^{x-1} (1-t)^{y-1} dt \quad (\text{A.1a})$$

$$\Gamma(x) = \int_0^\infty t^{x-1} e^{-t} dt \quad (\text{A.1b})$$

Both functions are related by the equation

$$B(x, y) = \frac{\Gamma(x)\Gamma(y)}{\Gamma(x+y)} \quad (\text{A.1c})$$

and the gamma function fulfills

$$\Gamma(x+1) = x\Gamma(x) \text{ and} \quad (\text{A.1d})$$

$$\Gamma(n+1) = n! \quad (\text{A.1e})$$

for all positive reals x and positive integers n .

Examine the integral

$$\frac{1}{2} B\left(\frac{2l+3}{2}, \frac{2N+2}{2}\right) = \frac{1}{2} \int_0^1 t^{\frac{2l+1}{2}} (1-t)^N dt = \int_0^1 t^{2(l+1)} (1-t^2)^N dt.$$

The expansion of the integrand into a binomial series yields

$$\begin{aligned} \frac{1}{2} B\left(\frac{2l+3}{2}, \frac{2N+2}{2}\right) &= \int_0^1 t^{2(l+1)} \sum_{\eta=0}^N (-1)^\eta \binom{N}{\eta} t^{2\eta} dt \\ &= \sum_{\eta=0}^N (-1)^\eta \binom{N}{\eta} \int_0^1 t^{2l+2\eta+2} dt = \sum_{\eta=0}^N \frac{(-1)^\eta}{2l+2\eta+3} \binom{N}{\eta}. \end{aligned} \quad (\text{A.2})$$

A. Appendix

This is the left-hand side of the equality we want to show. On the other hand, we can use (A.1c) and the properties (A.1d) and (A.1e) to find

$$\begin{aligned} \frac{1}{2}B\left(\frac{2l+3}{2}, \frac{2N+2}{2}\right) &= \frac{1}{2} \frac{\Gamma\left(l + \frac{3}{2}\right) \Gamma(N+1)}{\Gamma\left(l + N + \frac{5}{2}\right)} \\ &= \frac{N!}{2} \frac{\left(l + \frac{1}{2}\right)!}{\left(l + N + \frac{3}{2}\right)!} = \frac{2^N N!(2l+1)!!}{(2l+2N+3)!!}. \end{aligned} \quad (\text{A.3})$$

A.2. Hellmann-Feynman force formula

We want to derive Eq. (4.5). To do so, we perform the differentiation in Eq. (4.2). We obtain

$$\mathbf{F}_{\text{HF}}^c = -Z_c \frac{\delta}{\delta \boldsymbol{\tau}_c} \left\{ \int_{B_{R_c}(\mathbf{0})} \rho^c(\mathbf{s}_c) G(-\delta \boldsymbol{\tau}_c, \mathbf{s}_c) d^3 s_c - \frac{1}{4\pi} \oint_{\partial B_{R_c}(\mathbf{0})} V_C^c(\mathbf{s}_c) \frac{\partial G}{\partial s_c}(-\delta \boldsymbol{\tau}_c, \mathbf{s}_c) dS_2 \right\}.$$

By inserting the formulas for the Green's function (3.30) and (3.32), we can evaluate this expression to get

$$\begin{aligned} \mathbf{F}_{\text{HF}}^c &= Z_c \frac{\delta}{\delta(-\boldsymbol{\tau}_c)} \left\{ \sum_{LL'} \int_0^{R_c} \frac{4\pi}{2l+1} \frac{\rho_{L'}^c(s_c)}{s_c^{l-1}} \left[1 - \left(\frac{s_c}{R_c}\right)^{2l+1} \right] ds_c \delta_{LL'} (-\delta \tau_c)^l Y_L(-\widehat{\boldsymbol{\tau}}_c) \right. \\ &\quad \left. + \sum_{LL'} \frac{V_{CL'}^c(R_c)}{R_c^l} \delta_{LL'} (-\delta \tau_c)^l Y_L(-\widehat{\boldsymbol{\tau}}_c) \right\} \\ &= Z_c \sum_L \left\{ \frac{4\pi}{2l+1} \int_0^{R_c} \frac{\rho_L^c(s_c)}{s_c^{l-1}} \left[1 - \left(\frac{s_c}{R_c}\right)^{2l+1} \right] ds_c + \frac{V_{CL}^c(R_c)}{R_c^l} \right\} \nabla [r^l Y_L(\hat{\mathbf{r}})] \Big|_{r=0}. \end{aligned} \quad (\text{A.4})$$

Note that we already know the electrostatic potential at the time of the force calculation. Therefore, we inserted the spherical harmonic representation of the potential for the boundary values instead of the interstitial representation.

The last factor in (A.4) is the derivative of a constant for $l = 0$. For $l \geq 1$ it becomes

$$\nabla [r^l Y_L(\hat{\mathbf{r}})] \Big|_{r=0} = \mathbf{e}_i \left[\frac{r^i}{r} l r^{l-1} Y_L(\hat{\mathbf{r}}) + r^{l-1} r \partial_i Y_L(\hat{\mathbf{r}}) \right] \Big|_{r=0}.$$

Since the second term of the sum is r^{l-1} times $Y_{l\pm 1, m\pm 1}$ (see Eq. (5.8) for the context) and the spherical harmonic is bounded, the term is of the order r^{l-1} . Therefore, the expression vanishes for all values of l but $l = 1$. Thus, we have proven the validity of Eq. (4.5).

Bibliography

- [Abr65] M. Abramowitz. *Handbook of Mathematical Functions: with Formulas, Graphs, and Mathematical Tables*. Dover Publications, 1965.
- [And75] O. K. Anderson. Linear methods in band theory. *Phys. Rev. B*, 12:3060–3083, 1975.
- [BB06] S. Blügel and G. Bihlmayer. The full-potential linearized augmented plane wave method. In Johannes Grotendorst, Stefan Blügel, and Dominik Marx, editors, *Computational Nanoscience: Do It Yourself!*, volume 31 of *NIC Series*, pages 85–129, Jülich, February 2006. John von Neumann Institute for Computing, Forschungszentrum Jülich.
- [Bet11] M. Betzinger. *Orbital-dependent exchange-correlation functionals in density-functional theory realized by the FLAPW method*. PhD thesis, RWTH Aachen, 2011.
- [BFB10] M. Betzinger, C. Friedrich, and S. Blügel. Hybrid functionals within the all-electron FLAPW method: Implementation and applications of PBE0. *Phys. Rev. B*, 81:195117, 2010.
- [Bir47] F. Birch. Finite elastic strain of cubic crystals. *Phys. Rev.*, 71:809–824, 1947.
- [Blo28] F. Bloch. Über die Quantenmechanik der Elektronen in Kristallgittern. *Z. Physik*, 52:555–600, 1928.
- [Blo94] P. E. Blochl. Projector augmented-wave method. *Phys. Rev. B*, 50:17953–17979, 1994.
- [BO27] M. Born and R. Oppenheimer. Zur Quantentheorie der Molekeln. *Annalen der Physik*, 84:457–484, 1927.
- [Bro65] C. G. Broyden. A class of methods for solving nonlinear simultaneous equations. *Mathematics of Computation*, 19:577–593, 1965.
- [CA80] D. M. Ceperley and B. J. Alder. Ground state of the electron gas by a stochastic method. *Phys. Rev. Lett.*, 45:566–569, 1980.
- [Coo62] A. S. Cooper. Precise lattice constants of germanium, aluminum, gallium arsenide, uranium, sulphur, quartz and sapphire. *Acta Cryst.*, 15:578–582, 1962.

Bibliography

- [CP82] L. A. Cole and J. P. Perdew. Calculated electron affinities of the elements. *Phys. Rev. A*, 25:1265–1271, 1982.
- [Dir29] P. A. M. Dirac. Quantum mechanics of many-electron systems. *Proc. R. Soc. Lond. A*, 123:714–733, 1929.
- [HK64] P. Hohenberg and W. Kohn. Inhomogeneous electron gas. *Phys. Rev.*, 136:B864–B871, 1964.
- [HSE03] J. Heyd, G. E. Scuseria, and M. Ernzerhof. Hybrid functionals based on a screened Coulomb potential. *J. Chem. Phys.*, 118:8207–8215, 2003.
- [htt12] <http://www.flapw.de>, January 2012.
- [Jan74] J. F. Janak. Simplification of total-energy and pressure calculations in solids. *Phys. Rev. B*, 9:3985–3988, 1974.
- [KS65] W. Kohn and L. J. Sham. Self-consistent equations including exchange and correlation effects. *Phys. Rev.*, 140:A1133–A1138, 1965.
- [KSU95] A. Khein, D. J. Singh, and C. J. Umrigar. All-electron study of gradient corrections to the local-density functional in metallic systems. *Phys. Rev. B*, 51:4105–4109, 1995.
- [NM85a] O. H. Nielsen and R. M. Martin. Quantum-mechanical theory of stress and force. *Phys. Rev. B*, 32:3780–3791, 1985.
- [NM85b] O. H. Nielsen and R. M. Martin. Stresses in semiconductors: *Ab initio* calculations on Si, Ge, and GaAs. *Phys. Rev. B*, 32:3792, 1985.
- [NO11] N. Nagasako and T. Oguchi. Stress formulation in the all-electron full-potential linearized augmented plane wave method. *Journal of the Physical Society of Japan*, 80:024701, 2011.
- [Nye98] J. F. Nye. *Physical Properties of Crystals*. Clarendon Press, Oxford, 1998.
- [PBE96] J. P. Perdew, K. Burke, and M. Ernzerhof. Generalized gradient approximation made simple. *Phys. Rev. Lett.*, 77:3865–3868, 1996.
- [PW86] J. P. Perdew and Y. Wang. Accurate and simple density functional for the electronic exchange energy: Generalized gradient approximation. *Phys. Rev. B*, 33:8800–8802, 1986.
- [PW92] J. P. Perdew and Y. Wang. Accurate and simple analytic representation of the electron-gas correlation energy. *Phys. Rev. B*, 45:13244–13249, 1992.
- [PZ81] J. P. Perdew and A. Zunger. Self-interaction correction to density-functional approximations for many-electron systems. *Phys. Rev. B*, 23:5048–5079, 1981.

- [SBF⁺11] M. Schlipf, M. Betzinger, C. Friedrich, M. Ležaić, and S. Blügel. HSE hybrid functional within the FLAPW method and its application to GdN. *Phys. Rev. B*, 84:125142, 2011.
- [Sin91] D. J. Singh. Ground-state properties of lanthanum: Treatment of extended-core states. *Phys. Rev. B*, 43:6388–6392, 1991.
- [Sin94] D. J. Singh. *Planewaves, Pseudopotentials, and the LAPW Method*. Kluwer Academic, Dordrecht, 1994.
- [SK11] D. Sander and J. Kischner. Non-linear magnetoelastic coupling in monolayers: Experimental challenges and theoretical insights. *Phys. Status Solidi B*, 10:2389–2397, 2011.
- [Sla37] J. C. Slater. Wave functions in a periodic potential. *Phys. Rev.*, 51:846–851, 1937.
- [SW89] J. M. Soler and A. R. Williams. Simple formula for the atomic forces in the augmented-plane-wave method. *Phys. Rev. B*, 40:1560–1564, 1989.
- [SW93] J. M. Soler and A. R. Williams. Comment on "All-electron and pseudopotential force calculations using the linearized-augmented-plane-wave method". *Phys. Rev. B*, 47:6784–6786, 1993.
- [TADS02] T. Thonhauser, C. Ambrosch-Draxl, and D. J. Singh. Stress and pressure within the linearized-augmented plane-wave method. *Solid State Communications*, 124:275 – 282, 2002.
- [TJB⁺08] M. Torrent, F. Jollet, F. Bottin, G. Zérah, and X Gonze. Implementation of the projector augmented-wave method in the ABINIT code: Application to the study of iron under pressure. *Comp. Mater Sci.*, 42:337–351, 2008.
- [vBH72] U. von Barth and L. Hedin. A local exchange-correlation potential for the spin polarized case. *J. Phys. C: Solid State Phys.*, 5:1629–1642, 1972.
- [VWN80] S. H. Vosko, L. Wilk, and M. Nusair. Accurate spin-dependent electron liquid correlation energies for local spin density calculations: a critical analysis. *Can. J. Phys.*, 58:1200–1211, 1980.
- [WD92] M. Weinert and J. W. Davenport. Fractional occupations and density-functional energies and forces. *Phys. Rev. B*, 45:13709–13712, 1992.
- [Wei81] M. Weinert. Solution of Poisson's equation: Beyond Ewald-type methods. *Journal of Mathematical Physics*, 22:2433–2439, 1981.
- [WKWF81] E. Wimmer, H. Krakauer, M. Weinert, and Freeman. Full-potential self-consistent linearized-augmented-plane-wave method for calculating the electronic structure of molecules and surfaces: O_2 molecule. *Phys. Rev. B*, 24:864–875, 1981.

Bibliography

- [WP91] Y. Wang and J. P. Perdew. Spin scaling of the electron-gas correlation energy in the high-density limit. *Phys. Rev. B*, 43:8911–8916, 1991.
- [WWF82] M. Weinert, E. Wimmer, and A. J. Freeman. Total-energy all-electron density functional method for bulk solids and surfaces. *Phys. Rev. B*, 26:4571–4578, 1982.
- [YSK91] R. Yu, D. Singh, and H. Krakauer. All-electron and pseudopotential force calculations using the linearized-augmented-plane-wave method. *Phys. Rev. B*, 43:6411–6422, 1991.

List of Figures

1.1.	Uniaxial tensile stress transforms a bcc structure into a bct structure. . .	3
1.2.	Film (white) on different substrates (gray). In the middle figure, substrate and film are of the same material, the film is under no stress. On the left, the substrate has a greater lattice constant, leading to a tensile stress in the film (thin green lines). On the right, the substrate has a smaller lattice constant. This results in compressive stress in the film (red zigzag lines).	4
1.3.	Lattice structure optimization: Start with a guessed lattice geometry. If the resulting atomic forces are non-zero, shift the atoms in the unit cell and continue the optimization until the forces are sufficiently small. If the stress is non-zero, change the Bravais lattice vectors accordingly and continue the optimization until the stress vanishes.	5
2.1.	Components of the stress tensor. On each face of the cube, stress can act perpendicular to the surface normal or parallel to it. E.g. the stress component σ_{yy} causes the cube to expand or to shrink by ε_{yy}	7
2.2.	The textbook way of quantum mechanics follows the top, dotted path. Given a potential $V_{\text{ext}}(\mathbf{r})$, one calculates the eigenfunctions of the corresponding Hamiltonian. The electron density $\rho(\mathbf{r})$ is then found as the sum of the eigenfunctions squares. The theorem of Hohenberg and Kohn allows for the lower path from the ground state density $\rho_0(\mathbf{r})$ to the potential, allowing all three quantities to be the starting point of quantum mechanical calculations and introducing the equivalence between ground state density and potential.	10
3.1.	Schematic overview over electronic structure methods. Different parts of the Schrödinger equation can be handled by different techniques. The techniques are chosen with respect to the problem under consideration. [BB06]	15
3.2.	Division of space into an interstitial region between the atomic sites (IS) and spheres centered at the atomic nuclei, the so-called muffin-tin spheres (MT). In the APW method, the interstitial potential is a constant V_0 while the potential in the muffin-tin spheres is spherical with a radial function $V_{00}(r)$	18
4.1.	Infinitesimal displacement of atom c at $\boldsymbol{\tau}_c$ by $\delta\boldsymbol{\tau}_c$	41

List of Figures

5.1.	The stress components from the valence states, the double counting term, and the exchange-correlation energy of the strained system are calculated using a back-transformation to the unstrained coordinates.	49
5.2.	The stress components from the electrostatic energy of the strained system are calculated in strained coordinates. They are evaluated using the original density smeared over the strained lattice.	62
7.1.	(a) Birch-Murnaghan fit to total-energy data of aluminum, shifted by E_0 . (b) Negative derivative of the Birch-Murnaghan fit and pressure data without Pulay correction.	78
7.2.	Calculated results of the trace of the stress tensor and the pressure formulas. (a) shows the total stress and pressure, including the valence and discontinuity correction. (b) shows the kinetic stress and pressure of the valence states. (c) shows the core correction and the kinetic pressure of the core states. (d) shows the electrostatic stress and pressure. (e) shows the exchange-correlation stress (5.40b). It coincides with pressure by construction. (f) shows the Pulay correction without the core correction. . .	79
7.3.	Difference between stress and pressure. (a) shows the total difference. (b) and (c) show the difference between the kinetic stress and pressure components of the valence and core states, respectively. (d) shows the difference between electrostatic stress and pressure. This contribution dominates the difference between total stress and pressure. (e) and (f) correspond to figures 7.2(e) and (d). $6 \int \rho V_C d^3r$ is transferred from the exchange-correlation term to the electrostatic term. Thonhauser <i>et al.</i> use this convention.	81

List of Tables

7.1. Birch-Murnaghan fit to DFT data of aluminum	77
7.2. Results of the stress calculation of Thonhauser <i>et al.</i> [TADS02] (bold rows) and of the pressure and stress calculation of this thesis (indented lines below). Note that the variation in the unit-cell volume is part of the variation of the electrostatic potential in this thesis, but not in the publication of Thonhauser <i>et. al.</i> There it cancels with the electrostatic contribution in the term containing the exchange-correlation density (5.40b). We have adjusted our results to provide comparability.	82

Acknowledgments

It is only natural that a project of such importance to the author as his diploma thesis takes up a lot of time, resources, and the patience of his fellow people. I therefore wish to express my gratitude to a number of people who helped me greatly with this thesis.

First and foremost, I thank Prof. Dr. Stefan Blügel for allowing me to do my diploma studies at his institute at Forschungszentrum Jülich. He introduced me to the enthralling topic of stress calculations within the FLAPW method and supported me greatly with his insights, which he presented in his cheerful and inquisitive manner.

I also want to thank my second referee Prof. Dr. Marjana Ležaić for taking the time to appraise my work. I wish her and her partner only the best for their new 'project'.

The proofreading was done by the Doctors Gustav Bihlmayer, Christoph Friedrich and Daniel Wortmann, to whom I am grateful for fruitful discussions, too. Especially Dr. Friedrich made great efforts in helping me to work out the details of my thesis.

In addition, I give props to my colleagues for providing a comfortable and inspiring atmosphere at work.

Schließlich möchte ich auch meinen Eltern Edgar und Marthina Klüppelberg danken, die mir das Studium ermöglicht und mir immer liebend zur Seite gestanden haben. Besonders ihre Bemühungen, Alltagsorgen zu bereinigen, die mich vom Studium abgehalten hätten, sind zu erwähnen.

Selbstständigkeitserklärung

Hiermit versichere ich, dass ich die vorliegende Diplomarbeit mit dem Titel 'Calculation of stress tensor within the *ab-initio* full-potential linearized augmented plane wave method' selbstständig verfasst und keine anderen als die angegebenen Quellen und Hilfsmittel benutzt habe und dass die Arbeit in gleicher oder ähnlicher Form noch keiner Prüfungsbehörde vorgelegt wurde.

Aachen, den 1. Februar 2012

Daniel Aaron Klüppelberg